NGR-33-010-210 + NSG-1263.

040

(NASA-CR-149790) A PRACTICAL HADAMARD TRANSFORM SPECTROMETER FOR ASTRONOMICAL APPLICATION (Cornell Univ., Ithaca, N.Y.) 221 p HC A10/MF A01 CSCL 03A

N77-21001

Unclas

G3/89 21745

CORNELL UNIVERSITY

Center for Radiophysics and Space Research

ITHACA, N. Y.

CRSR 655

A PRACTICAL HADAMARD TRANSFORM SPECTROMETER FOR ASTRONOMICAL APPLICATION

by

Ming-Hing Tai

CENTER FOR RADIOPHYSICS AND SPACE RESEARCH
CORNELL UNIVERSITY
ITHACA, NEW YORK

January, 1977

A PRACTICAL HADAMARD TRANSFORM SPECTROMETER FOR ASTRONOMICAL APPLICATION

by

Ming-Hing Tai

DEDICATION

To my parents

献给 爸爸、妈妈

ACKNOWLEDGEMENTS

This project is by no means one man's product. Many people have devoted their talents to the completion of this project. I am just the one to make a summary of it.

My special thanks go to Prof. Martin Harwit, my thesis advisor. Martin set himself up as an admirable example: he always moved the heaviest equipment himself; tackled the most difficult jobs in the experiment so that he himself was responsible for any misfortunes; was earnest in discussions about problems with his student; and was modest in sharing the credit for the results. Above all, he truly expressed concern about his student, as a respectable advisor and as a warm friend.

My second thanks go to Dr. Daniel A. Briotta. Dan helped to automize the whole process and taught me the mini computer technique. Dan has shown me how to run the computer as though he were showing me how the lines in his palm run.

My thanks also go to the infrared astronomy group at Cornell. Prof. J. Houck has served on my committee and has always been available for discussion of astronomical and experimental problems. I especially thank him for his help in finishing up my degree while Martin was on sabbatical leave. Dr. Phillips built the spectrometer. The late L. King modified it. G. Stasavage built some electronic parts and H. Kondracki built the dewer. G. Melick helped with the observation, data processing and electronic parts, G. Gull with the field trip, and Drs. W. Forrest, Diward, and D. Shacck were involved in many valuable discussions. Thanks also go to Westy Dain for not only being always willing to help on chilly night's observations and tedious laboratory work, but also for proof reading my thesis.

I thank Prof. E.E. Salpeter for serving on my committee, Prof. A. Siever and Allen Chin for helping the He_3 cooled dewer, and Prof. P. Gierasch for always being available for discussing astronomical problems. I also thank G. Vincent for building many mechanical parts, B. Boettcher for figures and Eckelmaun for photographs.

The author thanks the staffs of the Kitt Peak National Observatory and McDonald Observatory for generous allotments of observing time and for assistance during the observing runs.

Finally, my thanks go to Divan Sun, Adeline Wu, and W.W. Chiu, for typing the thesis for me, and to N.H. Cheung, K.K. Mon, K.M. Lo and many of my Chinese friends for their continual help during these years.

Portions of this work were supported by the NGR 33-010-210 and NSG 1263.

TABLE OF CONTENTS

LIST OF FIGURES

LIST OF TABLES

忆 秦 娥

娄　山　关

一九三五年二月

西风烈，
长空雁叫霜晨月。
霜晨月，
马蹄声碎，
喇叭声咽。

雄关漫道真如铁，
而今迈步从头越。
从头越，
苍山如海，
残阳如血。

毛泽东主席

CHAPTER I

HISTORICAL INTRODUCTION TO HADAMARD TRANSFORM SPECTROMETRY (HTS)

The idea of modulating or encoding the optical output of a spectrometer goes back to the original work of Golay (1949) and Fellgett (1951). Its purpose is to allow many different wavelengths of radiation to fall on a detector simultaneously, and thereby to increase the signal-to-noise ratio (SNR) of the resulting spectrum. This improvement comes about because each element of the spectrum is effectively viewed a larger fraction of the total available observing time. One idea is to encode or modulate each spectral wavelength exiting the spectrometer output with an audio frequency that contains the optical wavelength information. The use of a conventional wave analyzer then allows recovery of the original optical spectrum. There are many variations of this technique.

In 1968, Ibbett et al and Decker et al independently suggested the use of sequentially stepped multiplex spectrometers. In both systems radiation enters a dispersive instrument through a single slit and is analyzed at a number of exit slits. Decker et al pointed out that two constraints should be imposed on the encoding scheme:

(1) To obtain the optimum signal to noise ratio, each spectral element should be viewed during exactly half the step positions.

(2) To impose the smallest dynamic range requirements on the

detector amplifier system, each step position should pass light from exactly half the spectral elements. They also worked out a scheme that satisfied the two constraints for masks having elements m=4n+2, where n is an arbitrary integer or zero. Ibbett *et al* introduced the Hadamard pattern for the mask. As discussed below, this is a pattern based on a set of binary orthogonal matrices first studied by the French mathematician Jacques Hadamard. Ibbett *et al* also described the application of their scheme to a real time computer aided measurement.

In 1969, Sloane *et al* worked out a number of binary cyclic coding schemes for multiplex spectrometry and evaluated the performance of each scheme in terms of a linear, least mean square, unbiased estimate. These schemes include a Hadamard matrix $\underline{H}$, and various modified Hadamard matrices, which these authors refer to as $\underline{G}$ matrix and $\underline{S}$ matrix (Fig. 1-1).

A Hadamard matrix $\underline{H}$ of order N is an N x N matrix H_N of +1's and -1's which satisfies:

$$H_N H_N^T = N I_N$$

where I_N is an N x N unit matrix

A modified Hadamard matrix $\underline{G}$ of order M is a partitioned matrix from the H matrix:

$$\underline{H} = \begin{bmatrix} 1 & \cdots & 1 \\ \vdots & & \\ \vdots & \underline{G} & \\ 1 & & \end{bmatrix} \qquad (M = N-1)$$

$$\underline{H} = \begin{bmatrix} + & + & + & + & + & + & + & + \\ + & + & + & - & - & - & + & - \\ + & + & - & - & - & + & - & + \\ + & - & - & - & + & - & + & + \\ + & - & - & + & - & + & + & - \\ + & - & + & - & + & + & - & - \\ + & + & - & + & + & - & - & - \\ + & - & + & + & - & - & - & + \end{bmatrix}$$

$$\underline{G} = \begin{bmatrix} + & + & - & - & - & + & - \\ + & - & - & - & + & - & + \\ - & - & - & + & - & + & + \\ - & - & + & - & + & + & - \\ - & + & - & + & + & - & - \\ + & - & + & + & - & - & - \\ - & + & + & - & - & - & + \end{bmatrix}$$

$$\underline{S} = \begin{bmatrix} 0 & 0 & 1 & 1 & 1 & 0 & 1 \\ 0 & 1 & 1 & 1 & 0 & 1 & 0 \\ 1 & 1 & 1 & 0 & 1 & 0 & 0 \\ 1 & 1 & 0 & 1 & 0 & 0 & 1 \\ 1 & 0 & 1 & 0 & 0 & 1 & 1 \\ 0 & 1 & 0 & 0 & 1 & 1 & 1 \\ 1 & 0 & 0 & 1 & 1 & 1 & 0 \end{bmatrix}$$

Figure 1-1. An 8 x 8 Hadamard matrix and two 7 x 7 cyclic matrices that can be derived from it.

where the first row and first column of H are all +1's. A feature of the G matrix is that it can be written in cyclic form-- a factor which we will show to be of considerable practical importance.

A modified Hadamard matrix S is a matrix obtained from G by replacing +1's by 0's and -1's by +1's.

The properties of H, G, and S will be discussed in section 2-6.

When we talk of encoding by means of a Hadamard matrix we have the following in mind. A mask is used to modulate - open or close - a series of entrance and exit slits in a spectrometer. If a certain slit location is open, we can designate it by a +1; if it is closed we can designate it by a 0; if it can be used to subtract from the signal incident on the detector, we designate it by -1. The sequence of +1's and -1's characterizing a mask in a given modulating position corresponds to a row of a matrix. The whole set of mask positions corresponds to the set of rows of the matrix. If the sequence of mask patterns corresponds to the rows of a Hadamard matrix we say we are encoding with a Hadamard pattern.

Sloane et al also introduced the idea of using a cyclic matrix for coding masks. This greatly decreases the experimental cost and facilitates operation, since any N slits of a single mask 2N-1 slits long can be used to provide one of the required mask patterns.

The first single entrance Hadamard spectrometer (HTS) was built by Decker and Harwit (1969). The spectrometer had a single entrance slit and 19 exit slits. The exit mask was stepped manually. The authors used this spectrometer to take the spectrum of the mercury vapor 1.7μ band to demonstrate the Hadamard transformed spectrum's fidelity and freedom from systematic errors.

With 19 exit slits, the HTS had a theoretical signal-to-noise advantage of 2.18 over the conventional spectrometer, which is rather hard to verify experimentally, Decker (1971) therefore proceeded to build a 255-slit HTS. In this spectrometer, the radiation, after being decoded by the exit mask, exits along the same path it comes in. This reverse pass de-disperses the beam and allows it to be brought to a focus at the entrance plane. Thus the dimensions of the focused image are roughly the same as the dimensions of the entrance aperture, and the detector size can be minimized. This is important since sufficiently large detectors sometimes do not exist, and if available tend to be noisy. Decker experimentally verified the theoretically predicted multiplex advantage of an HTS.

DeGraauw and Veltman (1970) were the first to use an HTS for astronomical work during the 1970 solar eclipse. Houck et al (1973) subsequently used an HTS to obtain near infrared spectra of Mars from airplane altitudes.

Besides putting an encoding mask at the exit plane, one can also put another encoding mask at the entrance plane of a spectrometer. In that way the radiation is modulated at both the entrance and exit apertures. Harwit et al (1970) worked out this scheme of doubly multiplexed dispersive spectrometry. The double multiplexing scheme allows one to increase the total amount of radiation that can be transmitted through a spectrometer. Furthermore, by a proper reduction of the data, one can also obtain a one dimensional picture of the source at the entrance plane. For a spectrometer of m entrance slits and n exit slits, one needs m x n data points to recover m spatial spectra, with each spatial spectrum containing n spectral elements. For a homogeneous source one does not need the spatial information, so (n + m - 1) data points will be enough to recover the spectra. Harwit et al (1974a)describe two schemes for recovering the spectrum with (n + m - 1) data points.

In 1975 Tai et al (1975a) finished the construction of a doubly coded Hadamard transform spectrometer. The spectrometer has 15 entrance slits and 255 exit slits, which can simultaneously obtain 15 spatial spectra, each having 255 spectral elements. Tai et al (1975b) went on to give an analysis of the errors in Hadamard spectrometry caused by imperfect masks.

Besides coding the radiation at both the entrance and the exit aperture, one can go one step further and use a two dimensional mask at the entrance aperture (Harwit, 1971). This yields a two dimensional picture at the entrance aperture, where each spatial point at the entrance has its own spectrum. To put it a different way, one obtains a two dimensional picture of the source at the entrance aperture for each color of the spectral elements.

Harwit (1973) experimentally verified the operation of imaging spectrometry, and Swift <u>et al</u> (1976) constructed the first Hadamard imaging spectrometer.

There are other discussions of Hadamard transform spectrometry in the literature, mostly of theoretical aspects. Nelson and Fredman (1970) give a more complete theoretical treatment of Hadamard matrix encoding. They also rediscovered a theorem due initially to Hotelling (1944) showing that the Hadamard matrix is the best design for a singly coding mask. Sloane and Harwit (1976) show the connection between Hadamard spectrometry and the mathematics of weighing designs in statistics.

There have been various comparisons of Hadamard transform spectrometry with other spectrometry. Larson <u>et al</u> (1974) makes a theoretical comparison of singly multiplexed Hadamard transform spectrometers and scanning spectrometers. They present a general mathematical framework for the comparison of relative performance and also verify their prediction by computer simulation of various characteristic spectra. Their results show that where the noise level is constant and independent of the incident photon flux, the determined multiplex advantage is $\sqrt{N/2}$, as predicted by Fellgett (1951). This is usually the case in a low energy region, such as the infrared. For a noise level that is signal-dependent, such as in the UV energy region, the detector is characterized by an output with statistics approaching a Poisson distribution and variance therefore proportional to the input signal. In that case the

HTS technique will be advantageous only for spectra that are characterized by a few well-defined and intense peaks on a very low intensity background. For spectra with high background, for dense spectra, or for spectra having very weak spectral features, the HTS will have no advantage over the conventional single slit (SS) technique.

Hirschfeld and Wyntjes (1973) compare Fourier transform and Hadamard transform spectrometry. They also describe various limitations of Hadamard transform spectrometry. This paper was followed by an exchange of notes between Decker (1973) and Hirschfeld and Wyntjes (1973) in the journal Applied Optics in which some of these limitations are disputed. These papers concern themselves with a number of practical matters on which opinions can vary. Here we mention these controversial papers mainly for completeness. Their contents will be discussed further below.

Wyatt and Esplin (1974) analyzed the effect of band width on noise equivalent power (NEP) for multiplex spectrometry with cryogenically cooled, cooled-background extrinsic long wavelength infrared detectors. They find that the NEP is directly proportional to band width, so multiplex schemes that require increased band width are not of real advantage. They further conclude that doubly encoded systems that are based on $m + n - 1$ measurements would have a real throughput advantage

Various other aspects of Hadamard matrices and Hadamard transform spectrometry which have not been mentioned above are covered in articles by: Baumert, Pratt et al (1969), Hirschy et al (1971), Allen et al (1972,1973), Kowalski et al (1973), Planky et al (1974), Oliver et al (1974).

In this thesis Chapter II will describe the mathematical properties of Hadamard matrices and their application to spectroscopy. Chapter III describes the Hadamard transform spectrometer, and gives results on laboratory performance. Chapter IV gives a comparison of Hadamard transform and Fourier transform encoding in spectrometry. The output of an HTS is fed into a mini computer. The computer performs a real time inverse Hadamard transform to recover the spectrum. Chapter V describes the algorithm and programming of inverse Hadamard transform. Chapter VI discusses observational results and their interpretation.

CHAPTER II

HADAMARD MATRICES

(A) Weighing Designs

In order to understand the mathematical advantage of Hadamard transform encoding, let us look at the following examples (Sloane *et al*, 1976).

Suppose four objects are to be weighed, using a spring balance which makes an error e each time it is used. Assume that e is a random variable with mean zero and variance σ^2.

First suppose the objects are weighed separately. If the unknown weights are ψ_1, ψ_2, ψ_3, ψ_4, the measurements are η_1, η_2, η_3, η_4, and the errors made by the balance are e_1, e_2, e_3, e_4, then the four weighings give four equations:

$$\eta_1 = \psi_1 + e_1 \qquad \eta_2 = \psi_2 + e_2$$

$$\eta_3 = \psi_3 + e_3 \qquad \eta_4 = \psi_4 + e_4$$

The best estimate of the unknown weights are the measurements themselves:

$$\hat{\psi}_1 = \eta_1 = \psi_1 + e_1$$

$$\hat{\psi}_2 = \eta_2 = \psi_2 + e_2$$

These are unbiased estimates:

$$E\hat{\psi}_1 = \psi_1$$

$$E\hat{\psi}_2 = \psi_2 \qquad \text{(E denotes expected value)}$$

with variance or mean square error

$$E(\hat{\psi}_1 - \psi_1)^2 = E\sigma_1^2 = \sigma^2$$

On the other hand, suppose the balance is a chemical balance with two pans, and the four weighings are made as follows:

$$\begin{aligned}
\eta_1 &= \psi_1 + \psi_2 + \psi_3 + \psi_4 + e_1 \\
\eta_2 &= \psi_1 - \psi_2 - \psi_3 - \psi_4 + e_2 \\
\eta_3 &= \psi_1 + \psi_2 - \psi_3 - \psi_4 + e_3 \\
\eta_4 &= \psi_1 - \psi_2 - \psi_3 + \psi_4 + e_4 \qquad (2\text{-}1)
\end{aligned}$$

This means that in the first weighing all four objects are placed in the left hand pan, and in the other weighings two objects are in the left pan and two in the right. (Note that the e are independent of the weights on the balance. This point is crucial). It is easy to solve for ψ_1, ψ_2, ψ_3, ψ_4, as long as the coefficient matrix for ψ is not singular. Thus the best estimate for ψ_1 is

$$\hat{\psi}_1 = \tfrac{1}{4}(\eta_1 + \eta_2 + \eta_3 + \eta_4)$$
$$= \psi_1 + \tfrac{1}{4}(e_1 + e_2 + e_3 + e_4)$$

The variance of Ce, here C is a constant, is C^2 times the variance of e, and the variance of a sum of independent random variables is the sum of the individuals variances. Therefore the variance of $\hat{\psi}_1$(and also of $\hat{\psi}_2$, $\hat{\psi}_3$, $\hat{\psi}_4$) is $\frac{4\sigma^2}{16} = \frac{\sigma^2}{4}$

Weighing the objects together has reduced the mean square error by a factor of 4. In effect the signal to noise ratio (SNR), which is given by the root mean square (rms) error is reduced by a factor of 2.

Finally, suppose the balance is a spring balance with only one pan, so only coefficients 0 and 1 can be used. A good method of weighing the four objects is:

$$\begin{aligned}
\eta_1 &= \phantom{\psi_1 +{}} \psi_2 + \psi_3 + \psi_4 + e_1 \\
\eta_2 &= \psi_1 + \psi_2 \phantom{{}+ \psi_3 + \psi_4} + e_2 \\
\eta_3 &= \psi_1 \phantom{{}+ \psi_2} + \psi_3 \phantom{{}+ \psi_4} + e_3 \\
\eta_4 &= \psi_1 \phantom{{}+ \psi_2 + \psi_3} + \psi_4 + e_4 \qquad (2\text{-}2)
\end{aligned}$$

In this case the variances of ψ_1, ψ_2, ψ_3, ψ_4, are $\frac{4\sigma^2}{9}$, $\frac{7\sigma^2}{9}$, $\frac{7\sigma^2}{9}$, $\frac{7\sigma^2}{9}$ respectively, a smaller improvement than in the previous case.

The theory of weighing designs is of immediate interest to multiplex optics, since the simultaneous measurement of the intensities of different bundles of rays is completely analogous to the simultaneous weighing of different groups of weights. In measuring the intensity of radiation passed through slits in a mask, we are effectively 'weighing' that radiation.

(B) General Mathematical Formulation

One can put the problem into a more general form. Let ψ_i be the i^{th} unknown, η_j be the j^{th} measurement, e_j be the error associated with the j^{th} measurement. Let w_{ji} be the weighing coefficient of the j^{th} measurement with the i^{th} unknown. Then

$$\eta_j = w_{ji}\psi_i + e_j \qquad \begin{matrix} i=1\cdots\cdots n \\ j=1\cdots\cdots n \end{matrix} \qquad (2\text{-}3)$$

In matrix notation:

$$\underline{\eta} = \underline{W}\,\underline{\psi} + \underline{e} \qquad (2\text{-}4)$$

With the notation < > for ensemble averages, the error e_i has the following properties:

(1) $\langle e_i \rangle = 0$

(2) e_i is independent of $\underline{\psi}$

(3) $\langle e_i e_j \rangle = 0$ if errors are assumed to be uncorrelated.

$= \sigma^2$ if $i=j$

The problem now is the following: (i) For a particular coding matrix W, what should be the decoding matrix A? i.e. What is A such that $\underline{\hat{\psi}}=\underline{A}\,\underline{\eta}$ where $\underline{\hat{\psi}}$ is an unbiased estimate of $\underline{\psi}$.

(ii) What is the best choice of $\underline{W}$ (or $\underline{A}$) that will minimize the error of measurement i.e. What is $\underline{W}$ such that

$$\varepsilon = < \sum_{j=1}^{n} (\hat{\psi}_j - \psi_j)^2 >$$

is a minimum.

In the absence of noise, i.e. n=0, it is clear from (2-4) that

$$\underline{\psi} = \underline{W}^{-1}\underline{n}$$

and therefore

$$\underline{A} = \underline{W}^{-1}$$

and

$$\hat{\underline{\psi}} = \underline{A}\ \underline{n} = \underline{\psi}$$

In the presence of noise,

$$\hat{\underline{\psi}} = \underline{A} \cdot \underline{n}$$

$$= \underline{A}\ \underline{W}\ \underline{\psi} + \underline{A}\ \underline{n}$$

and with the assumed properties of the noise $<\underline{\psi}> = \underline{\psi}$, one obtains

$$<\hat{\underline{\psi}}> = \underline{A} . \underline{W} <\underline{\psi}> + \underline{A}<\underline{e}>$$

$$= \underline{A}\ \underline{W}\ \underline{\psi}$$

Assuming no prior knowledge of the unknowns, one may use the unbiased condition $<\hat{\underline{\psi}}> = \underline{\psi}$. This again implies

$$\underline{A} = \underline{W}^{-1}$$

So with the assumed properties of noise and unbiased condition, the decoding matrix is just the inverse of the coding matrix.

One still has to find a coding matrix which will minimize the uncertainty, ε .

The second question can be solved in the following way: Let $\hat{\eta}_i$ be the i^{th} measurement in the absence of noise, then for each measurement

$$\begin{aligned}
\eta_i &= W_{i1}\psi_1 + W_{i2}\psi_2 + \cdots + W_{in}\psi_n + e_i \\
&= \hat{\eta}_i + e_i \\
\psi_j &= A_{j1}\eta_1 + A_{j2}\eta_2 + \cdots + A_{jn}\eta_n \\
&= A_{j1}(\hat{\eta}_1 + e_1) + A_{j2}(\hat{\eta}_2 + e_2) + \cdots \\
&\quad + A_{jn}(\hat{\eta}_n + e_n) \\
&= (A_{j1}\eta_1 + \cdots + A_{jn}\eta_n) + (A_{j2}e_2 + \cdots + A_{jn}e_n) \\
&= \psi_j + \text{noise}
\end{aligned}$$

The mean square of the noise term corresponding to the j^{th} unknown is therefore

$$\begin{aligned}
\varepsilon_j &= (A_{j1}^2 + \cdots + A_{jn}^2)\,\sigma^2 \\
&= \Delta_j^2\,\sigma^2 \qquad (2\text{-}7)
\end{aligned}$$

where

$$\Delta_j = (A_{j1}^2 + \cdots + A_{jn}^2)^{\frac{1}{2}} \qquad (2\text{-}8)$$

and Δ_j represents the improvement in the SNR for the weighing design, compared to the SNR for individual weighings.

Hence, the problem of maximizing the signal to noise ratio becomes the problem of minimizing ε_j; or Δ_j (Nelson and Fredman (1970)).

Sloane *et al* (1969) independently developed an expression for ε/σ^2 where

$$\varepsilon/\sigma^2 = \text{Trace } \underline{W}^{-1}(\underline{W}^{-1})^T$$

$$= \text{Trace } \underline{A}\,\underline{A}^T \qquad (2\text{-}9)$$

Equation (2-8) and (2-9) amounts to the same thing because it can be seen very easily that

$$\text{Trace } \underline{A}\,\underline{A}^T = \sum_{j=1}^{n} \Delta_j^2$$

The question of minimizing ε had been answered by Hotelling (Hotelling, 1944) and rediscovered by Nelson and Fredman. Hotelling has shown that for any choice of mask W with $|W_j| \leq 1$, the ε_i are bounded by $\varepsilon_i \geq \frac{\sigma^2}{N}$, and that it is possible to have $\varepsilon_i = \frac{\sigma^2}{N}$ for i=1,... N if and only if a Hadamard Matrix H_N of the order N exists (by taking $W=H_N$). This leads to the discussion of the Hadamard Matrix.

(C) Hadamard Matrix

A Hadamard matrix of order N is an NxN matrix H_N of +1's and -1's which satisfies:

$$\underline{H}_N \underline{H}_N^T = \underline{H}\underline{I}_N \qquad (2\text{-}10)$$

where I_N is an NxN unit matrix.

A Hadamard matrix has following properties: (Golomb(1964))

(1) Its row vectors (or equivalently, its column vectors) are mutually orthogonal.

(2) The Hadamard properties will not be disturbed by:

a. Interchanging rows,

b. Interchanging columns,

c. Changing the sign of every element in a row, or

d. Changing the sign of every element in column.

These properties enable the first row and column of every Hadamard matrix to be normalized to contain only +1's. If $\underline{G}$ represents the remaining M x M matrix (M= N-1), then $\underline{H}$ can be partitioned into

$$\underline{H} = \begin{bmatrix} 1 & 1\ 1\ 1 \ldots\ldots 1 \\ 1 & \\ 1 & \underline{G} \\ \cdot & \\ \cdot & \\ \cdot & \\ 1 & \end{bmatrix} \qquad (M= N-1)$$

It is conjectured that Hadamard matrices exist for all multiples of four. Further, if one of the following conditions is also satisfied,

(1) $N = P + 1$ P prime

(2) $N = P(P + 2) + 1$ P and P + 2 prime

(3) $n = 2^m$ m an integer

then $\underline{G}$ can be made cyclic. That is, the $(j + 1)^{th}$ row can be generated by shifting the j^{th} row one position to the left. For example, when N=8, we have matrices of the form shown in Fig. 1-1. Note that $\underline{H}$ and $\underline{G}$ are symmetrix.

Another choice for $\underline{W}$ is the matrix $\underline{S}$ obtained from $\underline{G}$ by replacing +1's by 0's and -1's by +1's.

The properties of the $\underline{H}$, $\underline{G}$ and $\underline{S}$ are discussed by Sloane et al. If rows i and j are any two rows of $\underline{H}$, $\underline{G}$ or $\underline{S}$, it can be shown that their dot product is:

In H_N : row i · row j $= \begin{matrix} 0 & i \neq j \\ N & i = j \end{matrix}$

In G_M : row i · row j $= \begin{matrix} -1 & i \neq j \\ M & i = j \end{matrix}$

In S_M : row i · row j $= \begin{matrix} M/4 & i \neq j \\ M/2 & i = j \end{matrix}$

The inverse of each matrix is:

$$\underline{H}_N^{-1} = \frac{1}{N}\underline{H}_N \; ; \; \underline{G}_M^{-1} = \frac{1}{M+1}(\underline{G}_M - \underline{J}_M) \; ; \; \underline{S}_M^{-1} = \frac{2}{M+1}(2\underline{S}_M \; \underline{J}_M)$$

where $\underline{J}$ is a M x M matrix consisting entirely of -1's and N= M+1.

Table 2-1 gives the value of Δ for different matrices. The matrix $\underline{I}$ represents the weighing scheme weighing each object separately. This corresponds to a conventional single slit spectrometer or to a wedge filter monochromator.

Table 2-1

MATRIX A	ELEMENTS OF A	Δ^{-1}	(FOR LARGE N)
$\underline{I}$	1,-0	1	1
$\underline{H}$	1,-1	$\sqrt{N}$	$\sqrt{N}$
$\underline{G}$	1,-1	$\sqrt{N}(2-\frac{2}{N})^{-\frac{1}{2}}$	$\sqrt{\frac{N}{2}}$
$\underline{S}$	1, 0	$\sqrt{N}(2-\frac{2}{N})^{-1}$	$\frac{\sqrt{N}}{2}$
*$\underline{F}$	cosine squared functions	$\frac{N}{4}\;\frac{2}{N+1}$	$\sqrt{\frac{N}{8}}$

* F is the Fourier Transform case which will be disscussed in Chapter IV.

If the number of measurements N is a multiple of 4, and the matrix coefficients are +1, the best weighing scheme is the Hadamard matrix H. ε will be reduced by a factor $\frac{1}{\sqrt{N}}$ compared to weighing the unknown separately. This is the maximum advantage a weighing scheme can obtain with weighing coefficient $|W_{ij}| \le 1$. If N is not a multiple of 4, or if the weighing coefficients are 0's and 1's, it is not possible to simultaneously minimize $\varepsilon_1 \ldots \varepsilon_n$ and some other criterion must be used (Sloane et al, 1976). Also the errors are uniformly larger than for the H-matrix, as shown for the G and S matrices in Table 2-1 above.

It is interesting to see that a spectrometer using the Fourier Transform, such as a Michelson interferometer, has a multiplex advantage a factor of $\sqrt{8}$ lower than the H-matrix and a factor of $\sqrt{2}$ lower than the S-matrix encoding instrument.

Following are some computer simulations for S-matrix transformations with various inputs (See Fig. 2-1(a) to (c)).

	INPUT	OUTPUT
1.	Constant	Constant
2.	Hadamard code: representing single line emission	Single line
3.	Single line: 1 at the 1st element and 0 for the rest. This represents an unknown impulse coming in during the	Hadamard code. Note, unlike the monochromater, the error propagates to other

INPUT	OUTPUT
observation.	elements.
4. Sine wave.	sine wave with different phase.
5. Square wave. The input is not a perfect wave because we have an odd number of elements. The input values have amplitudes 0 or 1 for each element.	Not a perfect square wave.
6. Straight line at a slope 1/255. This may represent a shift in baseline.	Refer to figure (2-1C).

(D) <u>Optical Realization of Hadamard Encoding</u>

We have made use of (modified Hadamard) S-matrices in two optical instruments: One is a Hadamard transform spectrometer having an encoding mask at the exit aperture. The other is a doubly encoded HTS which has encoding masks at both the entrance and exit apertures.

S codes can be used for both the entrance and exit masks for the HTS, with +1 standing for an open slot through which radiation is transmitted, and with 0 standing for a closed slot where radiation is blocked.

The cyclic property of the S-matrix is very desirable, for then only a single mask 2N-1 slots wide need be constructed. Successive encoding positions are generated by stepping the mask one slot width along its length. This avoids the consturction of N masks with N^2 slots.

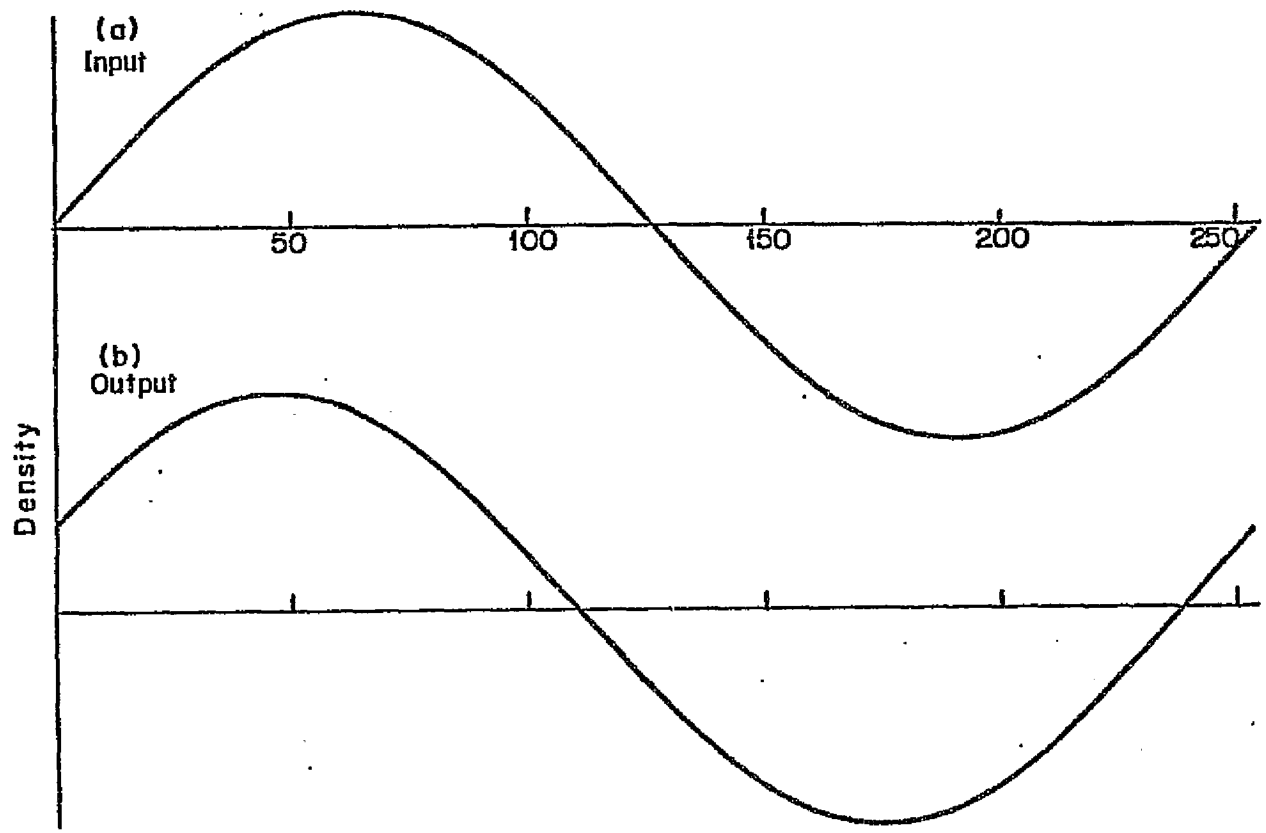

Figure 2-1a. Hadamard transformation of a Sine wave input.

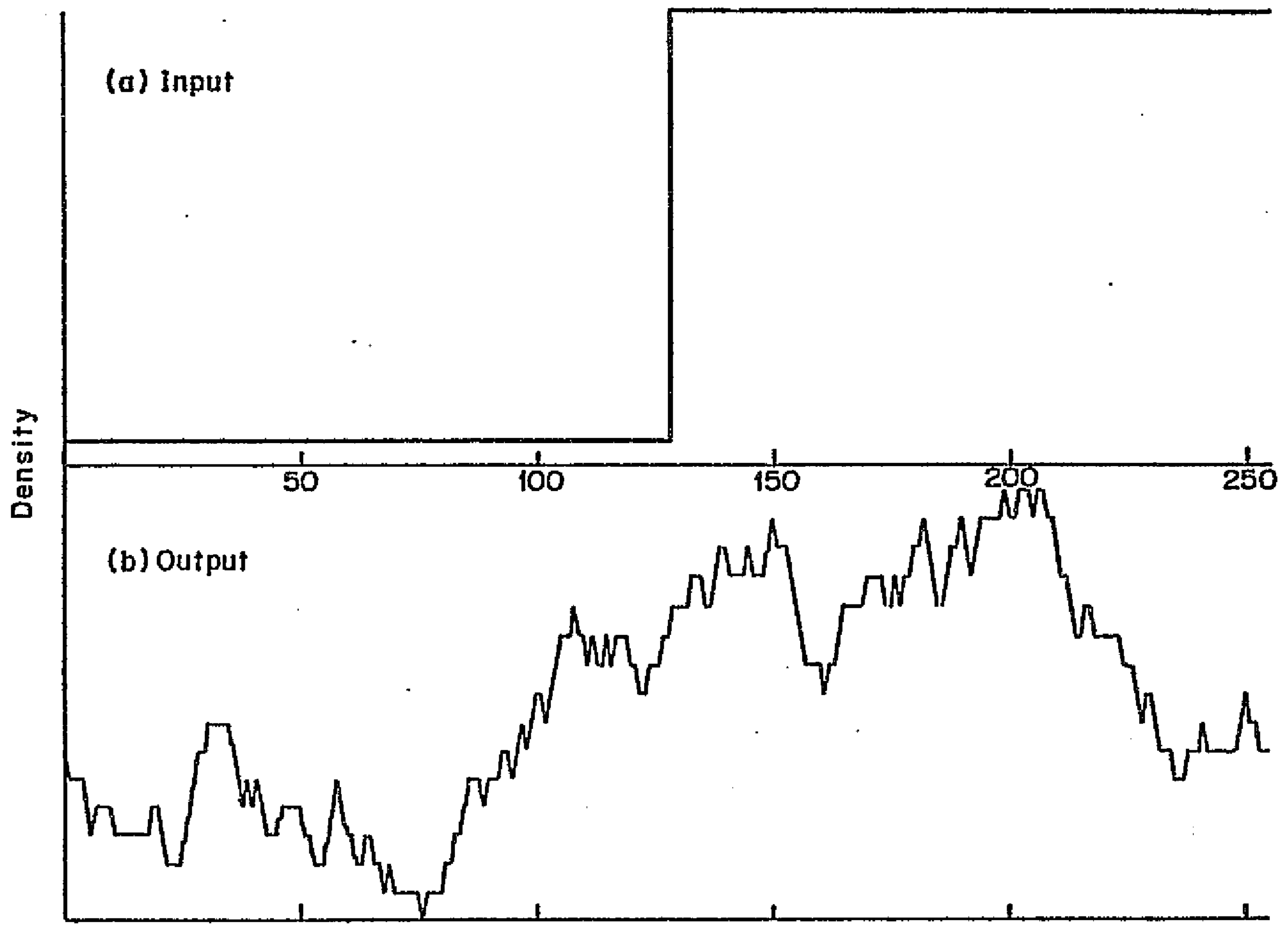

<u>Figure 2-1b</u>. Hadamard transformation of a square wave input.

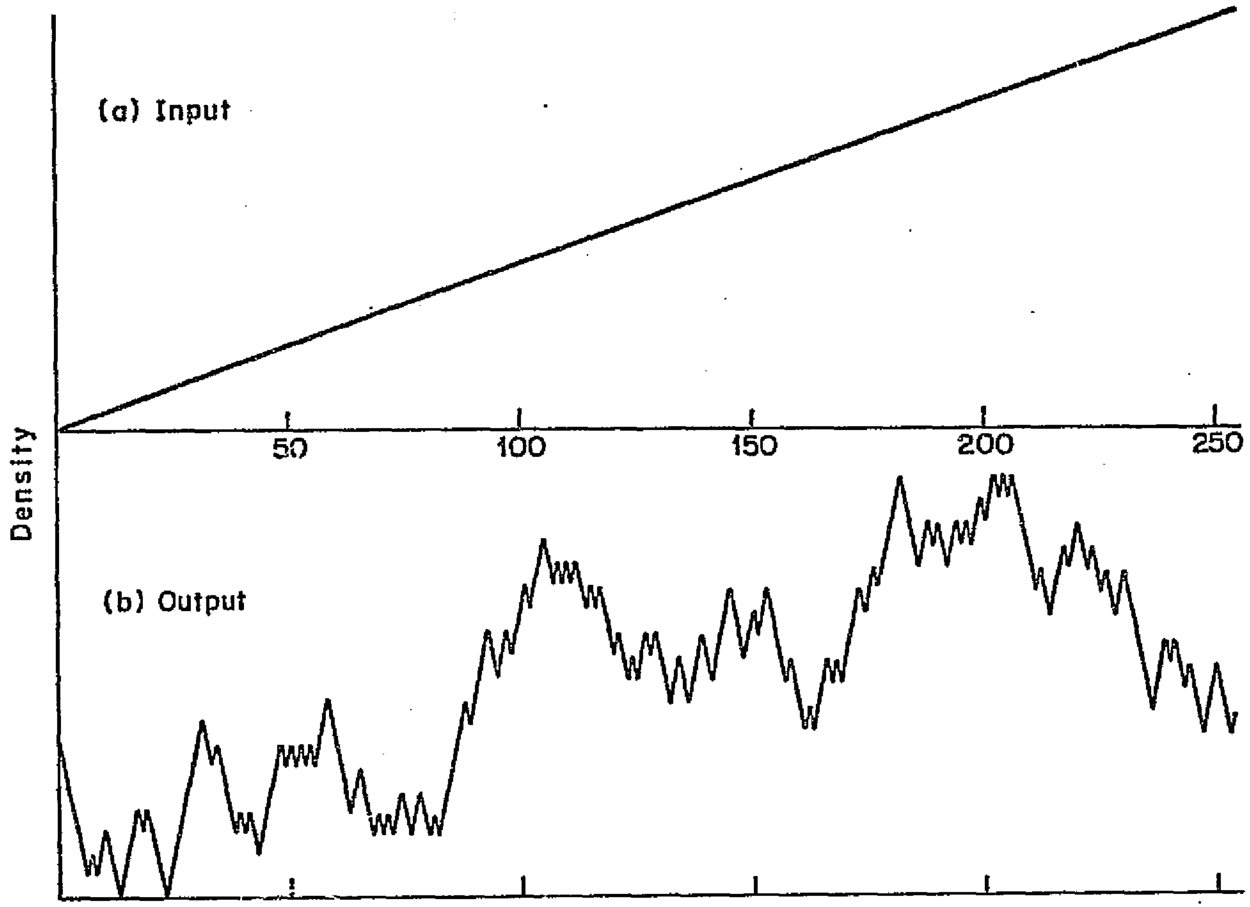

Figure 2-1c. Hadamard transformation of a straight line input.

Although H and G matrices have better coding efficiency than the S matrix, they introduce technical difficulties when used for spectrometer coding schemes. To utilize H and G matrices, one must measure the reflected as well as the transmitted radiation. In this case +1's represent reflecting slots and -1's represent transmitting slots. Therefore a minimum of two detectors must then be used, one in a subtracting mode, the other in the normal mode. The use of two detectors, however, increases the noise. Furthermore, the H matrix, with all elements +1 in the first row, makes the dynamic range of the detector system change by about a factor of two. Also its lack of the cyclic property does not allow one to generate the rest of the masks by the simple stepping technique mentioned above.

1. Hadamard Transform Spectrometer (HTS)

For the singly encoded HTS, we use the following optical arrangement (figure 2-2). Radiation passing through the single entrance slot is rendered parallel and directed to the dispersing element. The dispersed radiation is then de-collimated and focused upon the multi-slot mask at the exit aperture. The spectral elements transmitted by the mask pass through suitable post-optics and are collected onto a detector. One then makes N (in our case N=255) measurements by sequentially stepping the mask N times. The inversion procedure $\underline{\hat{\psi}}=\underline{S}^{-1}\underline{n}$ recovers the spectrum. Figure (2-3) gives a 255 cyclic S-matrix code for the exit mask.

Theoretically, the mean square error in the spectrum

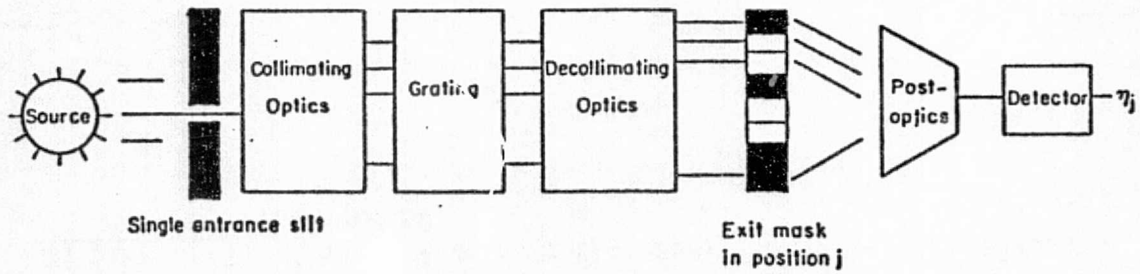

Figure 2-2. Schematic representation of HTS using the S code.

00000	00101	10001	11101	00001	11111	11001	00001
01001	11110	10101	01110	00001	10001	01011	00110
01011	11110	11110	01101	11011	10010	10100	10100
01001	01101	00011	00111	00111	10001	10110	00010
00101	11010	11110	11011	11100	00110	10011	01011
01101	01000	00100	11101	10010	01001	10000	00111
01001	00011	10001					

Figure 2-3. The 509 exit slit mask and the 255-element S code.

given by a monochromator is σ^2. For an HTS using the S code, this error is $\frac{1}{N}(2-\frac{2}{N})^2\sigma^2$ (Sloane et al, 1969). Hence the rms gain in S/N for the HTS is $G= \frac{N\sigma^2}{(2-\frac{2}{N})^2\sigma^2} = \frac{\sqrt{N}}{2-\frac{2}{N}}$. For N=255, $G\sim 8.0$ (figure 2-4 gives Decker's results. The experimental gain was measured as 8.0±0.3). Note that the scale in figure (2-4) are in arbitrary units, and the zero point appears to be shifted between parts (a) and (b).

2. Doubly Encoded Hadamard Transform Spectrometer (DHTS)

Figure (2-5) is a schematic representation of an optical system which has a number of entrance as well as exit slits. Instead of passing radiation through only one entrance slit, a mask M slits wide is placed at the entrance aperture. Radiation passed into the spectrometer through different combinations of open and closed slits. The dispersed radiation at the exit plane is analyzed in the same fashion as in the HTS. Encoding is accomplished by sequentially stepping one of the masks through its N different positions for each position of the other mask.

In a DHTS the entrance aperture is modulated by a P x P S matrix.

Let $\varepsilon=\varepsilon_{ir}$ be the P x P matrix whose rows represent P different entrance masks. $\varepsilon_{ir}=1$ for open slots and 0 for closed slots ($1\le i\le P$, $1\le r\le P$). Similarly let $\chi=\chi_{ij}$ represent the exit mask. When the entrance mask is in position i and the exit mask is in position j, the detector measurement η_{ij} is

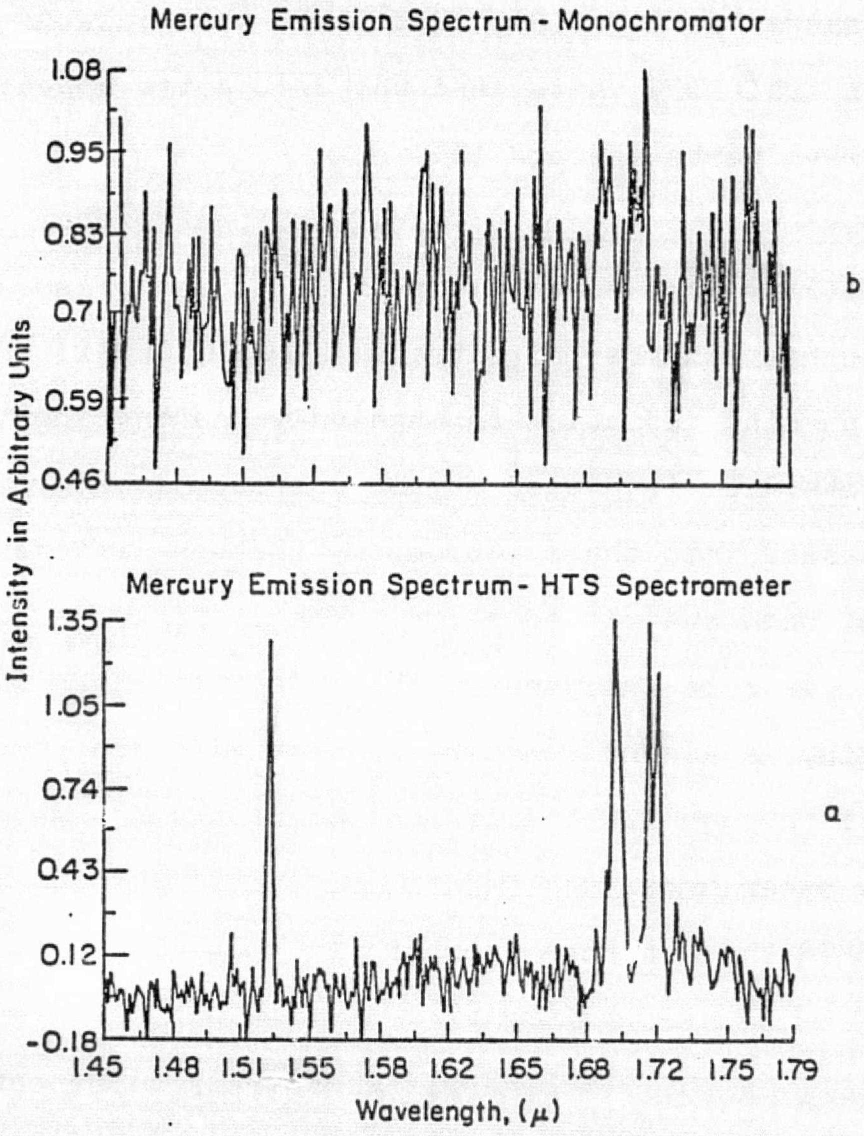

Figure 2-4. Comparison spectrum of the mercury emission lines in the 1.4-1.8μm region: (a, bottom) as obtained in the Hadamard-transform mode, (b, top) as obtained under identical conditions using the same optical system as a conventional monochromator. This figure is taken from Decker, 1971b.

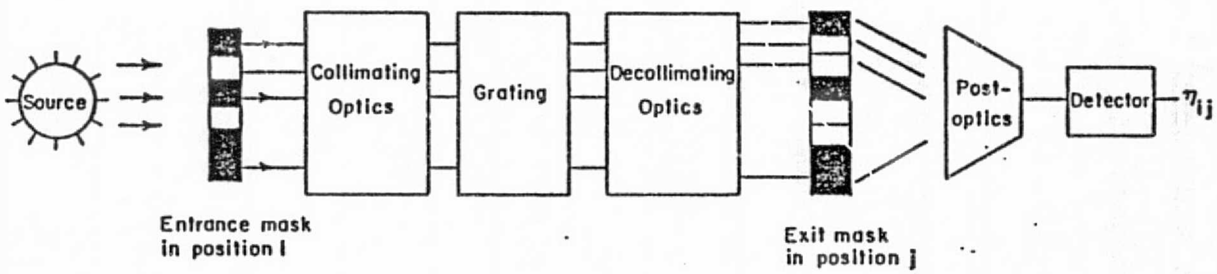

Figure 2-5. Schematic representation of DHTS.

$$\eta_{ij} = \sum_{r=1}^{P} \sum_{s=1}^{N} \varepsilon_{ir}\, \psi_{rs}\, \chi_{sj} + \nu_{ij} \tag{2-11}$$

where ψ_{rs} is the spectral element produced by radiation passing through the r^{th} entrance slot and the S^{th} exit slot, ν_{ij} is the noise in the $(i,j)^{th}$ measurement; it has the following properties:

$$\langle \nu_{ij} \rangle = 0 \qquad \langle \nu_{ij}, \nu_{k\ell} \rangle = \sigma^2 \delta_{ik} \delta_{j\ell}$$

If the instrument has no optical magnification, the spectrum of radiation that passes solely through the r^{th} entrance slot to first order is shifted by r spectral channels from the spectrum passing solely through the first entrance slot. Hence, only P+N-1 distinct spectral elements exist:

$$\psi_{-(P-1)}, \ldots \psi_{-1}, \psi_0, \psi_1, \ldots \psi_{N-1}$$

where

$$\psi_{rs} \equiv \psi_{r-s} \equiv \psi_t \qquad (t=r-s)$$

In matrix notation one may write

$$\underline{\eta} = \underline{\varepsilon}\, \underline{\psi}\, \underline{X}^T + \underline{\nu} \tag{2-12}$$

Employing the same analysis as one does for the HTS, i.e. using the unbiased condition $\langle \hat{\underline{\psi}} \rangle = \underline{\psi}$ and the properties of $\underline{\nu}$, one obtains

$$\underline{\hat{\psi}} = \underline{\varepsilon}^{-1}\underline{\eta}(\underline{X}^T)^{-1}$$

where

$$\underline{\hat{\psi}} = \begin{matrix} \hat{\psi}_0 & \cdots\cdots\cdots & \hat{\psi}_{-N+1} \\ \hat{\psi}_1 & \cdots\cdots\cdots & \hat{\psi}_{-N} \\ \vdots & & \vdots \\ \hat{\psi}_{P-1} & \hat{\psi}_{P-2} \cdots\cdots & \hat{\psi}_{-N-P+2} \end{matrix}$$

Each row i of $\underline{\hat{\psi}}$ represents a spectrum at the exit mask for radiation that enters the instrument through the i^{th} entrance position. Hence the j^{th} diagonal gives a one-dimensional spatial picture across the entrance aperture for the spectral element j.

One may obtain an average spectrum $\underline{\hat{\psi}_i}$ by averaging all the elements in each diagonal.

$$\hat{\psi}_i = \frac{1}{N-|t|} \sum_{r=1}^{P} \psi_{r,r-t} \qquad t \geq 0$$

$$= \frac{1}{N-|t|} \sum_{r=1}^{P} \psi_{r,r-t} \qquad t < 0$$

Harwit et al (1970) showed that if both the entrance and exit masks are S matrices and we define

$$\sigma_t^2 = \langle(\underline{\psi}_t - \underline{\hat{\psi}}_t)^2\rangle$$

Then

$$\sigma_t^2 = \frac{16}{(N+1)} \frac{N^2-1}{N-|t|} \cdot \sigma^2$$

$$\sim \frac{16\sigma^2}{(N-|t|)N^2} \qquad \text{for N large} \qquad (2\text{-}13)$$

where

$$t = -(N-1), \ldots\ldots (N-1)$$

If the total mean square error for the unknown is

$$\varepsilon = \sum_{t=\frac{-N-1}{2}}^{t=\frac{N-1}{2}} \sigma_t^2$$

where one sums only the central element, then for the S-code

$$\varepsilon = \sigma^2 \left[\frac{22.18}{N} + O\left(\frac{1}{N^2}\right)\right] \qquad \text{N large}$$

where σ^2 = constant $\frac{N}{T}$.

There are two points that should be made about the DHTS. (1) It has not been shown that Hadamard codes are the best codes for such an instrument. In fact some evidence suggests that Hadamard codes are not precisely optimum for this "two-ended" operation (Harwit et al,1974b). (2) For PxN data points the spectrum yields only P+N-1 spectral elements, plus a one-dimensional image. It is also possible to reconstruct the (P+N-1) elements with (P+N-1) data points only (Harwit et al, 1974b). Fig. (2-6) gives a 15 element cyclic S-matrix code for the entrance mask.

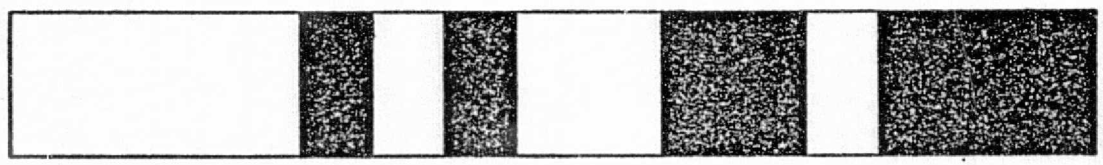

1 1 1 1 0 1 0 1 1 0 0 1 0 0 0

Figure 2-6. The 29 entrance slit mask and the 15-element S code.

Table 2-2 compares three different grating spectrometers. The first column represents the conventional single entrance and exit slot instrument. N measurements are made in time T, with a mean square error σ^2 in each. The second column is for a singly multiplexed instrument with an exit mask S, and is taken from Sloane et al (1969). The last column is for the doubly multiplexed system, using Equation (2-13) for σ_t^2, and has been multiplied by a factor of N to allow for having to make N^2 measurements in time T.

Table 2-2

	NO MASK	SHT	DHT
Δ^{-1}	1	$\frac{\sqrt{N}}{2}$	$\frac{N}{\sqrt{22.2}}$

(E) Errors in Hadamard Spectroscopy

During the manufacture of the masks, whether by deposition of metal or by removal of metal through an etching process, it is possible to obtain a systematic error that leaves each of the opaque portions of the mask either too wide or too narrow by a fixed amount. This will cause a systematic variation in signal passing through the slit. For example if the open slit is too narrow by a fixed amount ε, the light passing through an open slit position will be

I_o when the open slit is bounded by two open slits.

$I_o(1-\varepsilon)$ when the open slit is bounded by one open slit and one closed slit.

$I_o(1-2\varepsilon)$ when the open slit is bounded by two closed slits.

A similar analysis holds for open slits that are too wide, except that the minus sign in these expressions is replaced by a plus sign.

The spectrum of a single (spectral line resulting from such imperfect masks) is remarkably simple (Tai et al, 1975 b). Independent of the particular S-matrix mask to be used, there are always precisely four false blips present in the final spectrum. The amplitude of these blips is always the same for a fixed narrowing or widening of the transmitting slits. Two of the blips always surround the main spectral line, and a pair of adjacent blips always are some distance removed from that line. For the 255 element S-matrix, these two are located 24 and 25 elements away to the left of the parent line. The amplitude of the displaced blips is positive when the transparent slits are too wide and is negative when the slits are too narrow. In contrast, the two blips surrounding the parent line always are positive. Figure (2-7) shows the negative features accompanying the 1.7 μm mercury vapor doublet and the computer simulation of a pure spectral line input and its distorted spectrum. For the general case the reader may refer to Tai et al (1975 b).

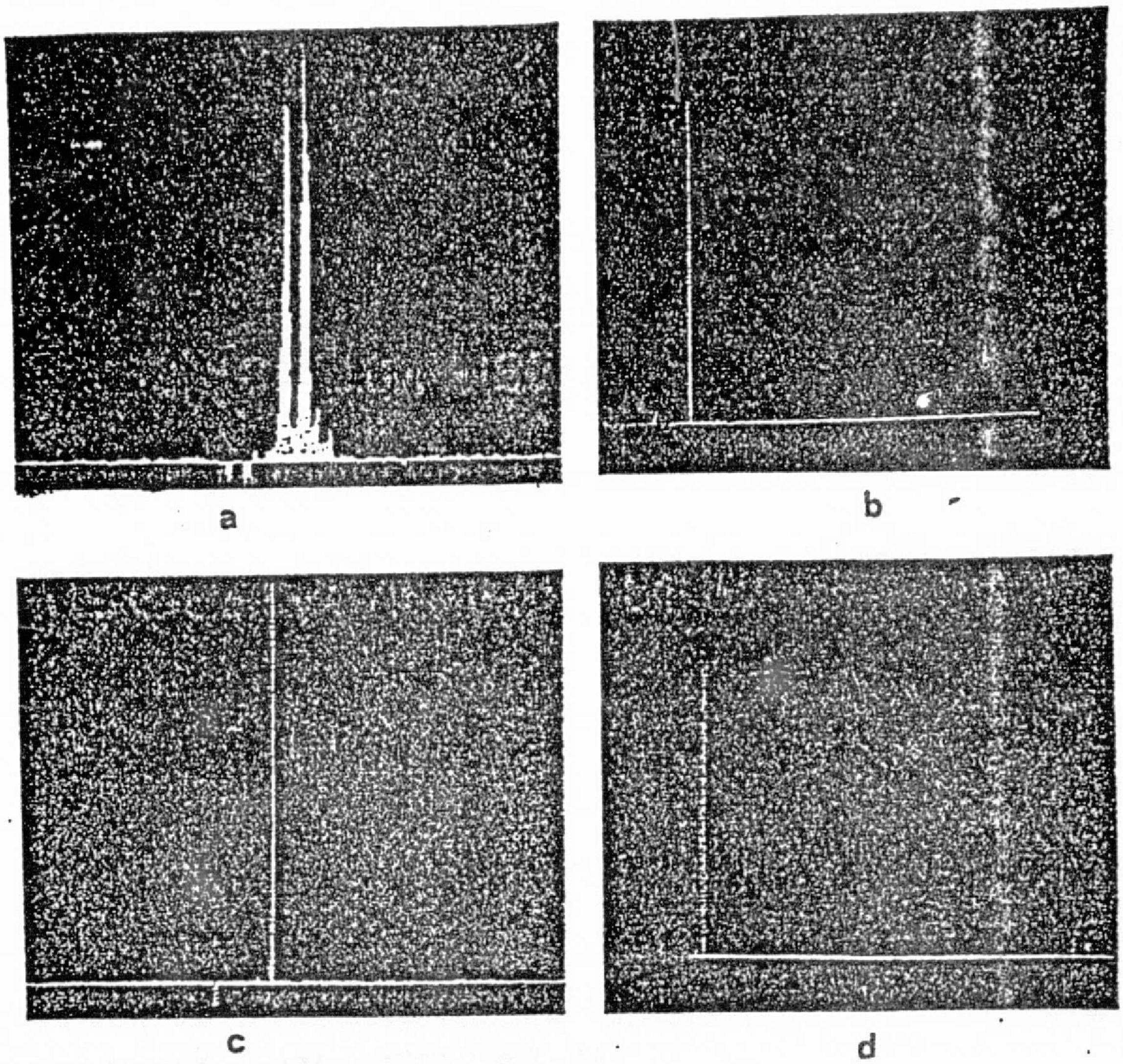

Figure 2-7. (a) Spectrum of the 1.7μm mercury vapor doublet showing negative peaks to the left at the emission peaks; (b) Shows the response we would obtain to a single spectral line with a perfect mask; (c) Shows the response for a single line with the radiation simulated as passing through a mask with slits too narrow because each opaque mask element protrudes into the adjacent transparent slot by a tenth of a slot width; (d) Shows the effect of simulating slits that are systematically too wide. Note that the main spéctral line has been placed in different positions for the synthetic runs (b),(c), and (d).

CHAPTER III

INSTRUMENTATION

(A) Multislit Spectrometer

A conventional spectrometer has four essential elements, an entrance slit, a dispersive device such as a grating or prism, a set of imaging optics, and an exit slit.

Such a spectrometer has two important parameters. The first is the "resolution" R, which is a measure of how well the spectrometer can separate two neighboring lines. The second parameter is the "throughput" E. This is a measure of the light gathering capability of the system. The two parameters, R and E, are lumped together into what is called "luminosity" L, defined as (Vanasse, 1974).

$$L = E \cdot R$$

For a conventional grating spectrometer having a grating of area A_g given by WH, where W and H are the width and height respectively of the grating, the throughput is determined by the product of A_g with the solid angle Ω subtended by the slit at the collimating mirror (or lens). The solid angle is given by

$$\Omega = \frac{w \cdot l}{F^2}$$

where w and l are the width and height respectively of the slit and F is the focal length of the collimating mirror

$$E \sim W \cdot H \cdot \frac{w \cdot h}{F^2}. \qquad (3\text{-}1)$$

The resolution of this instrument is

$$R = \frac{\lambda}{\Delta\lambda}$$

$$= nN$$

$$= n \cdot \frac{W}{d} \qquad (3\text{-}2)$$

where λ is the wavelength, $\Delta\lambda$ the closest wavelength that can be separated, n the order, N the total number of lines on the grating, W the width of the grating and d the spacing between rulings.

Since $d \sin \alpha = n\lambda$ (3-3)

substitute (3-2) into (3-3)

$$\frac{W}{R} \sin \alpha = n\lambda \qquad (3\text{-}4)$$

if the slit width is limited by diffraction, which is the minimum slit width, then

$$w \sim \frac{F\lambda}{W \cos \alpha} \qquad (3\text{-}5)$$

substituting (3-5) into (3-4) one gets

$$R \sim \frac{F}{w} \tan \alpha \qquad (3\text{-}6)$$

Comparing equation (3-1) and (3-6) one sees immediately that, for a fixed grating area W·H, and fixed optical system, E is proportional to the slit width w and R is inversely proportional to the slit width w. This means that an increase in luminosity of the system by increasing the slit width is made at the sacrifice of resolution, and vice versa.

From (3-1) and (3-6) one obtains

$$\begin{aligned} L &\sim E \cdot R \\ &\sim W \cdot H \cdot \frac{1}{F} \end{aligned}$$

Another feature of a conventional spectrometer is that it transmits only one narrow spectral range of light to the detector, and all other spectral elements are wasted. As a result, the instrument is inefficient.

Within the past two decades there has been much research done in an effort to design new spectrometric systems with a view to maximizing the luminosity L, and to observe a number of spectral elements simultaneously. This can provide a multiplex advantage, or a wide aperture advantage. Two quite distinct modulation techniques have been employed in the past. The first depends on the wave nature of radiation, and makes use of interferometry. The Fabry-Perot interferometer, Michelson interferometer, and Mach-Zehnder interferometer (Jacquinot, 1954, 1960; Vanasse and Sakai, 1967) are instruments of this type. The other technique employs dispersing spectrometers in which entrance and exit slits are replaced by opaque or transmitting masks. Golay's multislit spectrometer, Girard's Grill spectrometer and Hadamard spectrometers (Harwit et al, 1974a) are representative of these instruments.

A spectrometer, whether interferometric os mask-multiplexed, yields a multiplex advantage mainly for detector noise or amplifier noise limited applications. In these cases it can be shown that for N spectral elements, one can achieve of the order $N^{\frac{1}{2}}$ improvement in the overall spectral signal-to-noise ratio, S/N, over a conventional spectrometer (Chapter II).

For photon noise limited applications, the multiplexing advantage is cancelled by the N-fold increase in the photon noise attributed to the N-fold increase in the energy falling onto the detector. Nevertheless, for photon noise limitations, the throughput advantage can still be realized. The large throughput will become a disadvantage when the noise is background noise which increases faster than the noise due to the source (Harwit et al, 1974a).

In this chapter we will describe the experimental study of a Hadamard transform spectrometer (HTS) and calibration in the laboratory. Figure (3-1) is the flow chart of the whole process, starting with radiation from the telescope and ending with the output of the computer. Each component will be described.

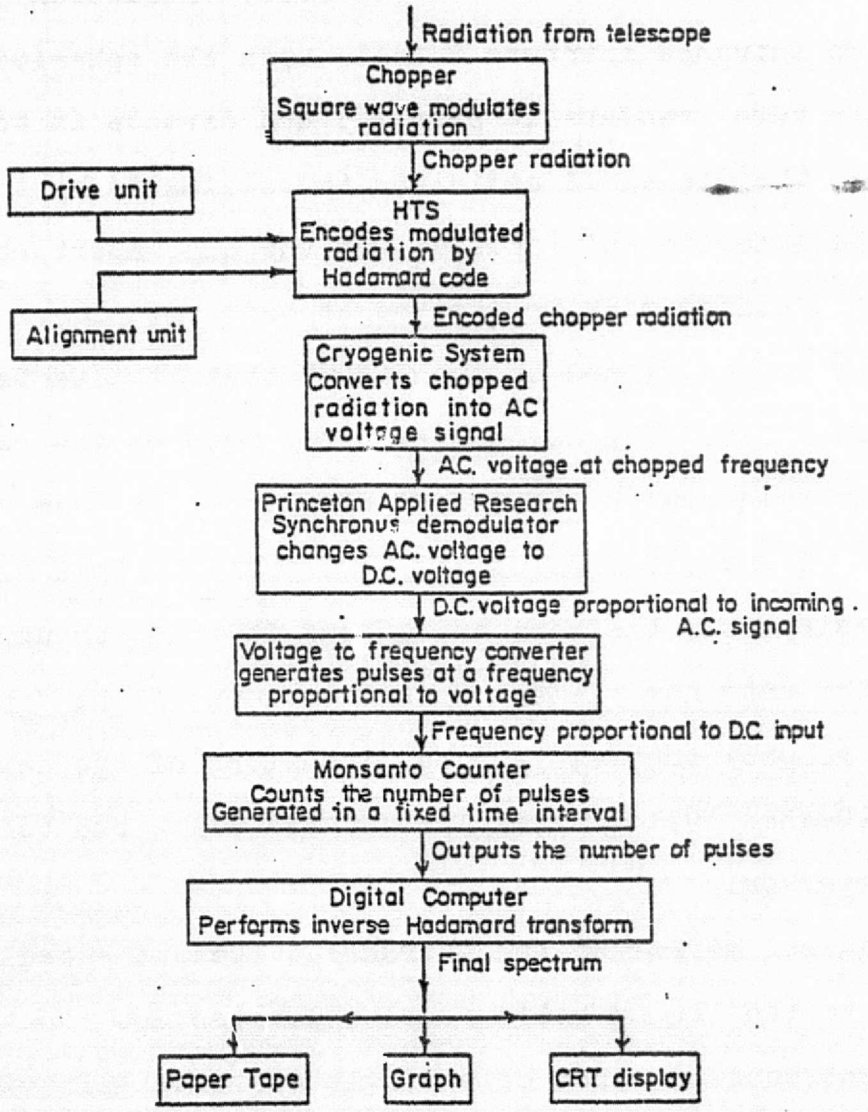

Figure 3-1. The flow chart of the data taking process, starting with radiation from the telescope and ending with the output of the computer.

(B) The Optics

1. Spectrometer

Fig. (3-2) shows the basic spatial design of the spectrometer. It works in the Ebert-Fastie mode. Radiation passing through the entrance aperture S falls upon the spherical mirror M which, in turn, renders it parallel and directs it to the grating G. The dispersed radiation is collimated by the other half of the spheroid and focused upon the exit aperture S'.. A 255-slot encoding mask is located at this position. The exit focal plane is positioned in such a way that it bisects a 90° corner reflection. The corner reflector returns the radiation through the spectrometer again and displaces the beam from the center of the principal plane to one side. This reverse process dedisperses the beam and allows it to be brought to a focus at the entrance plane. The dimensions of the focused image are roughly the same as the dimensions of the entrance aperture (Decker 1971). These procedures allow one to use a smaller detector.

A diagonal mirror at the entrance directs the dedispersed radiation to the liquid helium cooled post optics.

The entrance mask can be a single entrance slit with any width between zero to 1.5 mm for the 1x255 program, or it can be a fifteen S-matrix code with each slit having width 0.1 mm for the 15x255 element program. In normal use the height of of entrance slit is 3.5 mm. It can be increased up to 10 mm.

M_1 is a spherical mirror with a 49.5 cm focal length. On its back it is held in place with three teflon-tippled

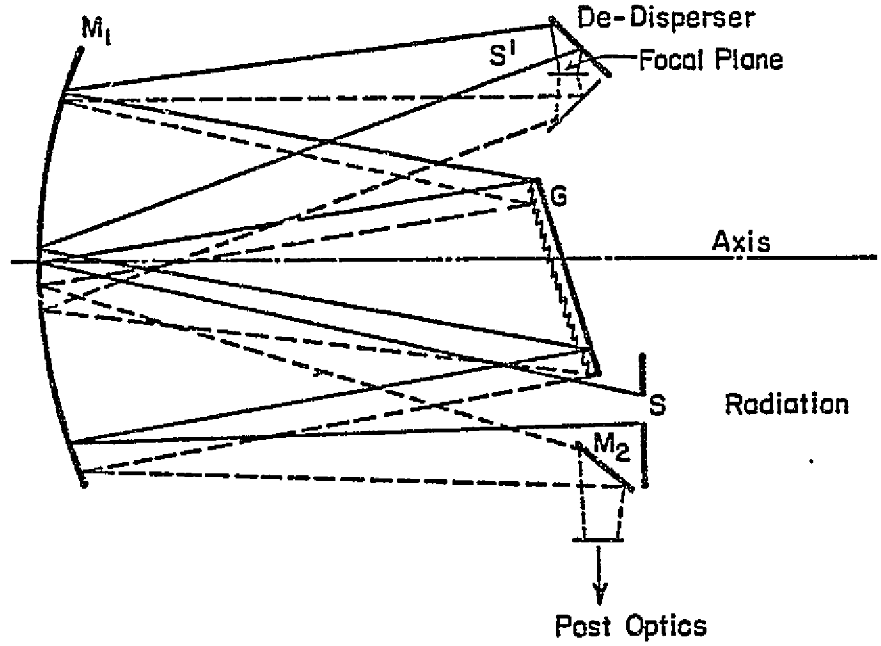

Figure 3-2. Optical path through the spectrometer. The dedisperser and exit mask are shown rotated by 90°.

screws. Three teflon-tippled springs bear on the front edges of the mirror. This design allows one to make slight adjustments in the position of M when aligning the instrument. The central part of the mirror is blocked off to reduce stray radiation.

G is a 75 mm x 75 mm grating with 20 lines/mm and blaze angle $5^{\circ}11'$. The corresponding blaze wavelength at first order is 9.03μ. Figure (3-3) is the calculated grating efficiency as a function of slit position, at two wavelengths. At 8μ the energy imaged within one slit width is 80% of the total. For 14μ the energy within one slit is 52%. The grating is mounted on a yoke which allows it to be adjusted in three mutually perpendicular directions. It is located at 0.82 focal length from the primary mirror M.

All mirrors inside the spectrometer are silver coated with a protective coating of SiO_2. The reflectivity of silver coating at 10μ is better than 97%.

For a multiplexing spectrometer which has N entrance and N exit slits, one wishes to image entrance slits S_1, S_2,....., S_n onto exit slits S_1', S_2',....., S_n' such that S_1 is imaged onto S_1' ,....., S_n onto S_n' at a particular wavelength λ. Let δ be the angle subtanded by S. Where δ and δ' are measured from the center of M. The grating equation for imaging S onto S' is

$$\text{Sin}\,\alpha + \text{Sin}\,\beta = \frac{m\lambda}{a} \qquad (3\text{-}7)$$

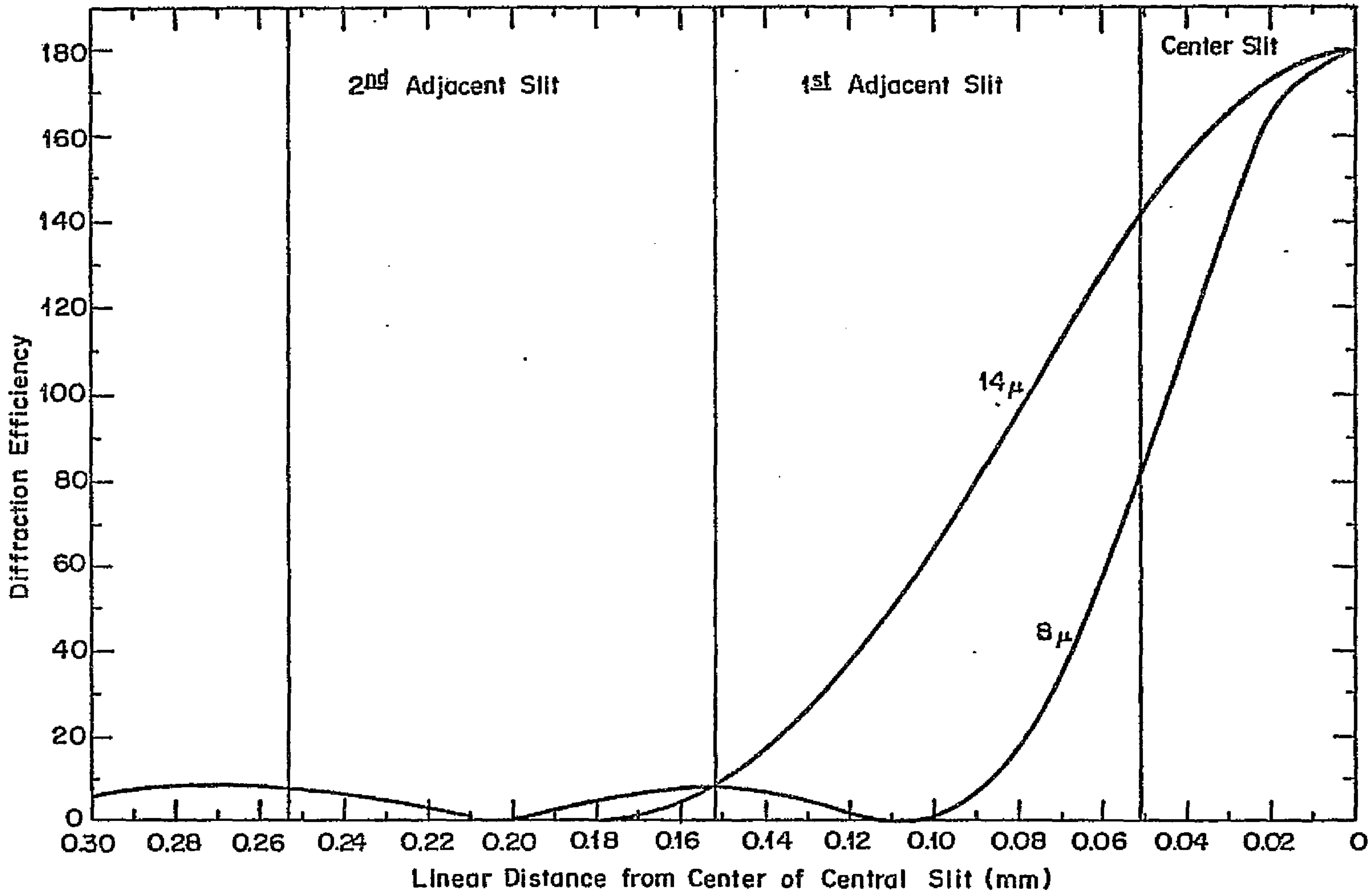

Figure 3-3. Grating diffraction efficiency as a function of slit position at 8 and 14μm.

Differentiating (3-7) with respect to α gives

$$\frac{d\beta}{d\alpha} = -\frac{\cos\alpha}{\cos\beta} \qquad (3\text{-}8)$$

The minus sign indicates that α and β change in opposite directions. $d\alpha$ is the width of the entrance slit and $d\beta$ is the width of exit slit, so $\delta \neq \delta'$ unless $\alpha = \beta$.

In our spectrometer, the exit slit width is 0.1024 mm, 2.4% larger than the entrance slit width. This is the effect of anamorphic dispersion- a magnification produced by the grating (3-8), when the lower limit on the slit width is set by diffraction. The total number of spectral elements that can be observed simultaneously is limited by the optical aberrations of any particular optical system, which set a limit on the total useful width over which the spectrum can be displayed.

2. Post Optics

The post optics consist of a liquid helium cooled Arsenic-doped silicon (As:Si) detector, with appropriate optics for focusing the radiation onto the detector (Fig. 3-4). Radiation enters the evacuated dewar through a barium fluoride window, passing through a filter with pre-selected band-width. The filtered radiation then passes through a cooled barium-fluoride filter and is focused onto the detector inside the housing by a gold coated mirror. A light baffle is partitioned in front of the detector housing.

Below is a brief discussion of each of the cryogenic components

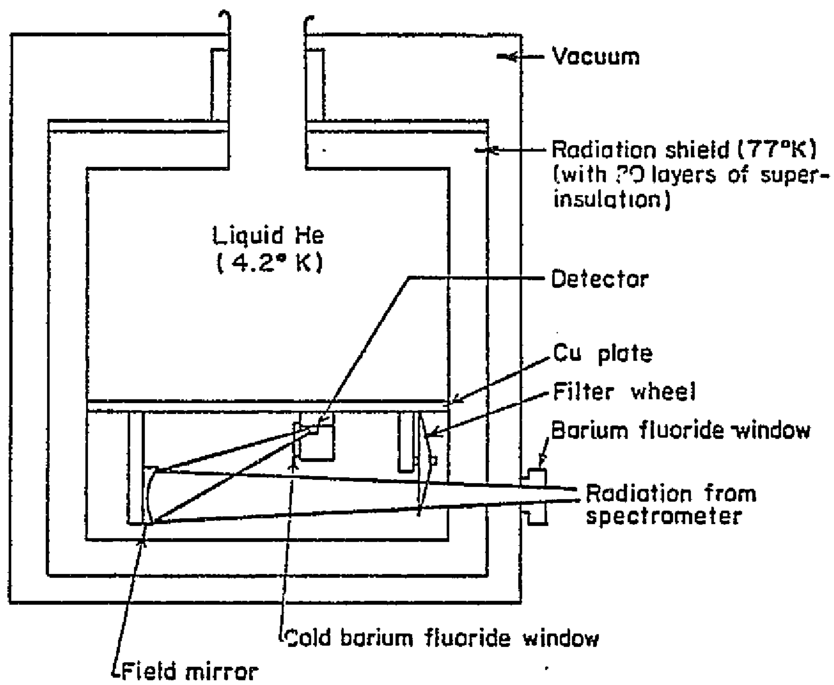

Figure 3-4. Liquid helium cooled post optics.

(a) Barium Fluoride Window

The barium fluoride window is 2 mm thick and 0.75" in diameter. It is used to cut off wavelengths longer than 14μ. It has a transmission efficiency of around 90% out to 11μ before it starts to cut off. At 14.29μ (700 cm^{-1}), its transmission efficiency is 50%.

(b) Filters

A liquid helium cooled filter wheel with 8 filter positions is housed inside the dewar. Table 3-1 gives a brief description of each filter.

Table 3-1

Filter position	Range	Band-width	Peak transmission efficiency
1	no filter		
2	closed (blocked by aluminum foil)		
3	8μ - 9.9μ	1.9μ	71%
4	8.7μ - 11.1μ	2.4μ	83%
5	11μ - 12.4μ	1.4μ	82%
6	11.1μ - 13.8μ	2.7μ	86%
7	8.4μ - 15μ	6.0μ	85%
8	glass	shorter than 2μ	

Filter positions 1 and 2 are for testing purposes.

The filter wheel is held in place by a spring-loaded screw.

The wheel was originally connected to the outside world through a stainless steel rod and could be changed to different positions by turning the rod. It was found that the stainless steel rod conducts too much heat from the outside into the helium containing can. When the stainless steel is replaced by a G-10 Glass Epoxy Lamitex rod, the holding time for the liquid helium of the dewar increases from 9 hours to 15 hours.

(c) Field Mirror

A gold coated mirror with focal length 7 mm and f/0.41 is used as a field mirror to focus the radiation onto the detector. The reflection efficiency for gold mirrors at 10μ is over 99%. The mirror has 3 degrees of freedom of adjustment, one translational and two rotational adjustments.

(d) Liquid Helium Cooled Barium Fluoride Filter

This barium fluoride window is also used to cut off the radiation longer than 14μ . Although the filter barium fluoride window cuts off radiation longer than 14μ from the outside world, it will emit radiation of its own because it is at room temperature. Since all the interference filters have a long wavelength leak between 20μ to 26μ, and since the detector will cut off radiation longer than 24μ only, there is still radiation from 20μ to 24μ that gets into the detector as background radiation. The insertion of the liquid helium cooled barium fluoride filter eliminates this peak. It was found to cut down the background radiation by a factor of four.

(e) Detector

An arsenic doped silicon detector with dimension 1.2 mm x

3.2 mm is positioned inside a housing, which has a baffle at its entrance.

Arsenic doped silicon is a N-type extrinsic semiconductor. When the detector absorbs radiation, free carriers are provided for the conduction band, thus changing the resistence of the detector. The following discussion follows the work of Putley. For further details, one can refer to Putley (1964) and Kittel (1966).

Let σ be the conductivity of the detector

e be the electric charge of the carrier

τ be the life time of free carriers

N be the density of free carriers, and

μ be the mobility of free carriers

Then,

$$\sigma_D = NeP\mu \qquad (3\text{-}9)$$

and

$$\Delta\sigma_D = \Delta J e\tau\mu\eta$$

$$= \frac{\Delta P}{h\nu} e\tau\mu\eta \qquad (3\text{-}10)$$

where

$\Delta\sigma_D$ is the change in conductivity of the detector

ΔJ is the number of photons incident in unit time

ΔP is the radiation power incident

ν is the frequency of the incoming photons, and

η is the quantum efficiency, i.e. nmuber of electrons freed per photon.

Since

$$R_D = \frac{1}{\sigma_D} \frac{\ell}{A} \tag{3-11}$$

where R_D is the resistance of the detector

ℓ is the length of the detector, and

A is the area of the detector

Then

$$\Delta R_D = - \frac{\ell}{A} \frac{\Delta \sigma_D}{\sigma_D^2}$$

$$= - \frac{\ell}{A} \frac{\Delta P}{h\nu} \frac{\eta}{N^2 e \mu \tau} \tag{3-12}$$

Let

$$I_D = \frac{V_B}{R_D} \tag{3-13}$$

where I_D is the detector current, and

V_B is the bias voltage across the detector

Then

$$\Delta I_D = - \frac{V_B}{R_D} \Delta R_D$$

$$= \frac{V_B}{R_D} \frac{\ell}{A} \frac{\Delta P}{h\nu} \frac{\eta}{N^2 e \mu \tau} \tag{3-14}$$

Let

$$V_o = I_D R_L$$

$$= \frac{R_L}{R_D} V_B \tag{3-15}$$

where V_o is the voltage across the load resistor

R_L is the load resistance

Then

$$\Delta V_o = \Delta I_D R_L$$

$$= R_L V_B \frac{\Delta P}{h\nu} \frac{A}{\ell} \eta e \mu \tau \qquad (3\text{-}16)$$

From equation (3-16) one can calculate ΔP from ΔV_o.

(f) Procedures for Alignment of the Optics

i) Place all components in their respective positions and line them up visually. Be sure there is no mechanical binding in the mask and in the driving mechanism.

ii) Using a laser, put the spot from the entrance slot on the middle of the grating. It is suggested that only one entrance slot be used.

iii) Adjust the grating tilt until the line of dispersed dots exits at the proper position at exit. As the grating is rotated, this line of spots should remain level, not displaced normal to itself.

iv) Put one half of the dedispersing mirror combination in place. Use a T square to line it up roughly. At this point, use a mercury emission lamp with proper f-number to simulate the beam coming from the telescope. A number of colored image of the single entrance slot will be seen at the exit.

v) Adjust the spherical mirror for coarse adjustment and the position of the dedispersing mirror as a fine adjustment to bring the image to a focus on the exit plane.

vi) Adjust the grating position in its yoke until the color image from the mercury lamp is parallel to the exit slit length.

vii) Adjust the angle of the dedisperser so that the color image reflected by it is perpendicular to the exit mask.

viii) Put in the other half of the dedisperser and line it up at an angle so the radiation falls back upon the grating. Adjust with fine adjustment screws so the grating is fully illuminated. The image of the grating will appear on itself when viewed from the diagonal, 45°, mirror which diverts the radiation to the dewar.

ix) Place the dewar on the spectrometer using ¼" spacers to represent the thickness of the dewar bottom cover. Adjust the 45° mirror so that the dedispersed image (with color) falls on the center of the filter on the filter wheel.

x) Turn the filter wheel to position one (no filter), so that radiation can fall on the field mirror. Adjust the field mirror until the dedispersed radiation impinges upon the detector. Be sure that all the light falls onto the detector. Be sure that the mirrors accept all the radiation.

xi) Insert the housing. Be sure that the incoming radiation is clear of the housing.

xii) Put in the liquid helium shield, and the radiation shield. Put on the nose. Use GE varnish and aluminum foil to reduce openings in the baffles so that they will transmit only the bright white fringes.

xiii) When the spectrometer is on the telescope, maximize the signal by tilting and rotating the dewar.

(C) The Electronics

The data-taking process is controlled electronically to ensure a smooth process. The operator only needs to turn the switch on. The spectrometer will then automatically take date in, process it, and stop at the end of the transform indicated by the operator. All the operator has to do in the whole observation is to keep the astronomical object in the beam. Figure 3-5 shows the block diagram of electronic and computer set up. The following are brief descriptions of the electronic parts incorporated in the system.

1. Alignment Sensor

The alignment sensor (figure 3-6) is used to synchronize a Monsanto electronic counter, and the computer with the spectrometer. The circuit is shown in figure (3-6). The exit mask is continuously moving. When the exit mask is at its starting position, i.e. the first 255 slots are at the exit aperture, a light pulse goes through an alignment slot on the exit mask and is detected by a photo-cell on the other side of the exit mask. Two transistors amplify the output light curve and two IC chips change the light curve into an alignment pulse. This alignment pulse, through the drive unit, readies the counter for counting, readies the computer to accept data, and to turn on an indicator light showing that the system is taking data. One can adjust the starting position of the exit mask by adjusting the intensity of the light. After 255 data points have been obtained, the exit mask is at its other end, and another alignment pulse turns off the counter and the indicator light.

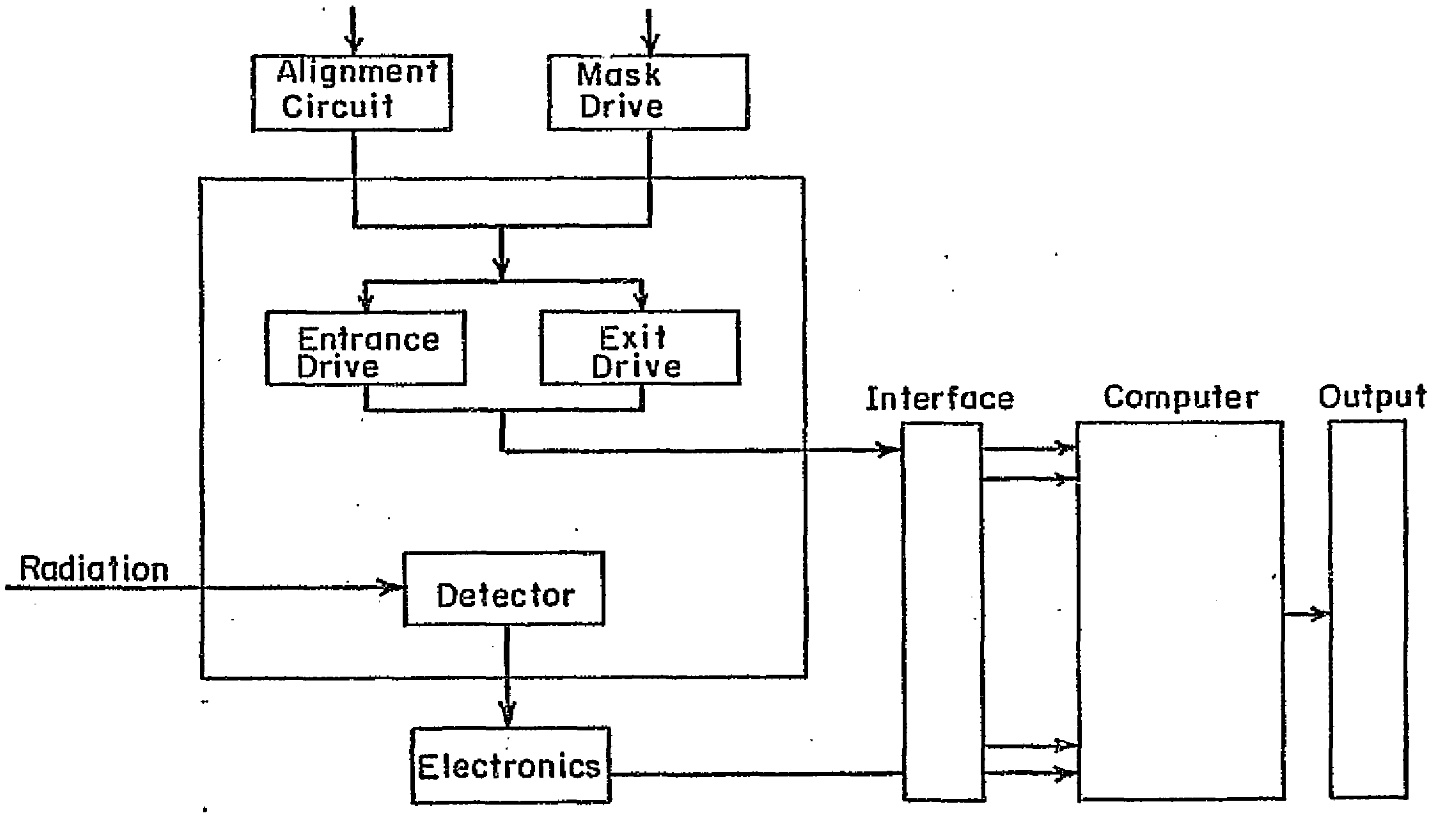

Figure 3-5. HTS drive unit block diagram.

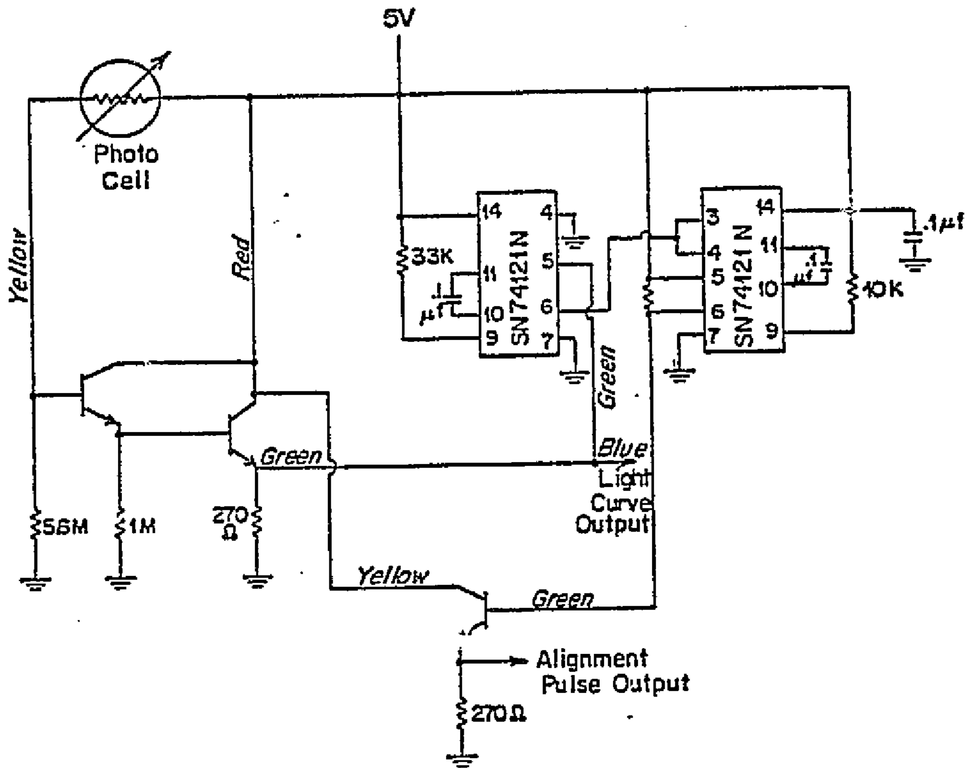

Figure 3-6. HTS alignment circuit.

The computer after taking 255 readings checks that the indicator light is off. This step ensures the synchronization of computer and spectrometer.

2. Drive Unit

A drive unit (Fig. 3-7) is used to drive the entrance and exit masks of the spectrometer. It can be set to be adjusted by pulse streams at 100 Hz, 200 Hz, or 400 Hz. The unit performs the following functions:

(a) It receives an alignment pulse from the sensor circuit(18) and generates a pulse to reset the counter for counting(17). The pulse will also ready the computer for taking the data.

(b) It drives the exit mask in a continuous mode at a displacement rate of one slot for every 41 pulses(18).

(c) After each set of 41 pulses the unit instructs the the mini-computer to read the integrated signal off the counter and then reset the counter for the next data integration.

(d) After 255 reset pulse the unit advances the entrances mask by one slot by sending the entrance mask advance motor 40 pulses (11).

3. Preamplifier

The circuit (Fig. 3-8) shows a transimpedance amplifier implemented with a Burr Brown operational amplifier. The circuit has the advantage of high speed, low susceptibility to microphonics, and detector operation at constant voltage with a high resistance load resistor.

Neglecting the voltage noise and current noise in the

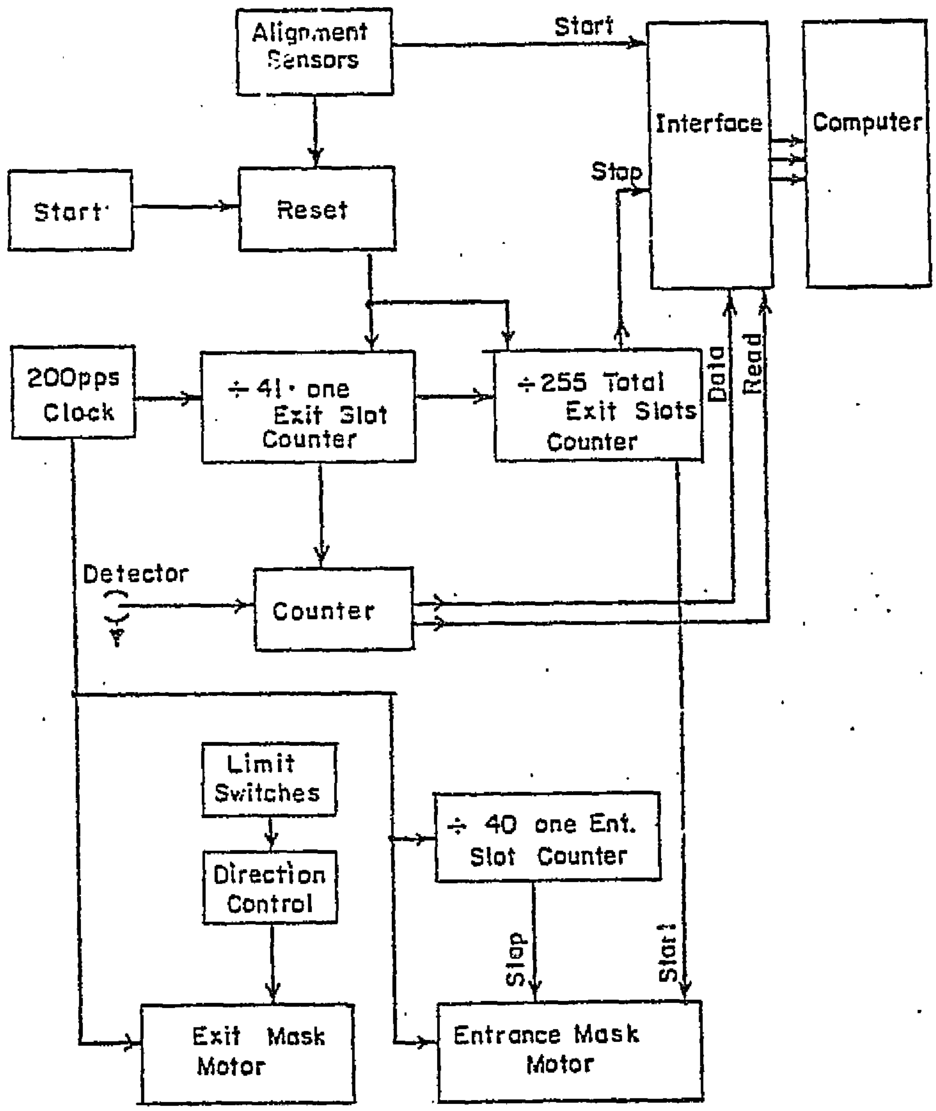

Figure 3-7. Logic diagram for mask motion and data processing.

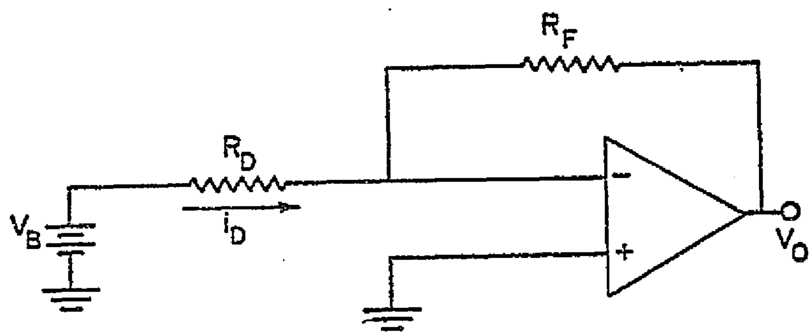

Figure 3-8. Basic detector bias and preamplifier circuit.

first order approximation, the current through the detector, I_D, also goes through the load resistor R_F because the input impedance of the operational amplifier can be taken to be very large, so

$$V_o = I_D R_F$$

$$= V_B \frac{R_F}{R_D} .$$

where V_o is the output voltage,

V_B is the constant bias voltage, and

R is the load resistance

(D) Laboratory Calibration

1. Calibration of Post Optics

Liquid nitrogen is used to calibrate the efficiency and sensitivity of the post optics. Liquid nitrogen is in a dewar with black paper along the wall to simulate a blackbody. Through a chopping device, the post optics will alternately see radiation from the liquid nitrogen and from the room. The difference between these two radiations gives the A.C. signal. D.C. measurements are obtained by putting liquid nitrogen directly in front of the dewar window. The following are the results of the calibration:

Dewar profile:	f_H = 7.6
	f_V = 10.3
Wavelength region:	8.7μ - 11.1μ

Band-width:	2.4μ
Bias voltage:	15μ
Load resistor at LH_2 temperature:	1.2 MΩ
A.C. power:	9×10^{-10} watt.
A.C. signal:	272.7 mv
A.C. noise:	4.4μv
(NEP) A.C. detector:	$5.2 \times 10^{-13}\ H_z^{\frac{1}{2}}$
(NEP) A.C. system:	$1.25 \times 10^{-12}\ H_z^{\frac{1}{2}}$
A.C. responsivity:	1.2 amp/watt.
D.C. power:	3.05×10^{-6} watt.
D.C. signal:	11.32V
D.C. noise:	4μv
(NEP) D.C. system:	$1.47 \times 10^{-12}\ H_z^{\frac{1}{2}}$
D.C. responsivity:	2.58 amp/watt.
Background noise:	$NEP_{Blip} = \sqrt{2\ P_{BG} h\nu}$
	$= 3.5 \times 10^{-13}$

where P_{BG} is the D.C. power

ν is the frequency that is assumed to be $10H_z$.

The system is a factor of 3.57 away from background limited.

2. Test of the Spectrometer

A mercury vapor lamp with emission at 1.7μ is used with the spectrometer to test the computer program. A PbS detector and an appropriate blocking filter isolates the 1.7μ doublet of mercury. The slit width and length for each mask is 0.15 mm and 3.5 mm. Fig. (3-9) is the mercury vapor spectrum at 1.7μ for the 1 x 255 mode. Fig. (3-10) is the mercury vapor spectrum

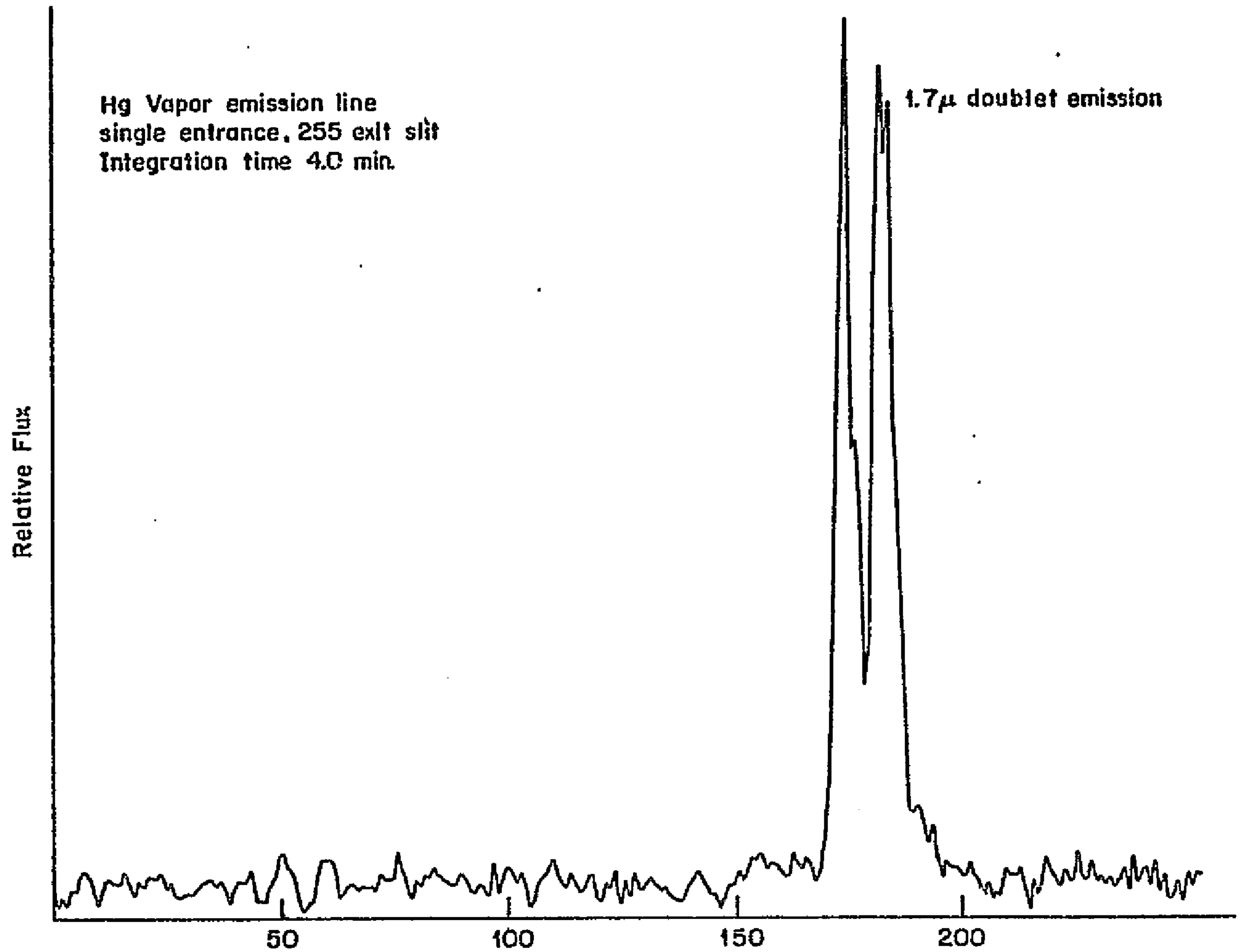

Figure 3-9. Spectrum of the mercury vapor 1.7μm line using the 1x255 mode.

for 15 x 255 mode. Figure (3-10a) shows the eighth of a series of fifteen individual spectra. Figure (3-10b) shows an average of all fifteen spectra, and (3-10c) shows all 15 spectra, each spectrum being displaced vertically from the next. The diagonal pattern near the right-hand edge represents a displacement of the peak between successive spectra. This represents the actual shift in spectral range between adjacent spatial elements.

Once it was clear that the instrument with the computer program worked properly in the 1.7μ region, the spectrometer was tested with the cryogenically cooled, arsenic-doped silicon detector. The transmission spectrum of polystyrene with a soldering iron as the source was obtained. The shap e of the filter profile and the transmission spectrum of polystyrene showed that the instrument worked in the 10μ region.

The wavelength calibration of the spectrometer is obtained by comparing the polystyrene transmission spectrum obtained by the spectrometer and the spectrum obtained by a Perkin-Elmen monochromator. The wavelength calibration is then checked against the moon spectra at 9.5μ where the atmosphere has strong absorption features.

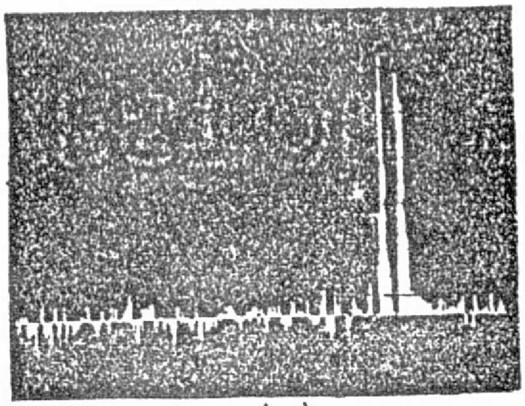

(a)

Figure 3-10.
Calibration spectra obtained for the mercury vapor emission lines at 1.69μm and 1.71μm: (a) The eighth of a series of fifteen individual spectra obtained;

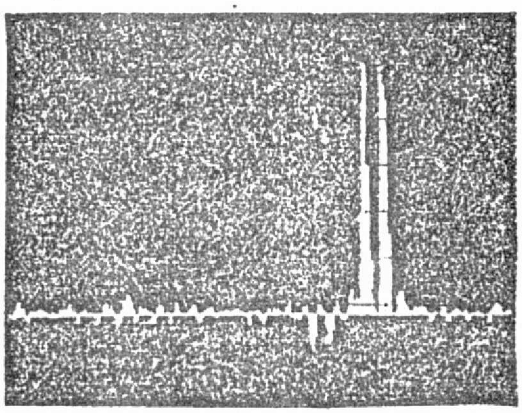

(b)

(b) An average of all fifteen spectra;

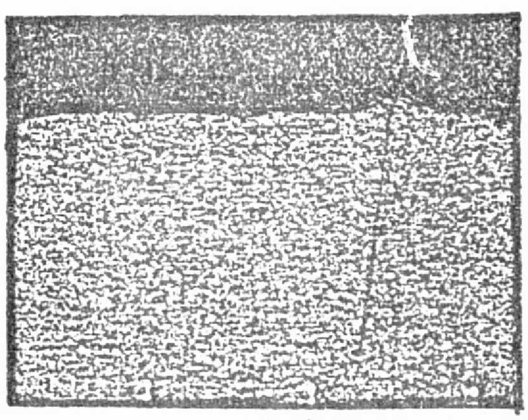

(c)

(c) A display of the fifteen spectra, each spectrum being displaced vertically from the next. The diagonal pattern near the right-hand edge represents a displacement of the peak between successive spectra. This represents the actual shift in spectral range between adjacent spatial elements.

CHAPTER IV

COMPARISONS BETWEEN FOURIER TRANSFORM AND HADAMARD TRANSFORM SPECTROSCOPY

Since the Michelson interferometer spectrometer (MIS) and Hadamard transform spectrometer (HTS) both have the multiplex advantage and the advantage of large through-put, there are a number of comparisons between them in the literature. In this chapter the comparisons are carried out in four different aspects: mathematically, computationally, optically and mechanically.

(A) Mathematically

Fourier transforms and Hadamard transforms can be viewed as using two different weighing schemes. Appendix A gives the mathematical analysis of the coding error for Fourier transform.

Let ξ be the path difference in a two beam interferometer. $P(\nu)$ is the power at wave number ν (i.e. the spectral density function). ν here is taken to be the inverse of wavelength, then $S(\xi)$, the power received for path difference ξ, is:

$$S(\xi) = \int_0^\infty P(\nu) \cos^2(2\pi\xi\nu)d\nu \quad . \qquad \text{A-1}$$

$$= 1/2P_o + 1/2\int_0^\infty P(\nu) \cos(4\pi\xi\nu)d\nu \qquad \text{A-2}$$

In the Fourier transform each spectral element can be viewed as having a phase modulation by a cosine squared term. Its argument depends on the stepped distance and the particular wavelength. In the Hadamard transform each spectral element is modulated by a step function of 1 and 0 for a S-matrix coding.

One can ask oneself whether these modulating or encoding schemes are equally efficient?

In table 2-1 we stated that for large N the multiplex advantage, or the efficiency, of the H-matrix coding of elements 1 and -1 is $\sqrt{N}$, the S matrix coding of element 1 and 0 is $\frac{\sqrt{N}}{2}$, and for a single detector MIS the Fourier coding is $\sqrt{N/8}$. This last figure is based on calculations shown in Appendix A. The other two values were described by Sloane et al (1968). The H-matrix is an orthornormal matrix. The element -1 means "subtract" the radiation, while the +1 element means "add" the radiation. No radiation is wasted and thus the coding scheme has the highest efficiency. For S-matrix coding half the slits are open, 1, letting light pass through; and half the slits are 0, blocking the light. Half the radiation is therefore wasted each time and one can intuitively see why the efficiency of the S-matrix is only half that of the H-matrix.

Although the S-matrix is less efficient, it has the important advantage that it is cyclic; that is, the $(i+1)^{th}$ column of the S-matrix is obtained by shifting the i^{th} column cyclically one place downwards. Instead of constructing a mask of N^2 slits for N spectral elements, one constructs only one mask with 2N-1 slits. Such a mask has two advantages. First, the cost of mask construction is reduced by $\sim N/2$ and the design of the advance mechanism is considerably simplified, since the total weight of the mask also decreases as $\sim N/2$. Secondly, it can be self-supporting and therefore permits the construction of a spectrometer which requires no transmission materials. In operation the mask is stepped one slit width - along the length of the mask- for each successive encoding position.

In the Fourier case, equation (A-2) of Appendix A

$$S(\xi) \quad = \quad 1/2P_o + 1/2\int_0^\infty P(\nu)\cos(4\pi\xi\nu)d\nu \qquad \text{(A-2)}$$

shows that half the power goes into $1/2P_o$, the first term on the right hand side, which is not modulated at all. This reduces the efficiency by a factor of two as in the S-matrix case. The other half of the power is modulated by a cosine term. Cosine modulation gives a factor $1/\sqrt{2}$ because cosines functions do not form an orthronormal set themselves. The total Fourier modulation efficiency is therefore $1/2(\sqrt{N}/2)$. Mathematically, the S-matrix is a factor of $\sqrt{2}$ better in SNR than the Fourier transform. The true Hadamard code, which cannot be realized experimentally, as yet, is a factor of $\sqrt{8}$ better that the Fourier code.

(B) Computer Requirements

Both MIS and HTS require a digital computer to decode the data. However, in the HTS case this reduces to nothing more than a series of additions and subtractions. Hence, as much as an order of magnitude in computer time can be gained over the Fourier decoding procedure required by MIS (Decker, 1971). In addition, HTS do not have the large zero path-length spike which is characteristic of MIS, and hence can be operated with a substantially lower dynamic range.

(C) Optics

HTS attempts to "liberate" the grating instrument from its inferior position and offers a possibility to convert a conventional scanning spectrometer into a multiplex instrument at a moderate cost. However, it is also the grating and optics that limit the capabilities of HTS.

1. Resolution

The resolution of a grating instrument is

$$R = \frac{\lambda}{\Delta\lambda}$$

$$= mN \quad (4\text{-}1)$$

$$= m\frac{W}{d} \quad (4\text{-}2)$$

where m is the order of diffraction. N is the total number of rulings in the grating. W is the width of the grating. d is the separation of lines.

The MIS introduces variable path differences between two interfering beams. The resolution is determined by the maximum permissible path difference in the interferogram.

$$\Delta\nu = \frac{1}{2x} \quad (4\text{-}3)$$

$$= \frac{1}{4\xi} \quad (4\text{-}4)$$

where x is the maximum path difference between interfering beams.

ξ is the displacement of one of the two mirrors from the white light fringe position, and

$\Delta\nu$ is the increment in wavenumber.

Since

$$R = \frac{\lambda}{\Delta\lambda}$$

$$= \frac{1}{\lambda\Delta\nu} \qquad \text{(Mertz a, P.5)}$$

$$\doteq \frac{2x}{\lambda} \qquad (4\text{-}5)$$

A MIS can have a resolutuion as high as $\sim 10^6$.

2. Slit Width

In the HTS, the minimum usable slit width is determined by the diffraction pattern

$$w \sim \frac{\lambda}{W} F \qquad (4\text{-}6)$$

where F is the focal length of the imaging mirror.

It has been argued that a boxcar profile is a poor match to a sine diffraction pattern(Hirschfeld, et al, 1973, Mertz, 1976 b). In the presence of diffraction, the transmission at each point of the mask will be a complex function of the spectral distribution, the mask position, and the relative width of the nearby transparent and opaque slits.

One way to correct this is to make the slits, wider than the diffraction limit, allowing the mask's transmission to approach the geometric optical limit. This way, however, not only the resolution of the instrument is reduced, but the total number N of spectral elements that can be observed simultaneously, also decreases.

There is another way to look at the same problem. The grating is an operator that changes the frequency domain into the spatial domain, so that intensity as a function of frequency, after passage by the grating, becomes a function of position. With diffraction effects included, the intensity has a new functional dependence on distance. The Hadamard mask code and the subsequent decoding process just translate this spatial distribution function back into its spectral domain. Therefore, an intensity pattern which is complicated by the diffraction pattern, after the Hadamard coding and decoding, should still show up the same intensity pattern. Since one knows the diffraction pattern for a given optical system, the diffraction effect on the spectral intensity distribution can be computed and corrected, so that the sine^2 diffraction effect would not make the slit width any larger than the diffraction limit. One point, however, should still be noted. The correction that would have to be applied is wavelength dependent because diffraction is wavelength dependent.

A similar problem exists in MIS (Stewart P.296) because the moveable mirror must be stopped when its maximum displacement is reached.

The sidelobes in the interferometric case is of the form

$$S(\omega') = \frac{\sin(\omega-\omega')T}{\omega-\omega'} \qquad \omega \simeq \omega' \qquad (4\text{-}7)$$

(Stewart P.295)

which has considerably stronger side lobes than the diffraction pattern. Here, T is the time for the mirror to travel from one end to the other, and ω is the central frequency. Various schemes of apodization have been introduced to compensate for the side lobes in the interferometric case.

3. Multiplex Number

The total number of elements N that can be observed simultaneously yields the multiplex advantages. In HTS, the total aperture size is limited by aberrations largely due to off axis radiations. The aperture width is (Hirschfeld, 1973)

$$w = F \cdot S_w \qquad (4\text{-}8)$$

where F is the instrument focal length and $S_w/2$ is a factor of the order of $0.05 \sim 0.1$, that describes how far off axis one can go before the aberration pushes the individual slit width up to the point where no further gain in N is possible. Since the minimum slit width, determined by diffraction effects, is $\sim 1.22\lambda f$, the total number N is

$$N = \frac{FS_w}{1.22\lambda f} \qquad (4\text{-}9)$$

and is of the order of 10^3.

For our HTS at Cornell, we have

$$F = 49.5$$

$S_w \sim 0.08$ (assume $\sim$ medium value)

$\lambda = 10.0\mu m$

$f = 7.5$

$N \sim 250$

Actually, however, Mertz and Flamand (1976) suggested that S_w values $>>0.1$ may be realized in practice.

The MIS has a very large effective value of N. This is its main gain. The total wave number range observed in MIS is

$$\nu_{max} - \nu_{min} = \frac{1}{4\Delta}$$

$$= \frac{1}{4\Delta\delta}$$

where Δ is the step size of the mirror, σ is the resolution in wave number. N for the MIS can be 10^6.

4. Spectral Range

The MIS also has a broad free spectral range. Its range is limited by the beam splitter efficiency which usually varies approximately as the cosine of the wavelength. HTS free spectral range is usually about one grating order. Its free spectral range can be increased by using order sorting, but this increases the technical difficulty. Although the HTS has a smaller spectral free range, it can be set to recover only those spectral bands of particular interest throughout any spectral regions (Decker, 1971). This is impractical with a MIS.

5. Throughput

The throughput is defined in section 1-A as the product of aperture A and angular acceptance Ω

$$E = A\Omega$$

For a MIS it can be shown that $\Omega R = 2\pi$ and

$$E_{MIS} = A_m \cdot \frac{2\pi}{R}$$

where R is the resolution of the instrument. A_m is the area of the interferometer mirror. Typically, $A \sim 1$ cm^2, and for $R \sim 10^3$, $E_{MIS} \sim 6 \times 10^{-3}$.

For the HTS, from equation (3-1) one obtains

$$E_{HTS} = A_g \left(\frac{w \cdot h}{F^2}\right)$$

where h and w are slit height and width and F is the focal length. For a double multiplexed spectrometer, the throughput of MIS and DHTS are about the same, of the order 10^{-2} cm^2. For the same throughput, the HTS may have a worse system transmission because the HTS requires a dedispersing process.

DHTS has the additional advantage that one can construct a one dimensional picture of the source.

(D) Mechanical Requirements

The HTS mask can be made self-supporting hence no beam-splitters or transmission optics, are required. Furthermore, in the MIS, construction tolerances usually involve dimensions and motions that have to be maintained to within fractions of wavelengths. For a HTS, the corresponding tolerances are fractions of a slit width, and these tolerances are normally two orders of magnitude more relaxed, so that this instrument will be more suitable for rugged applications and less costly.

It is clear from the above comparison that the MIS has the advantages of highest resolution, very large multiplex number and free spectral range. The HTS has the mechanical advantages and computational advantages for large N. The HTS can have on the order of 10^3 spectral elements and a resolution sufficient to resolve the rotational lines of many molecules. For most IR astronomical observations this will be sufficient. Furthermore, its potential for modifying the existing sacnning spectrometer at a moderate cost make this a very worthwhile field for further study.

CHAPTER V

PROGRAMMING FOR HADAMARD TRANSFORM SPECTRAL DATA REDUCTION

An 8K Computer Automation minicomputer model L.S.I. or model Alpha-16 can be used to interface with the output of a Monsanto scalar counter which digitized the output of the detector used with the Hadamard transform spectrometer. The computer processes each data point as soon as it receives it and when the data gathering run is completed, the computed spectrum is also ready within a fraction of a second. The final spectrum can be displayed on a cathode ray tube for quick visualization, or printed on paper by a teletype machine for more detailed analysis. Also, it can be stored on paper tape for future use.

There are two inverse transformation programs: 1 x 255 for the single entrance slit and 255 exit slit Hadamard transform spectrometer, HTS, and 15 x 255 for the 15 entrance slit and 255 exit slit instrument, DHTS.

(A) HTS Program

The inverse HTS program processes the raw data obtained by the combination of a single entrance slit and 255 exit slit. This program is in double precision format. Two areas in the memory are reserved by the program to store the final spectrum. The final spectrum can be stored in either the plus beam or the minus beam area. The plus and minus beams are arbitrarily named.

Data can come in at a rate of 10 data points per sec., 5 data points per sec., or 2.5 data points per sec., depending on how the clock driving the spectrometer is set. Since a complete pass has 255 points, each pass takes 25.5 sec., 51 sec., or 102 sec., depending on the data rate. Each pass yields one spectrum. One can take as many passes as one wants until one is satisfied with the SNR of the spectrum.

The whole program (Appendix B) is linked by the following subprograms: COMMAND, TRANSFORM, INPUT/OUTPUT, READ, CLEAR, PUNCH, GRAPH, DISPLAY, MATHMATICAL PACKAGE and MASK. The function of each subprogram is described briefly in the following sections.

1. COMMAND: This subprogram performs two functions. (a) It commands the computer to do one of the following functions: TRANSFORMATION, CLEAR, READ, PUNCH, GRAPH or DISPLAY. (b) If two distinct spectra are stored in two different beam areas, the COMMAND program can take the difference and ratio of the two spectra.

2. INVERSE TRANSFORM: This is the most important subprogram in the whole program. It will take data points from the counter, transform them and enter them into either the plus or minus beam areas, or it will read the data points from the paper tape into one beam area, transform them and enter them into the other beam area. This program is called the inverse transform, since it inverts the transformation performed by the coding mask, and

yields a spectrum. The program also performs the Hadamard transform, i.e. transforms the spectrum back to raw data, from either input.

The algorithm is based on the following idea: Let ψ_j be the j^{th} spectral element and w_{ij} be the weight of the j^{th} element of the i^{th} mask. w_{ij} equals 1 for transmitted radiation and 0 for blocked radiation. Each measurement then has a value

$$\eta_i = \sum_{i=1}^{255} S_{ij}\psi_j + \nu_i$$

where ν_i is the random detector noise satisfying the properties mentioned in Section II-B. $\underline{S}$ is the 255 x 255 matrix. η_i is the i^{th} data point entered into the computer. The computer's job is to decode η_i to reconstruct the original spectral values ψ_j. Therefore

$$\hat{\psi}_j = \sum_{i=1}^{255} S^{-1}_{ji}\,\eta_i$$

where $\hat{\psi}_j$ is the unbiased estimate of ψ_j and $\underline{S}^{-1}$ is the inverse of the S matrix.

According to the relation

$$\underline{S}^{-1} = \frac{2}{N}(2\underline{S} - \underline{J})$$

one obtains $\underline{S}^{-1}$ by keeping all +1's in the S-matrix and replacing all 0's by -1. The matrix obtained in this way is the inverse matrix of $\underline{S}$ except for a constant factor $\frac{2}{255}$, which only gives a different normalization.

To reconstruct the spectral values ψ_j one needs to add or subtract each measured value to n_i different bins, according to whether $\underline{S}^{-1}$ is plus or minus. Fig. (5-1) is a flow chart for the 1 x 255 transform program.

By a Hadamard transform we mean a program that transforms the spectrum back to its raw data*. This procedure is useful because by inspecting the raw data display which usually appears quite smooth, any bad data point can be easily identified, and for example, replaced by the average of its two adjacent data points. This procedure will improve the final spectrum.

The Hadamard transform turns out to be extremely easy. All one has to do is to change one statement in the inverse transform program. When S_{ij}^{-1} is -1, instead of negating the data, one just sets it to zero.

Data points are taken both with the exit mask moving in a forward and in a reverse direction. The inverse transform program takes care that when the exit mask moves in the forward direction, the spectrum is transformed into the plus beam area. When the exit mask moves in the reverse direction, the final spectrum is stored in the minus area. Not adding the

---

* The notation here may be a bit confusing. We use the $\underline{S}^{-1}$ to transform the raw data into an intensity spectrum. The inverse transform uses $\underline{S}$ to transform the intensity spectrum back into raw data.

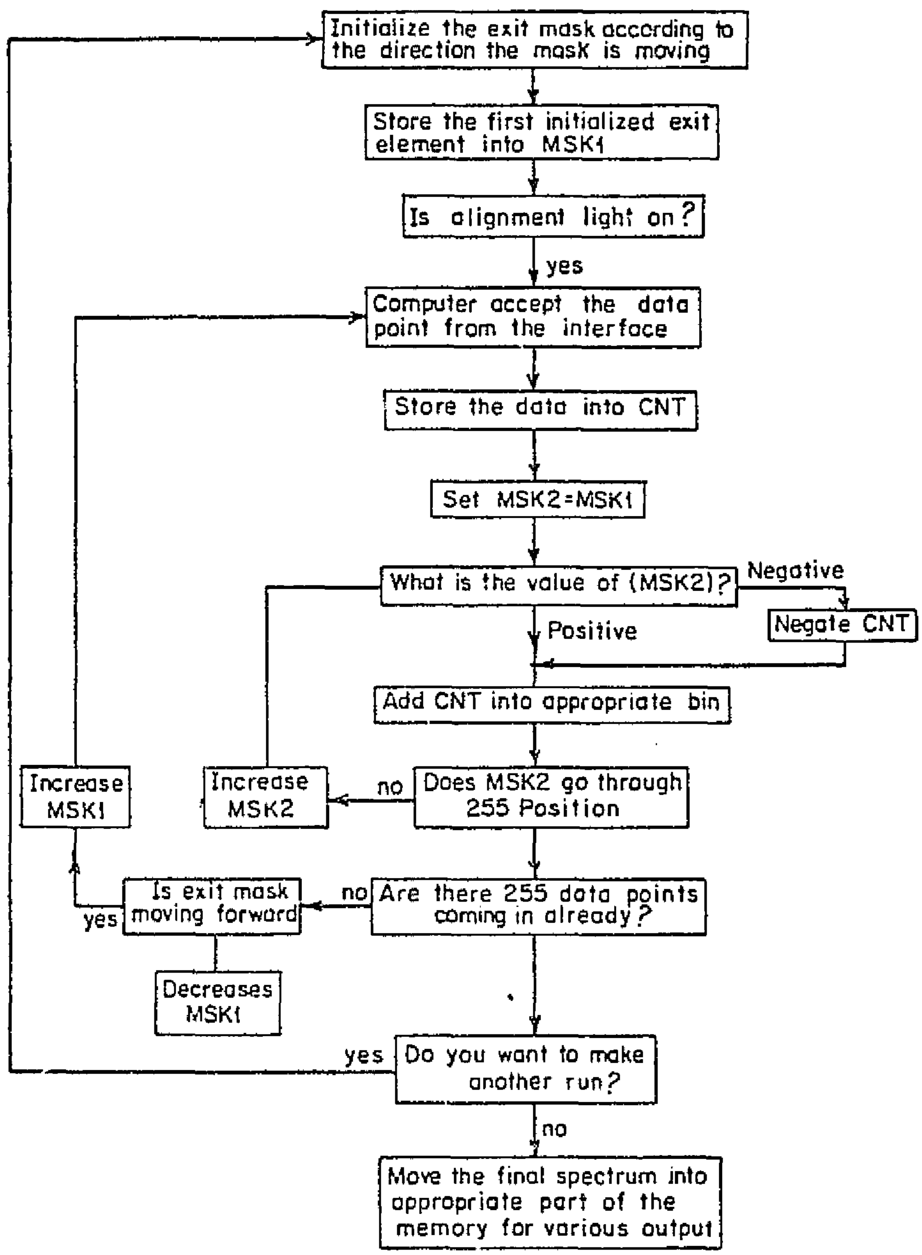

Figure 5-1. The flow chart of the 1x255 inverse transform program.

forward and backward spectrum eliminates a degradation of the final spectrum due to any asymmetry between the data taking for different directions of motion of the mask.

3. INPUT/OUTPUT: This program links up the computer, the teletype and high speed reader. It consists of the following functions: Keyboard Input, Paper Tape Input, Output to Teletype, Output Text from Buffer, Output Floating Point Number, Wait for Execute Signal, Command Error Exit, Carriage Return-Line Feed.

4. READ, CLEAR, PUNCH: This program reads the spectrum from the paper tape into either plus or minus beam areas for further maniputton, or punches the spectrum out from the beam area; it also can clear the beam area. The speed of teletype for reading is 100 words per sec. Hence it takes about 12 min. to read the spectrum. Punching has the same rate.

5. GRAPH: This program plots the graph on teletype paper, with its numerical value in floating point format. This procedure offers one the chance to inspect the spectrum in detail if it is needed. It takes about fifteen to twenty minutes to finish a spectrum, depending on the complexity of the spectrum.

6. CRT: A cathode ray display is interfaced with the output of the computer. It takes about 2 sec. to display the spectrum, with a factor of 5 higher resolution than the graph printed by the teletype on paper. One can display the spectrum at the end of any pass to see how good it is.

7. MATHMATICAL PACKAGE: This package is supplied by the Computer Automation library tape, with a little modification

from our own on its double precision part.

8. MASK: This part contains the $\underline{S}^{-1}$ matrix, the 255 elements exhibited in the first mask position plus an additional 254 elements representing the further cycling of this mask.

(B) DHTS

The doubly encoded Hadamard transform program processes the data obtained by the various combinations of fifteen entrance slots and 255 exit slots. It is a single precision program. It can accept data at a rate of 5 data points per sec. and 2.5 data points per sec. onl[illegible] because it takes a longer time to process each data p[illegible] the whole transform takes about 14 minutes. The final [illegible]um consists of 15 separate spectra, representing a one-dimensional color picture across the spectrometer entrance aperture. Each separate spectrum contains 255 spectral elements. The program can co-add all fifteen separate spectra yielding a sum spectrum with improved SNR.

The program consists of the following subprograms: COMMAND, TRANSFORM, DATA, INPUT/OUTPUT, READ, CLEAR, PUNCH, GRAPH, DISPLAY, ENTRANCE MASK, EX[illegible]ppendix C). Since most of the subprograms are [illegible] the same function as their counterpart in the 1 x 255 [illegible]pt written in single precision format, their descr[illegible]ll not be repeated here. Only the TRANSFORM, DATA, and [illegible] programs will be discussed because they are different from those in the 1 x 255 scheme.

1. INVERSE TRANSFORM: The program can accept data eigher from the counter or from paper tape. In order to eliminate any asymmetry due to the different directions of motion of the exit mask, the computer will accept data only when the mask is moving in a given direction, either forward or backward, depending on the operator. If one wants to save time, one can still choose the mode in which the computer will accept data in both directions of mask motion. Hence, the program provides six modes for operation: accepting data from the counter, in the forward, backward, or both directions, and accepting data stored on the paper tape, in the forward, backward and both directions. Figure (5-2) shows the flow chart for 15 x 255 program.

Let both the entrance and the exit masks be linear arrays encoded by Reed-Muller codes. Then the matrix of spatial-spectral elements ψ is related to the matrix of measurements η by

$$\underline{s}\ \underline{\psi}\ \underline{S} = \underline{\eta}$$

To obtain the spatial-spectral information about the viewed scenc we solve this equation by premultiplying the data matrix by $\underline{s}^{-1}$ and postmultiplying by $\underline{S}^{-1}$

$$\underline{\psi} = \underline{s}^{-1}\underline{\eta}\ S^{-1}$$

Now consider the element η_{11}. It is multiplied only by elements of the first column of $\underline{s}^{-1}$; and in turn it multiplies only the elements of the first row of $\underline{S}^{-1}$. To a given spectral-

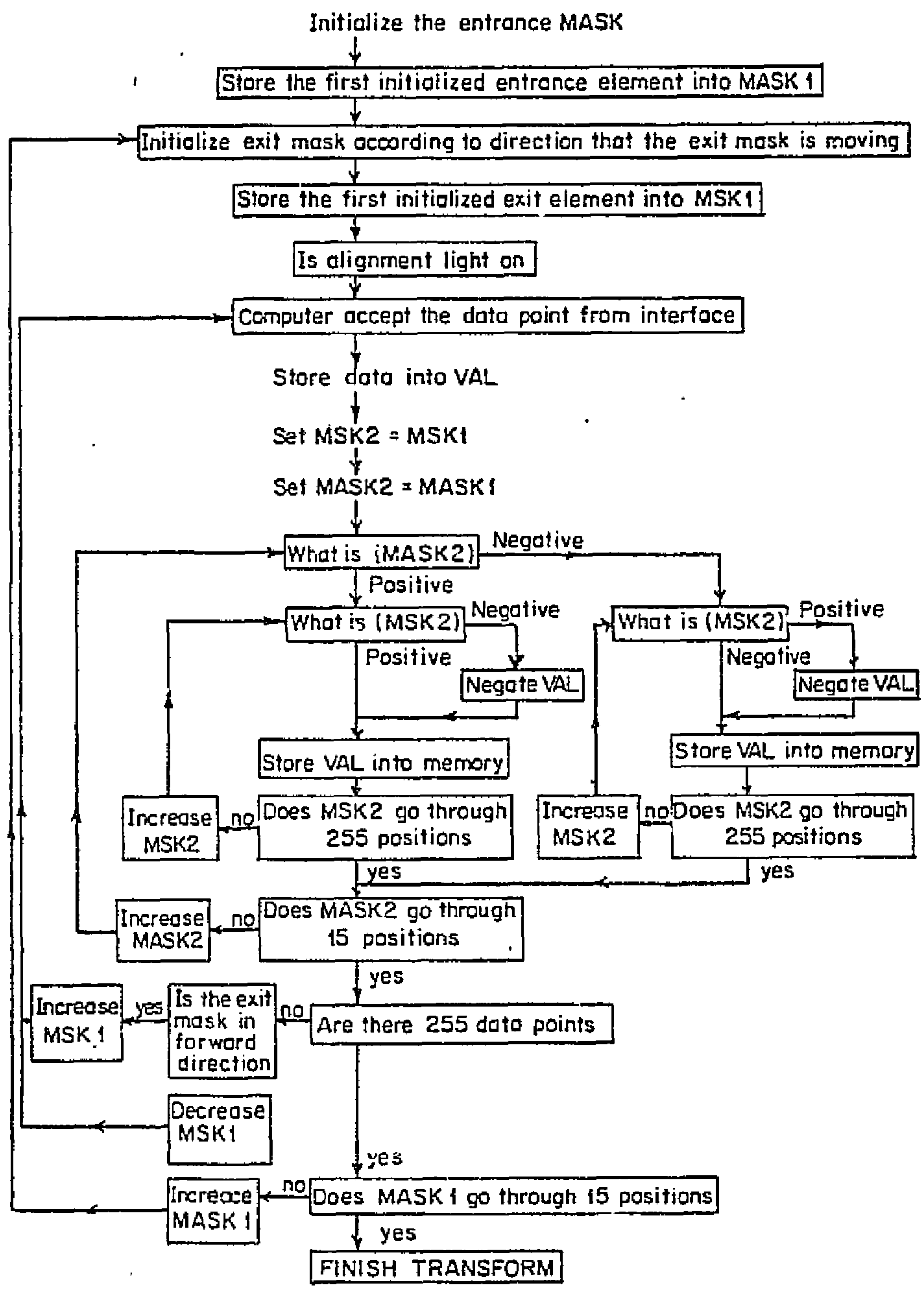

Figure 5-2. The flow chart of the 15x255 inverse transform program.

spatial element ψ_{ij}, it therefore contributes an amount $s_{i1}\eta_{11}S_{1j}$. But the elements s_{i1}^{-1} and s_{1j}^{-1} all have values, either +1 or -1, and the result is that each element ψ_{ij} of the matrix ψ receives a contribution $+\underline{\eta}_{11}$, or $-\underline{\eta}_{11}$ from the reading, η_{11}.

This procedure is generally valid. Any reading $\eta_{k\ell}$ will make additive contributions that can only have values $+\eta_{k\ell}$ or $-\eta_{k\ell}$ to each element ψ_{ij} of the ψ matrix.

For real time decoding we therefore need the following:

(a) A memory that consists of bins containing the contributions to the elements ψ_{ij} accumulated up to any given time t in the cycle of measurements. For a device that can resolve m spatial and n spectral elements, this memory reruires mn bins and of the order of mn memory words.

(b) For each acquired reading $\eta_{k\ell}$ we perform a series of additions of values either $+\eta_{k\ell}$ or $-\eta_{k\ell}$, one to each of the ψ_{ij} memory bins. But before that can be done, we need to decide on the assignment of + or - needed for a given bin. This is done in the following way.

We store the sequence of + and - signs in one column of $\underline{s}^{-1}$ and in one row of $\underline{S}^{-1}$ and in one cycled permutation of each of these vectors. Let us designate these signs by their positions in these two vectors, as $\underline{s}_i^{-1}$ and $\underline{S}_j^{-1}$, respectively, i=1,... m; j=1,... n. (Since each of these sequences is cyclic it can, respectively, be brought into its kth and ℓth cycling position after a measurement $\eta_{k\ell}$). The elements of the two vectors then are multiplied in all possible combinations to give a matrix having mn elements.

$$\Sigma_{ij} = s_i^{-1} S_j^{-1} \qquad i=1 \cdots m;\ j=1 \cdots n$$

Each element Σ_{ij} is either + or - depending only on whether the signs s^{-1} and S_j^{-1} are similar or dissimilar for a particular combination of i and j values.

The additions $+n_{k\ell}$ or $-n_{k\ell}$ to the bins ψ_{ij} are made as successive elements, Σ_{ij} are computed, so that the elements Σ_{ij} need never be stored. Figure (5-3) shows the relation of Σ_{ij} to a superarray containign the set of all elements that are constructed at various stages of the computation.

When only a restricted number of spectral elements are of interest, we need to compute elements ψ_{ij} representing only selected j values. This might be useful, for example, if only certain atmospheric CO_2 absorption lines needed to be studied, and the spectral elements between were of lesser interest. In that case only $\Sigma_{k+i-1,\ell+j-1}$ elements corresponding to given j values need to be used, and the computing time decreases as p/n, where n is the total number of available spectral elements, and p is the actual number of interest.

One starts with the inverse of the codes, s^{-1} and S^{-1}, for the entrance and exit masks stored in the computer. One stores 509 elements of the exit mask, i.e., the 255 elements exhibited in the first mask position plus an additional 254 elements representing the further cycling of this mask. Similarly one stores twenty-nine elements for the entrance mask,

C.2

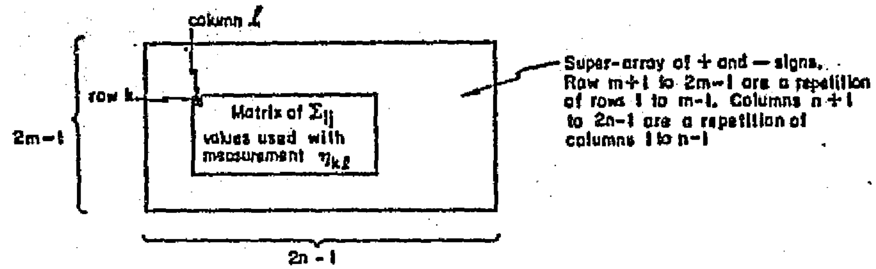

Figure 5-3. Matrices generated by the computer during the reduction of the spectral data.

representing the first fifteen elements used, plus the further cycling of fourteen elements.

For each reading $n_{k\ell}$ one essentially makes use of the matrix (figure 5-3) making use of elements k to k+14 of the stored entrance code and elements ℓ to ℓ+254 of the stored exit code. This matrix consists of + and - signs. When s_{ik}^{-1} and $S_{\ell j}^{-1}$ have the same sign, both being + or both being -, the matrix position ij is assigned a + sign, and the reading $n_{k\ell}$ is added to the accumulatively stored value of ψ_{ij}. If the elements s_{ij}^{-1} and $S_{\ell j}^{-1}$ have dissimilar signs, a - sign is assigned to ij and the reading $n_{k\ell}$ is subtracted from the stored ψ_{ij} values. This whole process takes ~100 msec, and is carried out while the succeeding intensity measurement is being made.

In pratice, we start with the first spatial element, i=1 and add or subtract the contributions to all the ψ_{1j} values, successively going from j=1 to j=255. We then repeat this procedure for i values going from 2 to 15. This whole procedure is carried out while the exit mask is moving from posiiton ℓ to ℓ+1 depending on whether the exit mask is moving forward or back. The entire process is then repeated for the next reading $n_{k,\ell+1}$. When the exit mask reaches its 255th position, ℓ remains unchanged, but the entrance mask moves from the position k to k+1.

For odd values of k, the exit mask moves in the direction of increasing ℓ values, and for even values of k, it moves toward decreasing values. In short, the exit mask moves back and forth as readings are taken. After the entrance mask has moved through all its fifteen positions, and the total 3825 readings have been taken and added onto or subtracted from the ψ_{ij} elements, the run is completed.

2. DATA: Instead of processing a data point immediately as it comes in, this program stores the data in the memory, so one can display the raw data points first, correct them if there are any obvious bad points, and then transform them. This program serves the same function as the inverse transform in the 1 x 255 system.

3. DISPLAY: The display program allows one to display the information in a number of different ways:

(a) One can call for the spectrum corresponding to any one of the entrance slit positions and display it individually.

(b) One can display the sum of the different spectra. In order to do this, one has to take into account that the spectrum for a given entrance slit is displaced by one spectral position from adjacent entrance slit position. In other words, the wavelength for element ψ^{-1}_{ij} corresponds to the wavelength for element $\psi_{\ell+1,j+1}$, because of the slightly displaced light paths through the spectrometer.

(c) Finally one can display all fifteen of these spectra simultaneously, with the zero baseline of each spectrum vertically displaced from the next one. While this format is somewhat crowded, it does allow a quick comparison of the individual spectra.

(C) Correction Program:

This program is shown in Appendix D written in BASIC language. It corrects the error introduced by the imperfect mask. Instead of correcting the mask which in practice is not possible, the program corrects the final spectrum. That is much easier.

As seen in section II-D, for any spectral line I_o, the distorted spectrum shows a line $I_o'=I_o(1-\varepsilon)$, two positive blips with amplitude $(1/2)(\varepsilon I_o'/1-\varepsilon)$ adjacent to the line on both sides, and two negative blips with same amplitude, i.e. $(\varepsilon/2)(I_o'/1-\varepsilon)$ at 24, 25 elements to the left. The correction program takes the intensity of every element, I_o', multiplies it by $\varepsilon/2$, adds it to the elements 24 and 25 positions to the left, and subtracts it from the two adjacent elements, one on each side of the line. The final spectrum is complete except for a different normalization factor. This is a linearized correction procedure valid only for small values of ε, $\varepsilon<<1$.

CHAPTER VI

ASTRONOMICAL OBSERVATION

(A) Correction Procedure

The correction of the spectra for telluric absorption and for instrumental response is a critical procedure. The correction is carried out by comparing the source spectrum (either stellar or planetary) with a lunar or solar spectrum which is taken on the same day at an airmass as close as possible to the star. The following procedures are used in the data reduction:

(1) Correct the raw star spectrum and lunar spectrum (or sun) for negative dip due to the imperfect mask as described in section II-D.

(2) Correct for different entrance slit width if necessary because different slit widths will give different resolution.

(3) Most of the astronomical infrared sources to be observed are weak sources, hence a positive offset is always added to the signal to prevent the signal becoming negative. (The electronics are confused by negative signals.) The correction procedure shown previously also take out this offset. One can take out the offset from the raw spectrum if one knows how large the offset is. Another way to correct this is by substracting a constant intensity from the stellar spectrum until the ratio of the stellar spectrum over the Moon spectrum,

around any large telluric absorption reigon, such as the ozone band, is optimally corrected. By optimal correction we mean that the atmospheric feature appears as neither a positive, nor a negative band. The Moon is a strong infrared signal and does not require an offset, so the result can be used as a calibration for base line.

(4) Align the stellar spectrum and the lunar spectrum by the telluric absorption feature. The final stellar spectrum is obtained by taking the ratio of the stellar spectrum and the lunar spectrum and multiplying it by the black body temperature of the Moon. The lunar temperature is obtained by noting the phase angle of the lunar east limb where it has usually been observed, and extrapolating the temperature from the value given by Linsky (1973). This procedure assumes the lunar infrared emissivity at 8-14μm as unity, which is not true. Murcray et al's (1970) results for the lunar emissivity of 8-14μm region are shown in figure (6-1). The observation was done from a balloon. The strong feature centered at 9.6μm is a result of telluric ozone absorption. Murcray's result has not been used in our analysis because in the region to be discussed, 8.5μm-14μm, the Moon's emissivity is about constant except for the ozone absorption.

(B) Observation of α-Orionis

The observations of α-orionis were carried out with the 50" infrared telescope at Kitt Peak National Observatory, Arizona, in May 1974. The beam size is 18 sec. x 47 sec. The Kitt Peak 50" telescope bolometer was used with the Hadamard spectrometer. The dewer has a band pass of 8 - 14μm. The spec-

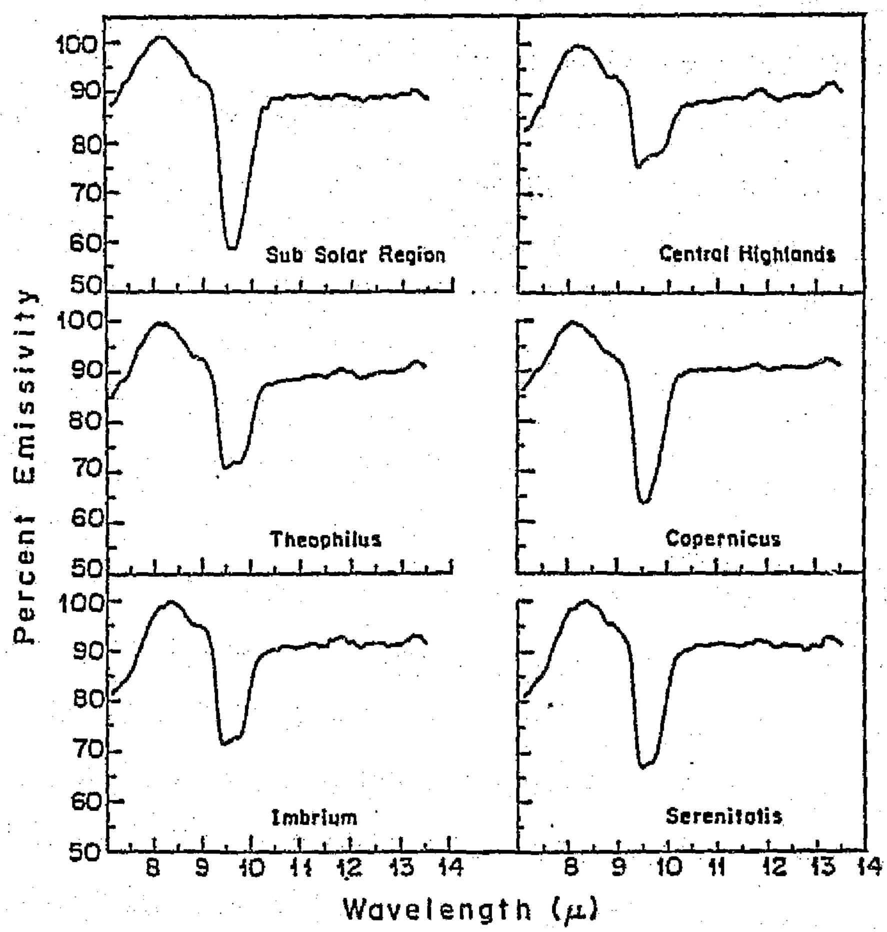

Figure 6-1. The spectral emissivity of various regions as calculated from the flight data (Murcray et al, 1970).

trometer operated in the 8-11μm region with a resolution $\lambda/\Delta\lambda$ around 500. The chopping frequency was 10 cycles per second.

Three runs were taken. Each run consisted of 10 scans of the sources. Two lunar spectra were taken on the same day for correction purposes. For the lunar temperature we used 383°K. Figure (6-2) shows the raw spectra of α-orionis and the Moon. The α-orionis spectrum is the sum of two independent runs.

Figure (6-3) shows the ratio spectrum of α-orionis corrected for lunar temperature. Except for the region immediately around the ozone band all the telluric absorption features are gone. The region between 9.35μm to 9.7μm is unreliable because the ozone band has a very low transmission.

α-orionis is a late type super-giant with temperature around 3000°K. A stellar continuum corresponding to a 3000°K blackbody is also shown in figure(6-3), normalized to arbitrary units. The broad emission feature around 10μm, which is due to silicate emission, is clearly shown in the spectrum. This 10μm 'silicate' emission feature of α-orionis has been previously discussed by others.

Woolf and Ney (1969) renormalized Gillett *et al*'s spectra (1968) of α-orionis and interpreted the 10μm emission as coming from circumstellar dust which absorbs starlight and reradiates at infrared wavelengths. Since the emission is far more sharply peaked than a black body, the wavelength dependence of the emission probably closely mimics the wavelength dependence of the opacity of the material. In the same paper, Woolf and Ney

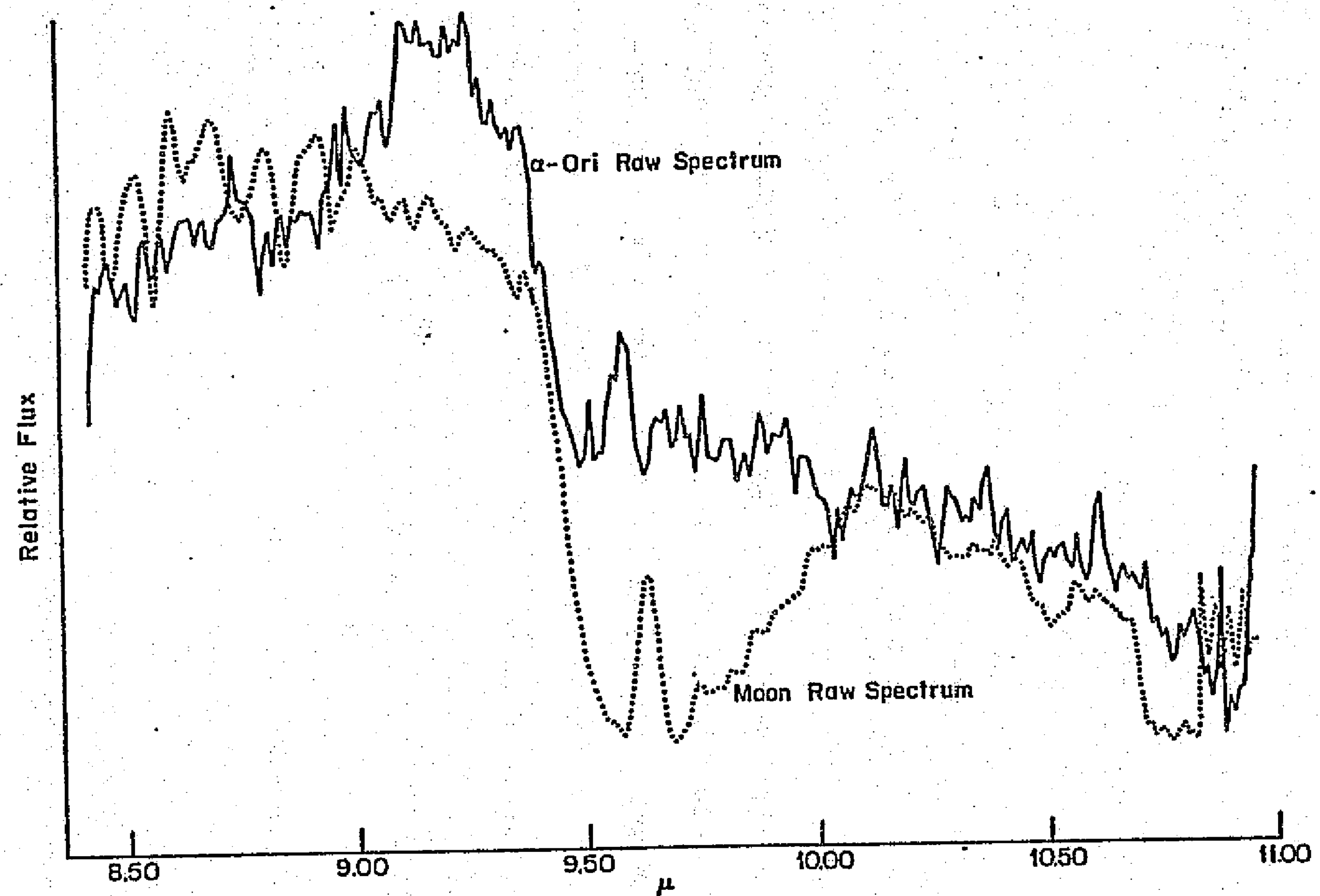

Figure 6-2. The raw spectra of α-orionis and the Moon.

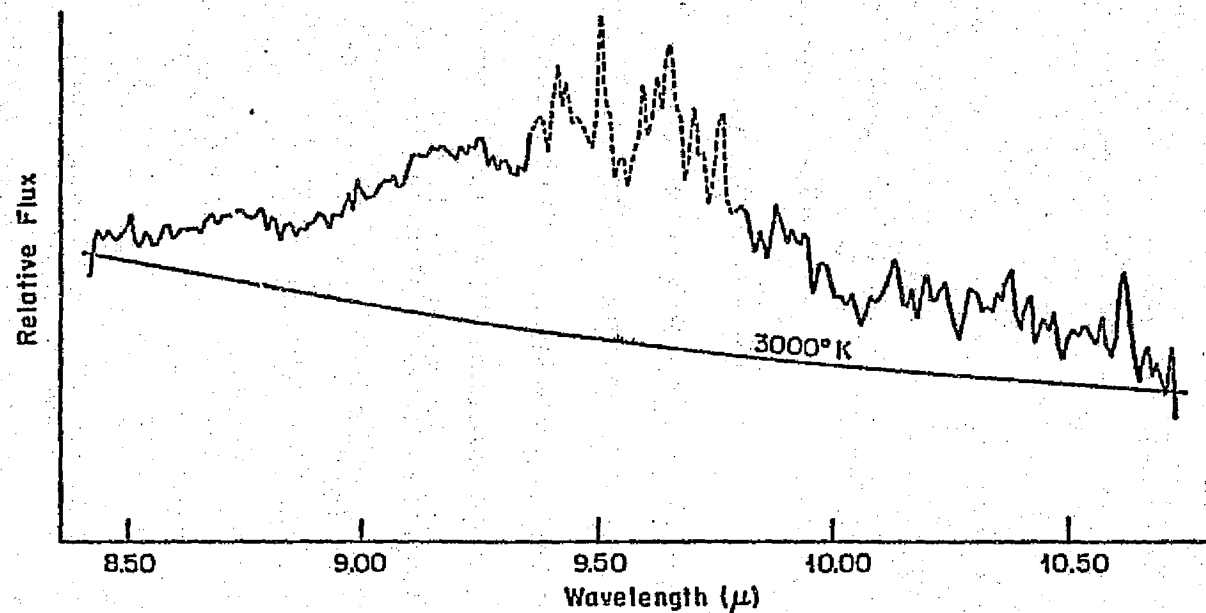

Figure 6-3. The ratio spectrum of α-orionis to the Moon corrected for lunar temperature.

also proposed that it is silicate grains which one is observing in the circumstellar dust cloud. This suggestion has been strengthened by high resolution spectra of Gamown et al (1972) with resolution $\lambda/\Delta\lambda$=250 from 850 cm^{-1} to 1100 cm^{-1}. The emissivity of silicate grains should have a second peak near 20μm. This second emission feature was observed by Low and Swamy (1970) in narrow-band photometry of α-orionis. Another supporting piece of evidence for the silicate model of the α-orionis dust cloud comes from observations of silicon monoxide (SiO). Silicon monoxide is expected to be among the most abundant molecules present in the atmospheres of cool stars of normal composition. It is also a reagent in the condensation mechanism thought to produce circumstellar silicate grains (Mass et al, 1970). The presence of silicon monoxide in α-orionis was confirmed by Cudubacк et al (1971). They observed SiO absorption features around 4μm.

The silicates are expected to form from the material ejected by cool stars. Gilman (1969) calculated what solids would condense from gas of stellar composition as it moved away from a star and cooled. This is critically dependent on the ratio of oxygen to carbon in the gas. These elements first combine to form carbon monoxide; the subsequent development depends on which of the two is left over when all the other has been used up in this way. If carbon predominates, graphite will be the principal condensate, or under certain circumstances silicon carbide. If oxygen wins, the grains which should form are the silicates of calcium, magnesium, aluminium and iron;

combinations of these are responsible for the 10 and 20μm spectral features. Aluminium and calcium silicate may be rare because of the low cosmic abundance of aluminium and calcium. Woolf and Ney (1969) expected magnesium silicate, $MgSiO_3$, with some iron silicate, $FeSiO_3$, to be most abundant. For recent work on dust grains one can refer to Salpeter's paper (1974 a) on the theory of nucleation and dust grains in carbon-rich stellar atmosphere and his paper (1974 b) on formation and flow of dust grains in cool stellar atmospheres.

Laboratory spectra exist for silicate absorption features (Day, 1974). Any fine feature of the astronomically observed silicate emission may be washed out by different particle sizes and shapes, uncertainty in temperature and mixture of composition. Gammon et al (1972) examined the excess in XY Seg and O Cet and concluded that the type of silicates involved are basic rather than acidic. Day (1974) synthesized the amorphous magnesium silicate and obtained an absorption band quite similar to the material causing the interstellar 10μm absorption feature. He suggested that the existance of disordered structures seems a more reasonable expectation than crystalline terrestrial-type minerals. For the momnet, the nature of the silicates is certainly at an unsettled stage.

Penman (1976) had measured the middle infrared reflectivities of five silicate minerals, and used Kramers-Konig analysis to obtain the optical constants of the samples. He then used the optical constants in Mie computations of the absorption properties of very small mineral grains. The final absorption cross-section spectra compared to the observed 10μm silicate of the source W3/IRS5. All the calculated spectra have sharper features than the astronomical features due to the application of Mie theory. However, the hydrated silicate, Chloritite (hydrated Mg/Fe/Al silicate) and serpenlenite (hydrated Mg/Fe silicate) fits the observed astronomical positions correctly. They fall almost exactly at the center of the astronomical features.

To the author's knowledge only two spectra of α-orionis in 8-14μm exist in the literature. Gillett et al (1968) (figure 6-4a) obtained results in the wavelength region from 2.8 to 14μm, with a resolution $\lambda/\Delta\lambda=50$. Treffers and Cohen (1973) (figure 6-4b) obtained a spectrum from 8-14μm, and in the 20μm region with resolution 1000. Gillett's and Treffers and Cohen's spectra are shown in figure (6-4). Compared with our result, all show the 10μm emission feature if Gillett's black body curve is lowered instead of being drawn tangent to the observed data at 10μm. Our spectrum shows a rather rapid dip at wavelengths beyond 10μm while Treffers and Cohen show a slower nearly constant decline. Further high resolution observations should clear this matter up. Our own instrument now operates at a resolution similar to that of Treffers and Cohen, and if used on a telescope as large as the 120 inch Lick Observatory reflector that they used, sufficiently high signal to noise ratios should be obtained.

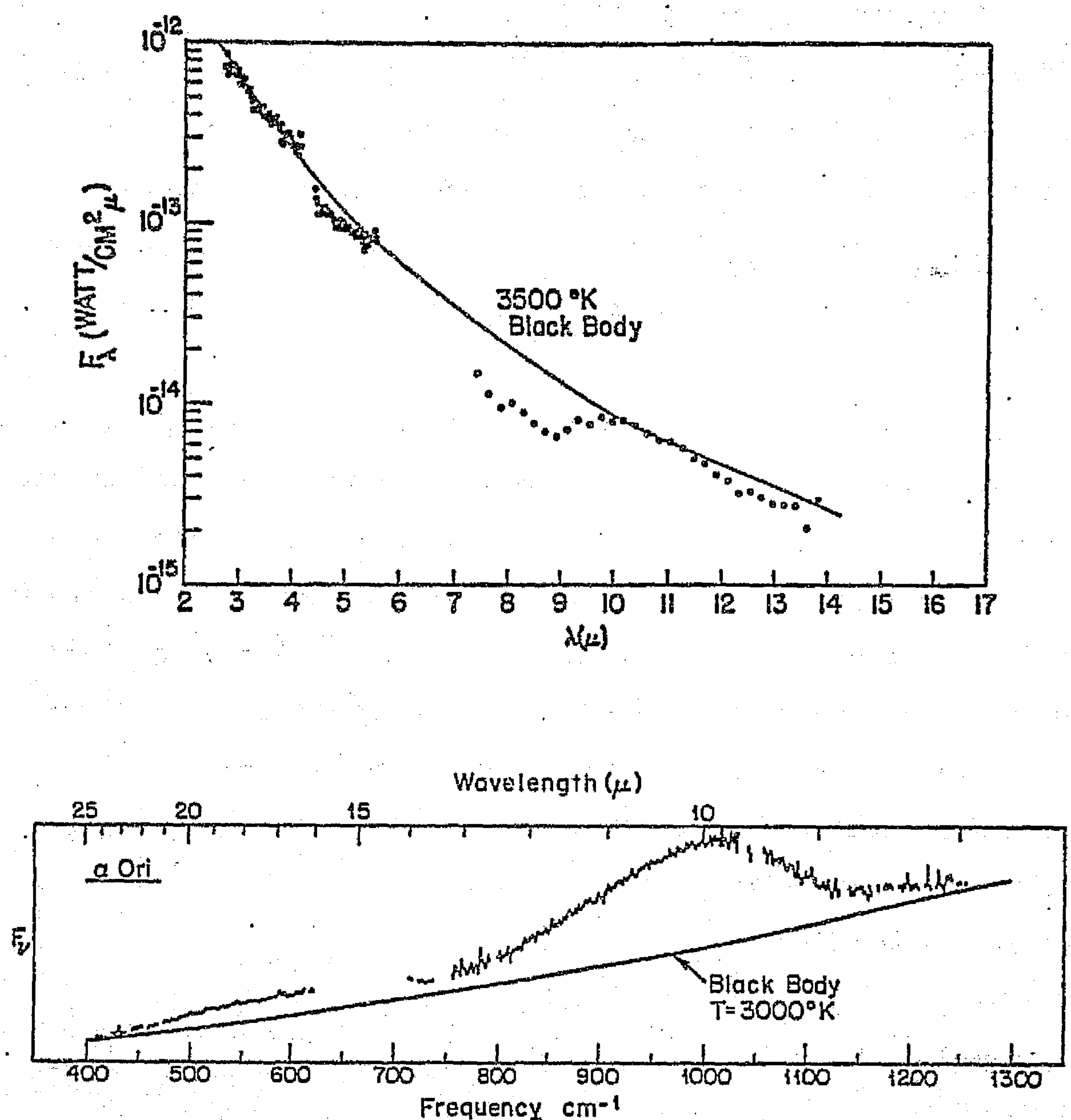

Figure 6-4. (a) Low resolution spectrum taken by Gillett et al(1969). Different symbols represent spectra taken on different nights. (b) High resolution spectrum taken by Treffers and Cohen (1973).

(C) Observations of Jupiter

The observations of Jupiter were also carried out with the 50" infrared telescope at Kitt Peak. The beam size is 18" x 47". The Kitt Peak bolometer assigned to the 50" telescope with band pass 8-14μm was used with the Hadamard spectrometer. For our Jupiter observations, the spectrometer operated in the 10.8-13.4μm region with an effective resolution $\lambda/\Delta\lambda$ around 250. The chopping frequency was 10 cycles per second.

Two runs were taken. Each run consisted of twelve scans of the whole Jovian disk. Two lunar spectra were taken on the same day for correction purposes. For the lunar temperature we used a value of 383°K. Figure (6-5) shows the raw spectrum of Jupiter and the Moon. Both the Jovian and lunar spectra are the sums of two independent runs. Figure (6-6) shows the ratio spectrum of Jupiter corrected for lunar temperature. The arrows labeled by H_2O show the position of telluric water vapor features. Most of the telluric features have been cancelled properly.

Jupiter is covered by clouds which in the visible part of the spectrum are seen from earth. Current models show three distinct cloud layers (figure 6-7, Ingersoll). The lowest layer is water ice, with maximum density at about 270°K. The middle cloud is solid ammonium hydrosulfide (NH_4SH) at about 200°K. Lewis and Prinn (1970) suggested that ultraviolet radiation from 2200 to 2700 Å is not absorbed by H_2, He, CH_4 and absorbed a little by NH_3. Therefore, the radiation in this

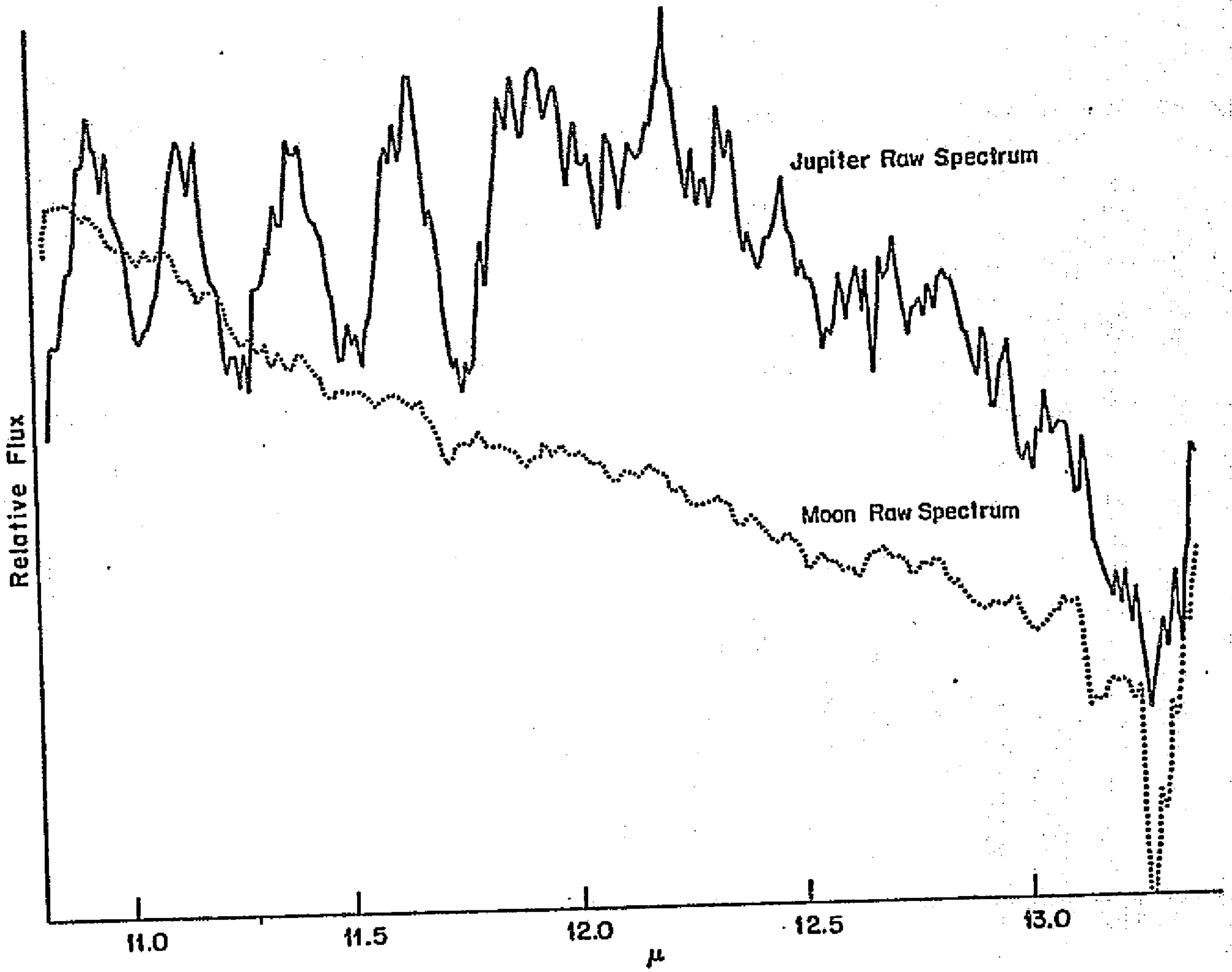

Figure 6-5. The raw spectrum of Jupiter and the Moon.

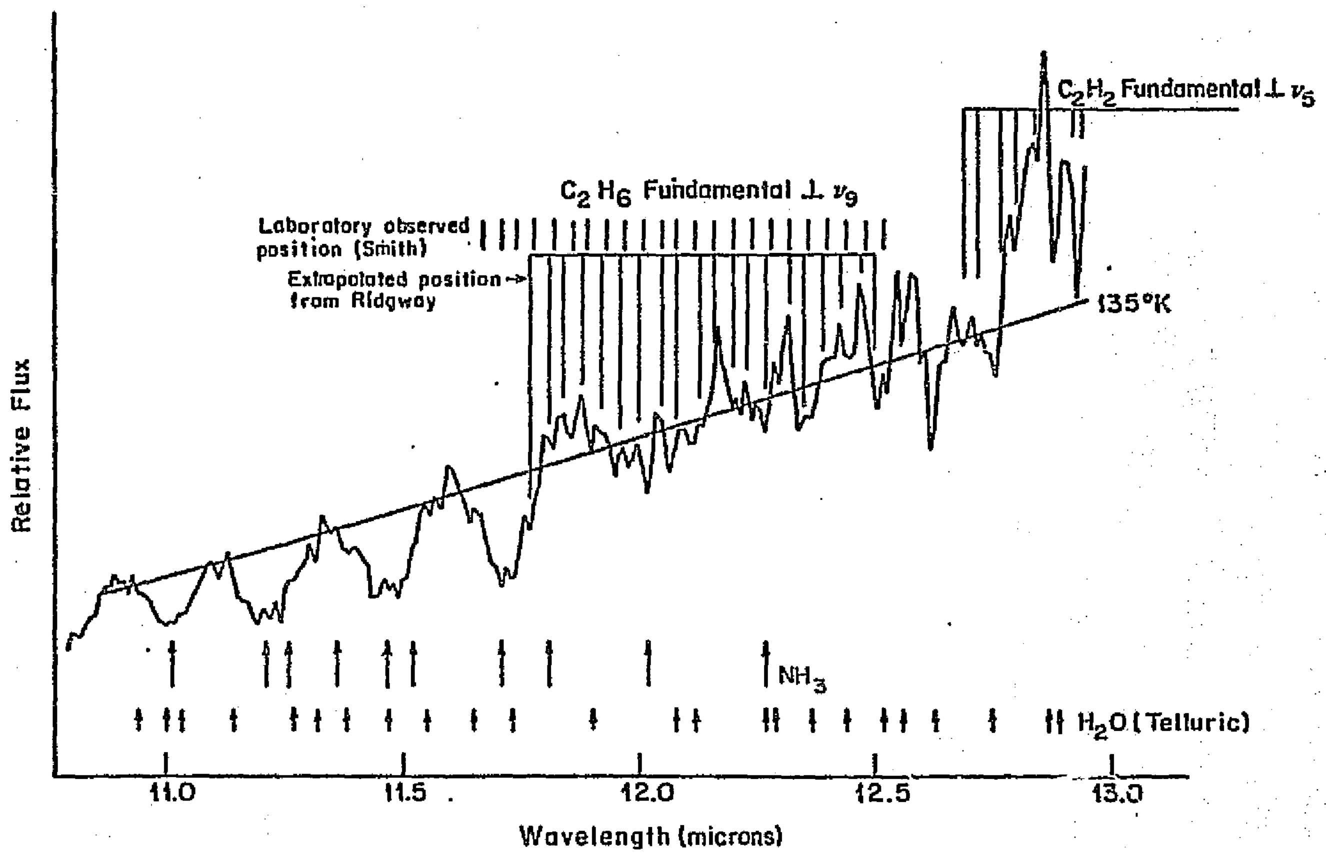

Figure 6-6. The ratio spectrum of Jupiter to the Moon corrected for lunar temperature.

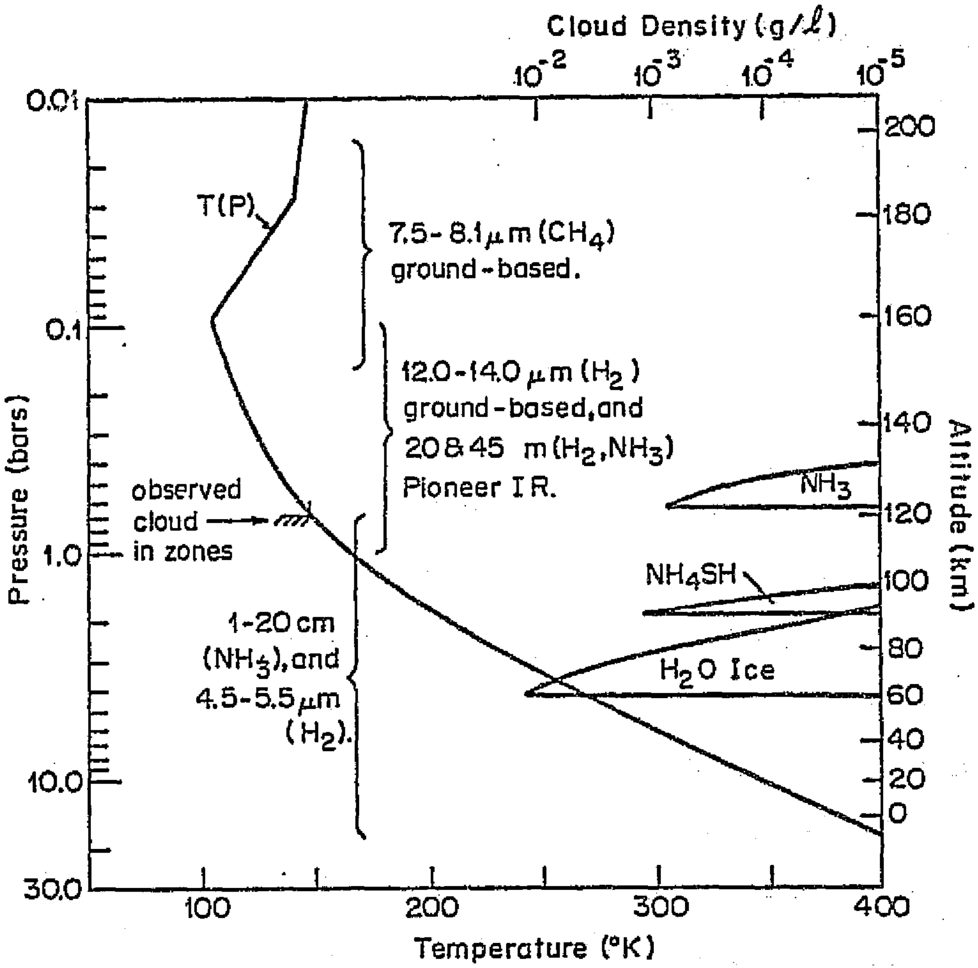

<u>Figure 6-7.</u> The atmospheric profile of Jupiter for a solar-composition model.

region may reach the ammonium hydrogen cloud and photolyze hydrogen sulfide there into hydrogen polysulfides (H_2S_x), elemental sulfur, and ammonium polysulfides $\left[(NH_4)_2S_x\right]$. All of these species are yellow, orange, or brown and may explain the color of zones. However, Sagan and Salpeter (1976) suggested that even under the most optimistic assumption that every H_2S photo dissociation event leads to polymerics, the implied optical depth falls short by two orders of magnitude from matching the observed values. Moreover, pure polymeric sulfur fits the observed optical properties of the Jovian red chromophores only poorly (Rages and Sagan,1977). The upper cloud is solid ammonia at around 150°K. Solid ammonia is whitish and probably forms the white zones on the Jovian disk. The color of the Great Red Spot may be due to high altitude ultraviolet photolysis of phosphine (PH_3) into P_2H_4 and amorphous red phosphorus. The total depth of the cloud system is about 70 Km, and the pressure range probably runs from about 0.5 bar at the top to 4.5 bar at the cloud base. It is the cloud tops and above where the 10μm infrared radiation originates. Our spectrum measures a color temperature of 135°K which is consistent with Ingersoll's picture. The radiation should come from the cloud tops because the Jovian atmosphere at 10.5 to 13μm has appreciable opacity, as discussed in the next paragraph.

The main constituents of the Jovian atmosphere are hydrogen molecules, helium molecules, methane and ammonia, with minor constituents hydrogen sulfide, water, ethane and acetylene. Table 6-1 shows their observed abundance ratio by number.

TABLE 6-1

Solar composition atmosphere (fraction by number)

Species	(1)	(2)
H_2	0.886	0.870
He	0.112	0.128
H_2O	1.05×10^{-3}	8.80×10^{-4}
CH_4	6.30×10^{-4}	6.17×10^{-4}
NH_3	1.52×10^{-4}	1.49×10^{-4}
H_2S	2.90×10^{-5}	2.56×10^{-5}

(1) Weidenschilling and Lewis (1973).

(2) Podolak and Cameron (1974); Cameron (1973).

The table is taken from Ingrosell.

The abundances of hydrogen, methane, ammonia, and helium seem consistent judged from solar atomic abundances. For detailed information one can refer to McElroy (1973).

The opacity due to hydrogen molecules is caused by pressure induced dipole absorption. The hydrogen molecule has no permanent dipole moment, and consequently, no permanent dipole spectrum. Gaseous H_2, however, has a weak pressure - induced dipole spectrum which absorbs significantly over the long path lengths and low pressure of the Jovian atmosphere. The induced dipole moment results from two distinct physical process (Kranendonk and Kiss, 1959). The first takes place when the permanent quadrapole moment of one molecule induces a dipole moment in another molecule by virtue of the neighbor's polarizability. This is a long range interaction. The second physical process takes place when the overlap forces of the two adjacent molecules cause an asymmetrical distortion of their electronic charge clouds. The net induced dipole moment is modulated by the relative translational and rotational motion of the colliding pair and this modulation produces the absorption of infrared radiation. The translational spectrum is predominant at long wavelengths with its peak at 100μm at 100°K (Trafton and Munch, 1969). In our wavelength region (10.5 - 13μm) its contribution to the opacity is negligible. The rotational hydrogen collisional spectrum, however, has its peak at 17μm and contributes a continuous opacity in our wavelength region (Th. Encrenaz, 1972).

The helium molecule also has no permanent dipole moment.

Its opacity comes from the collision with the hydrogen molecules and resembles the H_2-H_2 collision process. The collision is less important due to the smaller abundances of helium.

Ammonia is an important source of opacity at 10μm under Jovian atmospheric conditions. The 10μm band of ammonia arises from transitions through the ν_2 mode. In the ν_2 mode of vibration, the nitrogen atom oscillates vertically relative to the plane of the hydrogen atoms (figure 6-8a). The nitrogen atom is able to penetrate through the potential barrier to the other side of the hydrogen plane. This inverted position leads to inversion splitting of the levels of the ammonia molecules. The splitting generates both symmetric and antisymmetric energy levels with a given vibrational quantum number.. The 10μm band of ammonia arises from transitions from the ground vibrational state to the first excited state in the ν_2 mode (figure 6-8b). Another transition, from the first excited symmetric vibrational state to the second excited asymmetric state is also in 10μm range, but the contribution due to this "hot band" is small for the low temperature in the Jovian atmosphere.

The ammonia is clearly seen in abosrption in the spectrum. The centers of the bands are shown by the arrows labeled NH_3. The ammonia absorption has been observed by different groups.

Gillett <u>et al</u> (1969)(figure 6-9) observed Jupiter from 2.8-14μm with low resolution $\lambda/\Delta\lambda=50$. Briefly, their results show the following: The spectrum has a depression at 3.3μm caused by CH_4. Solar heating of the upper atmosphere via this band results in warming of the upper atmospheric layers. This

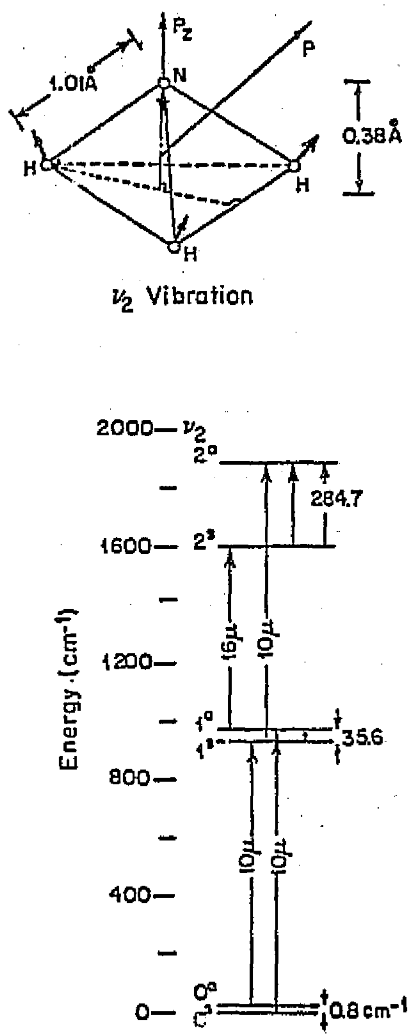

Figure 6-8. (a) Schematic representation of the NH_3 molecule. The components of angular momentum and the motion in the ν_2 vibrational mode are also shown. (b) Energy levels of the ν_2 vibrational mode of ammonia. Superscripts a and s refer to the antisymmetric and symmetric levels which arise due to inversion splitting.

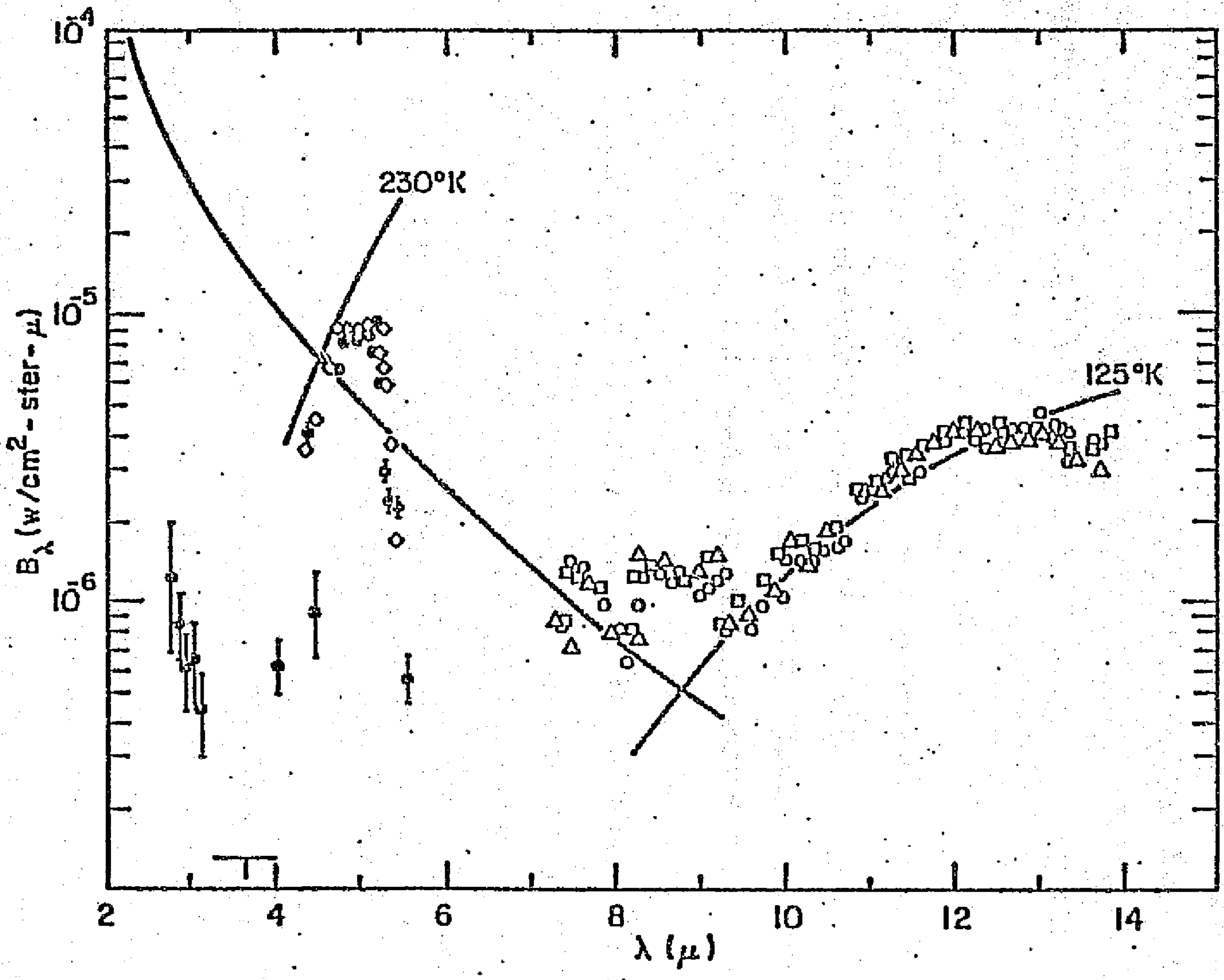

Figure 6-9. Low resolution spectrum taken by Gillett *et al* (1969). Different symbols represent spectrum taken on different nights. This figure is taken from their paper.

proceeds until energy is radiated at the same rate via the 7.7μm band of CH_4. Ammonia absorption around 10μm was also detected. Judging from the CH_4 emission, these authors were the first to suggest a temperature inversion on Jupiter caused by solar heating of the 3.3μm band of CH_4. They also showed that the NH_3 band at 10μm is saturated, and calculated that the H_2 abundance at 12.5μm, assuming a temperature of 125°K, is 12 km-atm. with a pressure $P_{H_2} \sim 1/4$atm.

Aitken and Jones (1972) obtained a Jovian spectrum from 8 - 13μm at a resolution $\lambda/\Delta\lambda \sim 143$(figure 6-10). The ammonia absorption band is again seen. They estimated that the ammonia abundance in the band is about 2.7 cm-atm. and a lapse rate $\Gamma = \frac{\partial T}{\partial h}$ at 13μm given by H=-30K, where H is the scale height ~20km.

The most recent published infrared spectrum is by Lacy et al (1975) who used the Lick Observatory 120" telescope. High resolution spectra were obtained at 890 cm^{-1}(11.24μm) with $\lambda/\Delta\lambda$=1780. Medium resolution data were observed from 1000 cm^{-1} to 850 cm^{-1}(10 ~ 12.75μm) with $\lambda/\Delta\lambda$ from 250 to 333 (figure 6-11 a,b). The authors also calculated synthetic spectra, assuming that NH_3 and H_2 are the only sources of opacity. Their conclusions from comparison between observed and computed spectra follow: All of the prominent lines in their observed spectrum are saturation NH_3 bands broadened to a width many times the pressure - broadened line width. The observed 135°K continuum is primarily formed by the wings of the NH_3 line. The H_2 opacity may be important if NH_3 is unsaturated

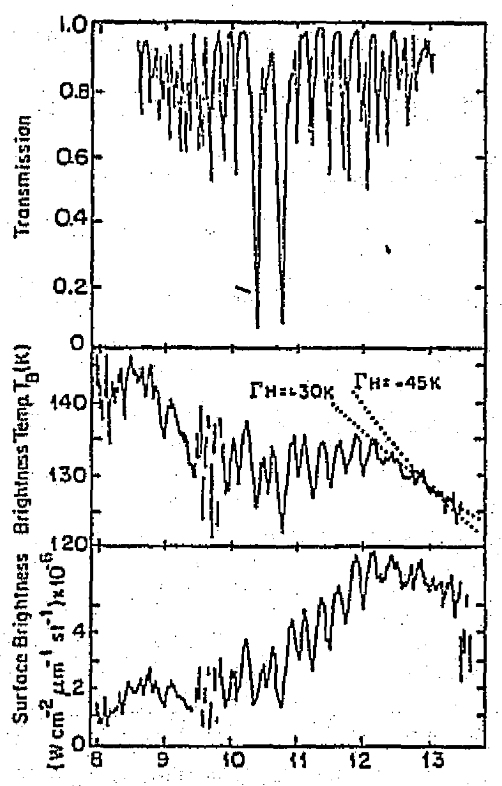

Figure 6-10. (a) Room temperature absorption spectrum of ammonia, p=0.06 atmos, w=0.6 cm atmos. (b) Brightness temperature; (c) Surface brightness of the central region of Jupiter from 8 to 13.5μm. (Taken from Aitken and Jones).

near 135°K. A pressure of 0.125 atm. at 135°K is required to form the continuum. The minimum temperature in their synthetic model is 118±5°K while the observed minimum temperature is 123°K, about 5°K larger than the derived temperature due to incomplete resolution of the features. The lapse rate at 135°K is 7.5±2.5°K/SH. Gillett et al (1969) estimated the lapse rate at the NH_3 saturation level is 4°K/SH. A discrepancy occurs in the comparision of the medium resolution data between 870 and 890 cm^{-1}. In this region the Jovian spectrum seems to be depressed by about 2°K relative to the calculated curve. The authors suggested that it may be due to an as yet unidentified minor constituent of the Jovian atmosphere.

Our spectrum has about the same resolution as the medium spectra of Lacy et al's and so the two spectra can be compared. The line positions match well. The vertical matching shows a drift towards longer wavelength. Figure (6-11a) is obtained by matching points A and B. The short wavelength side matches but the end of the long wavelength side is about 1.5 times higher. Also our spectrum seems to match the theoretical curve better at 870 to 890 cm^{-1}. Figure (6-11b) is obtained by matching A' and B'. Then the long wavelength side matches better than before but the short wavelength side is different. Also now our spectrum matches better with Lacy et al's observed result at 870 - 890 cm^{-1}. A conclusion about the discrepancy at 870 cm^{-1} between Lacy's observed and calculated spectra can not be reached at present until there is a better way for matching our and Lacy's et al's spectrum. Also it is not clear

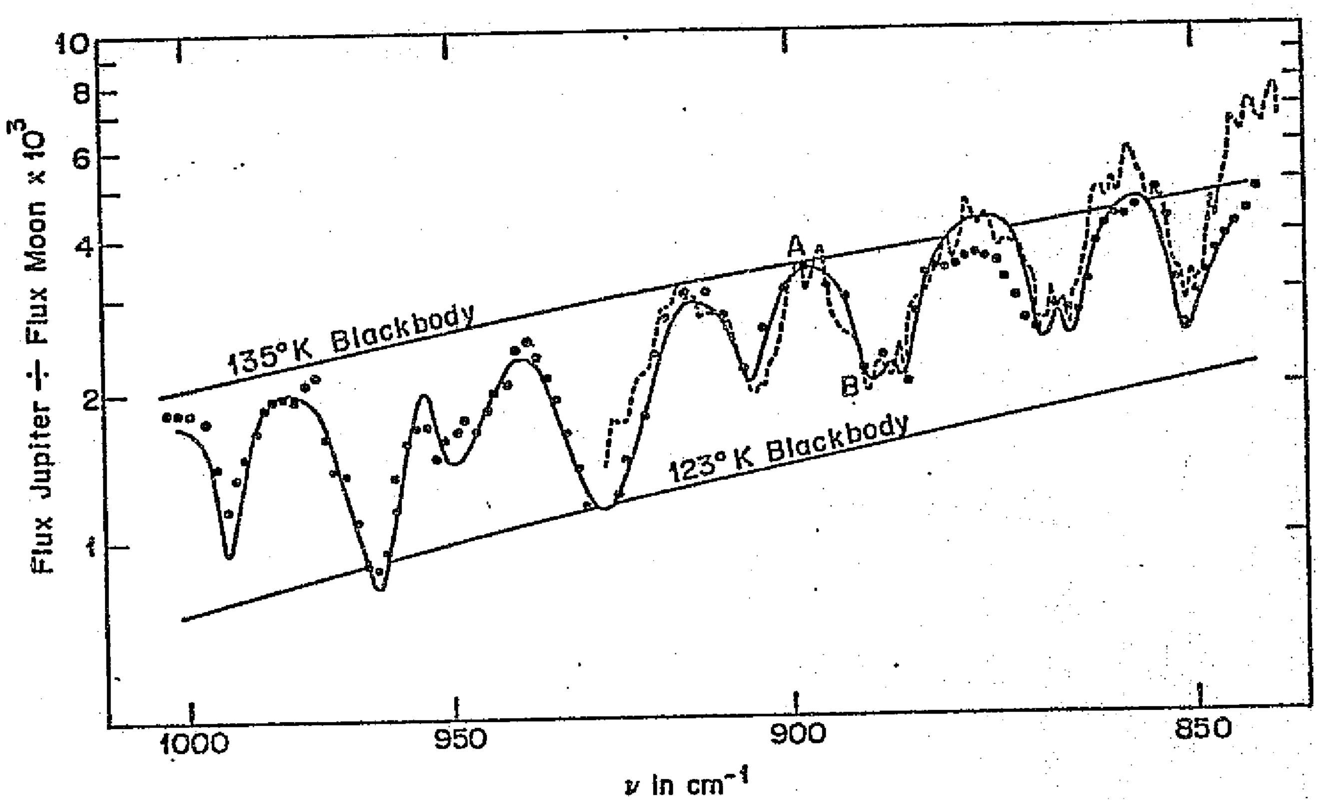

Figure 6-11a. Spectrum of the N and S polar regions of Jupiter at 3-4 cm^{-1} resolution divided by the spectrum of the Moon. Data points are shown as solid circles, and the solid line represents the best fitting synthetic spectrum calculated from the model calculated by Lacy *et al* (1975)(The graph is taken from Lacy *et al*). The dotted curve is our observed spectrum by matching Lacy's spectrum at points A and B.

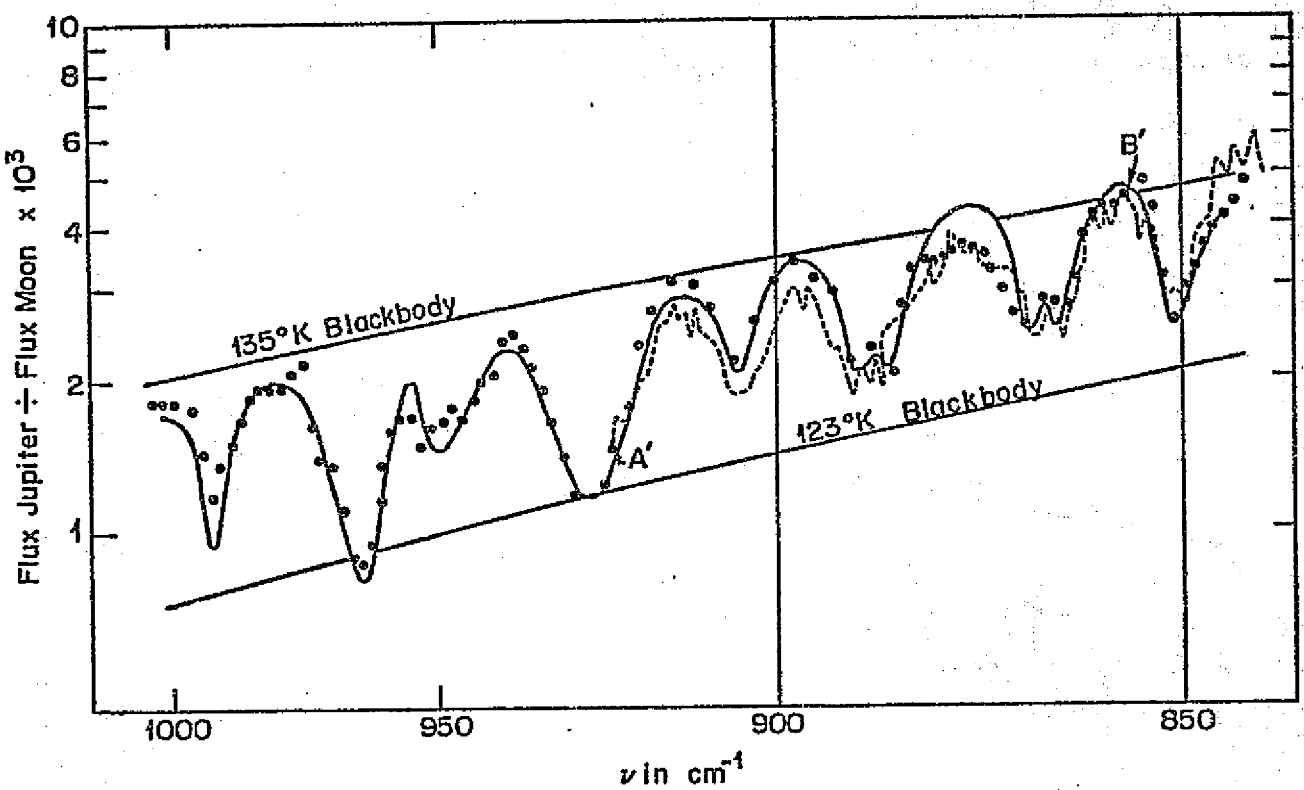

Figure 6-11b. Same as 6-11a except matching our spectrum with Lacy's at A' and B'.

whether the difference in matching of our spectrum and Lacy et al's between long wavelength and short wavelength is real or not. There could be several reasons for the difference. It could be due to the inaccuracy of the end of the spectra, because the short wavelength side is the end of our spectrum and the long wavelength side is the end of Lacy's spectrum; or it may just be due to the matching technique. More effort is needed to clearify this point.

The absorption due to NH_3 is much less important beyond 12μ, so one may be able to use the H_2 opacity to estimate the lapse rate in that region. The lapse rate can be estimated by the equation

$$T_B(\lambda_1) - T_B(\lambda_2) = \frac{\Gamma H}{2} \ln \frac{a(\lambda_1)}{a(\lambda_2)}$$

where $T_B(\lambda_1)$ is the brightness temperature at λ_1

$T_B(\lambda_2)$ is the brightness temperature at λ_2

Γ is the lapse rate

$a(\lambda_1)$ is the absorption coefficient at λ_1

$a(\lambda_2)$ is the absorption coefficient at λ_2

H is the scale height

If one chooses λ_1=11.95, λ_2=12.34 with measured brightness temperature T_1=133.94, T_2=133.64, $\alpha(\lambda_1)$, $\alpha(\lambda_2)$ are taken from Calpa and Ketebaar (1957), one obtains a result $\Gamma H=-43.2^\circ K$ for an H_2 opacity dominated atmosphere. Gillett et al (1969) calculated the adiabatic lapse rate $(\Gamma H)ad=-42^\circ K$ for an H_2 atmosphere, while Aitken and Jones (1972) measured a value of $\Gamma H=-30^\circ K$ from their spectrum. Our value seems closer to the value calculated by Gillett rather than to Aitken's. It is emphasized here that the estimate is based on the assumption that the H_2 opacity is the dominant opacity at wavelengths 11.95μ and 12.34μ, which may not be true.

Methane has a strong emission band at 7.7u but does not have any band structure in our region. Methane has two important contribution to the overall thermal structure of the Jovian atmosphere. The first one is that methane has an absorption band at 3.3μm which absorbs solar energy and reradiates at 7.7μm producing an inversion temperature layer with a maximum temperature of 150°K at an altitude 160 - 200 km. Secondly, methane is photo dissociated by ultraviolet light in the upper atmosphere. This results in products such as ethane (C_2H_6), acetylene (C_2H_2), and ethylene (C_2H_4). Strobel (1973) estimated that column densities of C_2H_6, C_2H_2, C_2H_4 above the cloud top are approximately 10^{21}, 3×10^{16}, $3 \times 10^{15} cm^{-2}$ respectively. C_2H_6 and C_2H_2 were first observed by Ridgway (1973) using the 60" Kitt Peak solar telescope in the 750 - 875 cm^{-1} (11.42 - 13.33μm) range with resolution $\lambda/\Delta\lambda$=770, (figure 6-12a). The lines are shown in strong emission at the 140°K temperature. The apparent lines are superpositions of many lines, each group corresponding to a subband. Ridgway calculated that the mixing ratios are $N(C_2H_6)/N(H_2)=4 \times 10^{-3}$ and $N(C_2H_2)/N(H_2)=8 \times 10^{-5}$. The ratio $N(C_2H_6)/N(C_2H_2)$=50 where Strobel predicts about 200. Combes et al (1974)'s (figure 6-12b) observation confirms the presence of very strong emission lines of C_2H_2 and C_2H_6. The abundance of

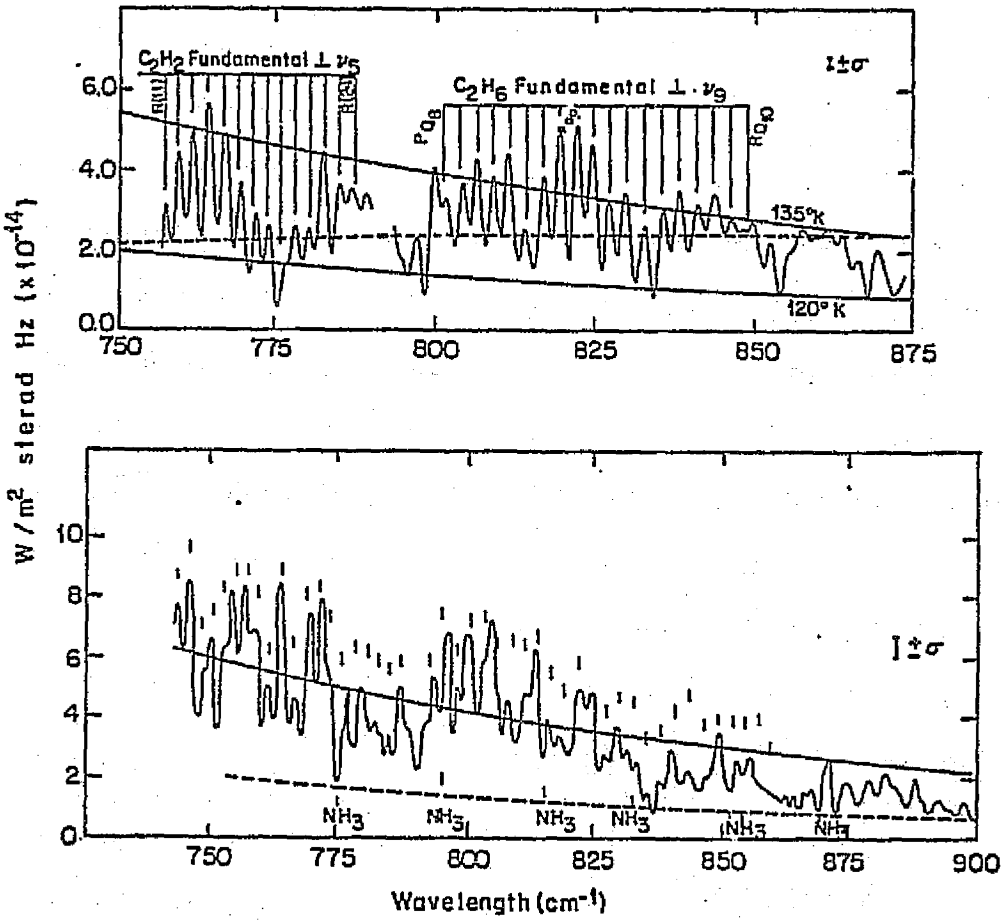

Figure 6-12. (a) Thermal emission spectrum of Jupiter corrected for absorption in the earth's atmosphere observed by Ridgway (1973). The dashed line is the predicted form of the H_2 continuum. (b) The ratio of the Jovian spectrum to the atmospheric absorption spectrum observed by Combes et at (1974). The solid and dashed lines are the blackbody curves at 135°K and 120°K respectively.

ethane estimated from Ridgway's spectra depends strongly on the distribution of gas temperature, which is not well-determinded. If the temperature in the mesospheric inversion layer turns out to have a maximum value of 150°K, the observations indicate ~ (Ridgway 1974) 2×10^{-2} gm cm^{-1} of ethane in this high temperature region. Sagan and Salpeter (1976) estimate the column density of ethane molecules to be 3×10^{-3} gm cm^{-2} by assuming that ethane is produced by photolysis of methane by solar ultraviolet photon and destroyed mainly by eddy diffusion into the troposphere, followed by pyrolysis in deeper, hotter layers. This would be in very serious conflict with the observations, especially since only a small fraction of the theoretical column density refer to the hotter inversion region.

The ethane emission band is also shown in our spectrum (figure 6-6). In the figure the indicated emission line position was extrapolated from Ridgway's spectrum, and the laboratory observed position by Smith (1949) are also shown for comparison. Our positions agree with Ridgway's reasonable well, while Smith's seem displaced from ours by 0.01μm,possibly due to a uncertainty in position calibration. Only a portion of the C_2H_2 spectrum can be seen in our spectral coverage. The abundance of C_2H_6 is not estimated here because the absolute amplitude of our spectrum is not well calibrated.

Our spectrum contains both ammonia and ethane features while other observers have not shown both. This will be useful because one can compute the synthetic spectra including both. Ammonia will provide us with information about the top of the cloud layer while ethane provides us with the information about the inversion layer. A synthetic spectrum including both ethane and acetylene would be interesting because the inclusion of these new gases would affect the models, especially around the inversion. Acetylene would appear around 13μm. The absorption of solar radiation by CH_4 at 3.3μm used to be thought to be radiated solely by CH_4 at 7.7μm. The 7.7μm emission intensity is a critical test of a temperature inversion model and the emission intensity calculated by Wallace et al (1974) is within 25% of the value observed by Gillett et al (1969). If ethane and acetylene do contribute to emission in the thermal infrared, there must be some additional source of solar absorption in order to produce the observed inversion temperature. Additional absorption at this altitude, perhaps due to particles, is suggested by the low ultraviolet albedo of Jupiter in the wavelength region 2100 to 3600 Å (Wallace, Caldwell and Savage, 1972).

Terrile and Westphal (1976) had imaged Jupiter at high spatial resolution at 8 - 14μm. All images reveal a belt and zone structure similar to visible photographs. In the 8 - 14μm broad-band data, belts appear to be about 2°K hotter than the zone. The lowest belt-zone contrast is found in the hydrogen opacity dominated region at 12.5μm, while images at 9.5μm have the greatest contrast. This is consistant with the dynamic picture that zones are rising columns of air and belts are sinking columns of air. Ammonia gas being carried upward in zones will freeze out and form a thick cloud on top of the zones, giving a low infrared temperature to the zones, and the crystalized NH_3 particle will be carried down to the deep atmosphers in the belt where they will get sublimated. One can look deeper into clouds in the belt because of the lack of the ammonia cloud on top of it and therefore see a higher infrared temperature. Although there are a number of high resolution spectra of good spectra for methane. The observation of methane will be interesting not only because it provides us with information about the inversion layer, it is also useful to find out the temperature profile. If the temperature profile of the Jovian atmosphere is known, one can use it to find the ammonia abundance profile. Ammonia itself is not a very good tool for probing the temperature profile because it has a low vapor pressure and its variation is very sensitive to temperature changes. Observations of methane at 3.3μm and 7.7μm, should be able to accomplish this.

The Hadamard transform spectrometer described in this thesis would be able to make these observations, with small modifications that would permit observations to be made at these wavelength. In addition, observations should be undertaken at 8.0 to 9.5 microns where neither ammonia nor methane have strong absorption features. At these wavelengths one would be observing the clouds. In this 8.0 to 9.5 micron region our instrument should be able to image the bands and zones of Jupiter, to probe for spectral differences and cloud features. Such observations should increase our understanding of Jupiter's cloud structure.

(D) Observations of Mercury

The observations of Mercury were made with the newly built Cornell 25" telescope at Mount Pleasant, Ithaca, New York. The telescope has a focal ratio f/13.5 . The spectrometer's acceptance beam size is 7.8" x 78" . The dewar described in section III-B was used with the spectrometer. The spectrometer operated in the 10.5∿13μm region with a resolution $\lambda/\Delta\lambda$ around 300. The chopping frequency was 10 cycles per second.

The observational procedure was carried out a little differently from the observations of α-orionis and Jupiter. First, Sun spectra were used for correction spectra rather than lunar spectra. There are no known molecular lines in this region. Its temperature at 11.10μm is 5030°K(Saildy & Goody). The observations were made on August 3, 1976. At that time the Sun was about an hour away from Mercury, and was observed through roughly the same air mass as Mercury. Secondly, Mercury is so faint in broad day light that we were unable to see it in visible light. The way to find Mercury was the following: We pointed the telescope in the correct region and scanned for the infrared signal. The signal is so strong that one can see it go off scale on the synchronous demodulator. The pointing accuracy of the telescope is 6 sec. of time in right ascension and 25 sec. of arc in declination. Thirdly, since we could not see Mercury visually for tracking, we adapted a different method for tracking Mercury. Since our computer programming is set up in such a way that the data taken when the mask is moving forward and moving backward are stored in different areas, we only took data when the mask was moving forward. When the mask was moving backward we maximized the signal to assure correct pointing and waited for the next forward pass. Any noise introduced when moving the telescope for maximizing the signal would have gone into the backward-pass data bins and those data points were thrown away anyway. Since each pass takes 51 sec. only, Mercury remained at essentially the same position during the forward data taking pass.

Two runs of Mercury and two runs of the Sun were taken. Each run consisted of ten scans of the sources. Figure (6-13) shows the raw spectra of Mercury and the Sun. Since Ithaca has a lot of moisture in the air during the summer time, the correction for atmospheric features is more difficult than at Kitt Peak and is done in a different way. A constant was added to the Mercury spectra such that atmospheric features in the Mercury/Sun ratio spectrum were minimized. This step ensures that the atmospheric features are largely corrected. The Mercury spectrum which has a constant added to it was then multiplied by another constant to make its amplitude as close to that of the solar spectrum as possible. The solar spectrum was then subtracted from the modified Mercury spectrum. The multiplication of the Mercury spectrum by a constant assured that atmospheric features in the two spectra had similar amplitudes before the subtraction step. This difference spectrum was then added to a "perfect" solar spectrum which is calculated according to the blackbody function appropriate to the solar temperature. What one gets from these procedures is:

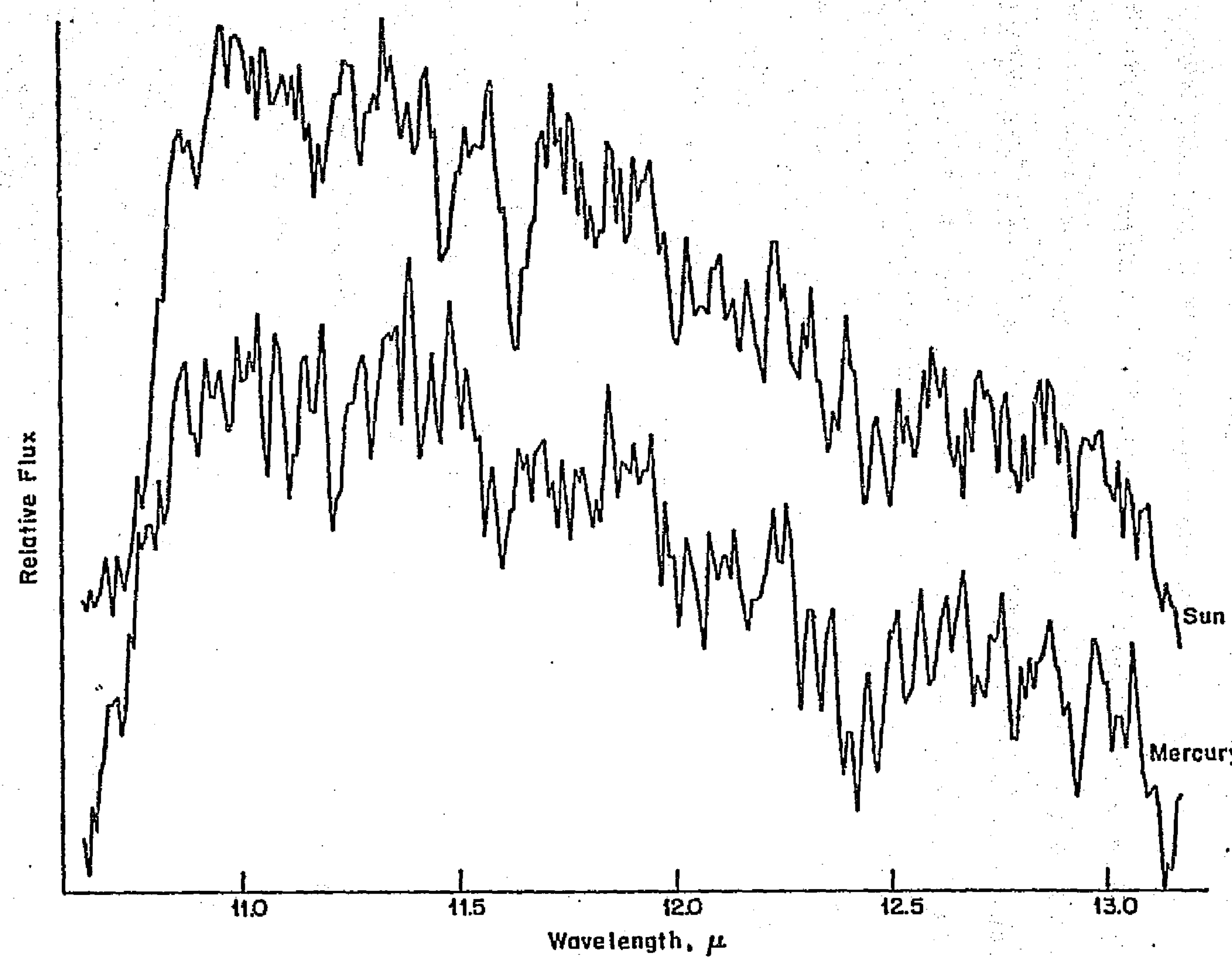

Figure 6-13. The raw spectra of Mercury and the Sun.

Final Mercury Spectrum

= observed corrected Mercury spectrum - observed solar spectrum + perfect solar spectrum

= ("perfect" Mercury spectrum + noise in the Mercury spectrum) - ("perfect" solar spectrum + noise in the solar spectrum) + "perfect" solar spectrum

= "perfect" Mercury spectrum + (noise in the Mercury spectrum - noise in the solar spectrum)

Any systematic noise such as emission and absorption due to the sky or to the telescope will be subtracted away. The advantage of this method is that the final spectrum is obtained through subtraction rather than by division. Division, in the low signal portion of the spectrum, produces deceptive high noise spikes in the ratio spectrum. The method we have used tends to eliminate these.

Since this will be the first high resolution Mercury spectrum obtained, we will calculate Mercury's disk integrated infrared temperature and compare this temperature with the observed one. Morrison and Sagan (1967) had calculated the infrared brightness temperature of the center-of-disk as a function of phase angle and heliocentric longitude, but there is no disk integrated infrared temperature available in the literature. In the following we will discuss the factors that may affect the brightness temperature, and then present a method of calculating the disk integrated infrared brightness and compare it with our observation. A good review of thermophysics of Mercury is given by Morrison (1970).

In 1965, Pettingill and Dyce (1965) used radar to discover that Mercury has a rotation period of 59 days, two thirds of the orbital period, instead of an 88 day synchronous rotation around the Sun. This implies that Mercury has a solar day, on the planet, about 176 terrestrial days long, equal to two orbital revolutions in three rotations. Mercury's non-synchronous rotation leads to time-dependent thermal emission of the planet due to the diurnal variation of the insolation. This diurnal variation would not happen for a synchronously rotating Mercury. The diurnal variation changes the brightness temperature as a function of both phase angle and heliocentric longitude. It also allows a measurement of the thermal properties of Mercury's surface.

Because of the high eccentricity of Mercury's orbit, (e=0.2), the diurnal cycle of insolation is markedly different from longitude to longitude, and can differ by a factor of 2.5. The eccentricity enters in two ways. First, the variation in distance from the Sun produces a solar constant that varies by more than a factor of 2 from perihelion to aphelion. Second, the changing orbital angular velocity causes the apparent speed of the Sun across the sky to vary; near perihelion the angular velocity of revolution actually slightly exceeds the angular velocity of rotation, and the apparent planetocentric solar motion is retrograde (figure 6-14, Soter and Ulrichs, 1967). The two effects of the eccentricity reinforce one another, with the larger flux coming at a time when the angular rate of the Sun across the sky is largest. The two longitudes (180° apart)

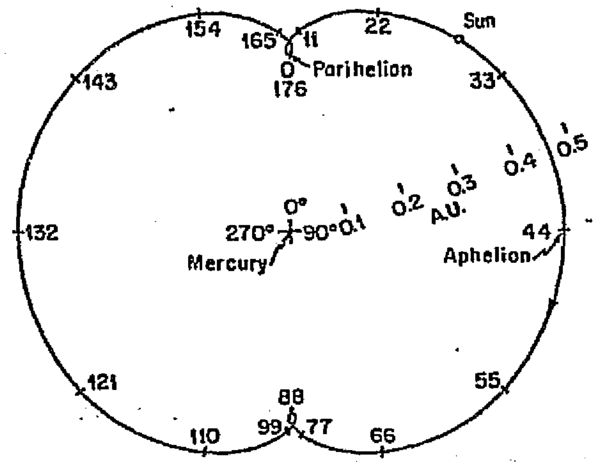

Figure 6-14. Diurnal path of the Sun about Mercury, drawn to scale. The relative positions of the Sun are marked at 11 day intervals with the planet held as a fixed reference. Planeto-graphic longitude are indicated for Mercury. (Taken from Soter and Ulrichs, 1967).

that see the Sun overhead at perihelion receive more than two and a half as much energy per period as the longitude 90° away, where the Sun is always small and rapidly moving while near the zenith.

Besides the insolation geometry, a possible atmosphere on Mercury will also affect the thermal emission. CO_2 is a major product for a possible secondary atmosphere, furthermore, since CO_2 could have been photodissociated and reduced to CO by preferential loss of oxygen, Fink et al (1973) had set up a search for a possible Mercury atmosphere of CO_2 and CO. They set up an upper limit 1.0×10^{-4} mb surface pressure for CO_2 and 2.0×10^{-5}mb for CO. Mariner 10's results also suggest that Mercury has no atmosphere although it may have a thin layer of He and other inert gas trapped by Mercury's magnetic field.

The optical observations of Mercury show that the integral spectral reflectivity of Mercury is quite similar to that for the integral moon (McCord and Adams, 1972). The Bond albedo of Mercury (de Vancouleurs, 1964) is 0.058.

In our model calculation we assume the following things. This model has been described by Murdock (1974):

1. The emission from the dark side at the phase angle we observed is negligible. On the day we made our observations, August 3, 1976, the illuminated portion amounted to 0.973 of the total disk and the dark portion was 0.017. The dark side temperature is about 110°K, which at 10μm has a flux 6.7181×10^{-8}watt-cm^{-2}-μ^{-1}-sr^{-1}. The flux for 500°K at 10μm is 7.1007×10^{-3}watt-cm^{-2}-μ^{-1}-sr^{-1}, so the contribution from the dark side

is negligible.

2. At infrared wavelengths, the radiation that reaches the observer originates very near the surface, so the infrared temperature is assumed equal to the insolation temperature. Soter and Ultichs' (1967) results show that the day time temperature is independent of the thermal properties of the surface material and determined largely by the insolation temperature.

3. The infrared emissivity we assumed was 0.9, which is the lunar value. We choose this value since Mercury's surface may be similar to the lunar surface.

In figure (6-15) we choose two coordinate systems on Mercury surface. The unprimed system is the "solar system" with the z-axis pointing towards the Sun. A is the subsolar point. The hemisphere above the plane BCD facing the Sun is the illuminated part. The primed system is the "earth system' with the z'-axis pointing towards the earth. A' is the subearth point. The hemisphere above the plane B'C'D' facing the earth is the portion that is being seen from earth. The two systems are different by an angle α with the x-axis as the common axis.

If the surface is in equilibrium with sunlight and cannot conduct heat away, the subsolar point temperature is:

$$T_o = \left(\frac{S(1-A)}{\sigma\varepsilon R^2}\right)^{1/4} \qquad (6\text{-}1)$$

where S is solar constant at earth, equal to $1.360\text{x}10^{6}$ erg $cm^{-2}s^{-1}$

A is the Bond albedo for Mercury, assumed to be 0.058.

σ is the stefan-Boltzmann constant equal to $5.67\text{x}10^{-5}$ erg $cm^{-2}s^{-1}$

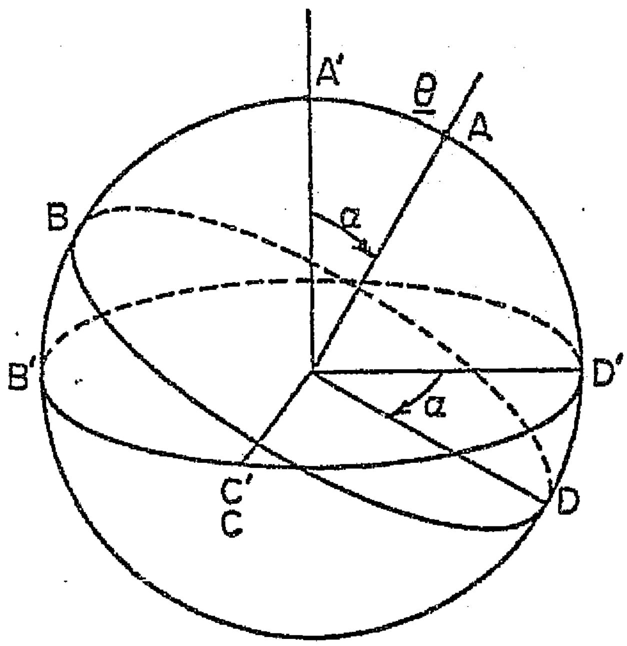

Figure 6-15. Two coordinate systems on the surface of Mercury. The unprimed system is the "solar system" with the Z-axis pointing towards the Sun. A is the subsolar point. The primed system is the "earth system" with the Z'-axis pointing towards the earth. A' is the sub-earth point.

ε is the infrared emissivity at 10μm from the surface, assumed to be 0.9

R is the distance between Mercury and the Sun in astronomical units

Mercury's subsolar point temperature varies with distance from the Sun as $R^{-1/2}$ and therefore is a function of heliocentric longitude due to the eccentricity we discuss above.

In the unprimed system the temperature distribution on the surface will be concentric isothermal bands around the subsolar point. The temperature of a band at colatitude θ is given by

$$T(\theta) = T_o \cos^{1/4}\theta \qquad (6\text{-}2)$$

The total intensity at any wavelength region will be composed of the contributions at that wavelength from many isothermal regions each with its own apparent area.

Since one is interested in the flux coming to the earth one will have,

$$dF'_\lambda = I_\lambda(\theta',\phi')\, dA' \qquad (6\text{-}3)$$

$$= I_\lambda(\theta',\phi')\, r^2 \sin\theta' d\theta' d\phi' \qquad (6\text{-}4)$$

$$= E_\lambda(\theta',\phi') \cos\theta' r^2 \sin\theta' d\theta' d\phi' \qquad (6\text{-}5)$$

where dF'_λ is the flux at wavelength λ coming from the area dA'

I_λ is the intensity at (θ',ϕ')

dA' is the differential area on Mercury

r is the radius of Mercury

$\Xi_\lambda(\theta',\phi') = I_\lambda(\theta',\phi')/\cos\theta'$ is the component of flux that radiates toward the earth.

$\Xi_\lambda(\theta',\phi')$ is a complicated function of (θ',ϕ') bacause the temperature distribution is a complicated function of (θ',ϕ'). However, one can convert the system to the "sun coordinate" where $\Xi_\lambda(\theta,\phi)$ is a simple function.

Since $dA' = dA$ (6-6)

$$\cos\theta' = \cos\theta\cos\alpha - \sin\theta\sin\phi\sin\alpha \qquad (6\text{-}7)$$

equation(6-5) becomes

$$dF_\lambda = \Xi_\lambda(\theta)\,[\cos\theta\cos\alpha - \sin\theta\sin\phi\sin\alpha]\,r^2\sin\theta d\theta d\phi$$

where

$$\Xi_\lambda(\theta) = \frac{C_1}{\lambda^5}\,\frac{1}{e^{C_2/kT(\theta)}-1} \qquad (6\text{-}8)$$

where $C_1 = 1.1909 \times 10^4$ watt $cm^{-1}\mu^{-1}sr^{-1}$

$C_2 = 1.4388 \times 10^4\,\mu K$

and $T(\theta)$ is given by (6-2)

so

$$F_\lambda = r^2\int d\theta\int d\phi\; \Xi_\lambda(\theta)(\sin\theta\cos\theta\cos\alpha - \sin^2\theta\sin\phi\sin\alpha) \qquad (6\text{-}9)$$

The integral (6-9) can be separated into two parts, for $\theta \le \underline{\theta}$

where $\underline{\theta} = \frac{\pi}{2} - \alpha$ (6-10)

is the limit of the cap shared by both the Sun and the earth, i.e. the limit of integration over $d\theta$ can ϕ go from 0 to 2π. For $\theta > \underline{\theta}$, the limit of the integral over d is constrained by the physical condition that some part on ϕ that is illuminated by the Sun can not be seen from the earth.

So (6-9) becomes

$$F_\lambda = r^2\int_0^{\theta} d\theta\int_0^{2\pi} d\phi \; \Xi_\lambda(\theta)(\sin\theta\cos\theta\cos\alpha - \sin^2\alpha\,\sin\phi\sin\alpha)$$

$$+ r^2\int_{\theta}^{\frac{\pi}{2}} d\theta\int_{\phi_1(\theta)}^{\phi_2(\theta)} d\phi \; \Xi_\lambda(\theta)(\sin\theta\cos\theta\cos\alpha - \sin^2\theta\sin\phi\sin\alpha) \qquad (6\text{-}11)$$

To find $\phi_1(\theta)$ and $\phi_2(\theta)$ one notices that ϕ is given when $\theta'=90°$.

From (6-7)

$$\cos\theta' = \cos\theta\cos\alpha - \sin\theta\sin\phi\sin\alpha$$

$$\theta' = \frac{\pi}{2} \Longrightarrow \sin\phi = \cot\alpha\cot\theta \qquad (6\text{-}12)$$

and

$$\phi = \sin^{-1}(\cot\alpha\cot\theta) \qquad (6\text{-}13)$$

Since ϕ will also be symmetric about the y-axis, equation (6-11) can be rewritten as:

$$F_\lambda = r^2\int_0^{\frac{\pi}{2}-\alpha} d\theta\int_0^{2\pi} d\phi \; \Xi_\lambda(\theta)(\sin\theta\cos\theta\cos\alpha - \sin^2\theta\sin\phi\sin\alpha)$$

$$+ \int_{\frac{\pi}{2}-\alpha}^{\frac{\pi}{2}} d\theta\int_{\pi-\sin^{-1}(\cot\alpha\cot\theta)}^{2\pi+\sin^{-1}(\cot\alpha\cot\theta)} \Xi_\lambda(\theta)(\sin\theta\cos\theta\cos\alpha - \sin^2\theta\sin\phi\sin\alpha) \qquad (6\text{-}14)$$

After evaluating the integral one obtains the following:

$$F_\lambda = 2\pi r^2\cos\alpha\left[\Xi_\lambda(\theta)\,\frac{\sin^2\theta}{2}\right]_0^{\frac{\pi}{2}-\alpha} + \pi r^2\cos\alpha\left[\Xi_\lambda(\theta)\frac{\sin^2\theta}{2}\right]_{\frac{\pi}{2}-\alpha}^{\frac{\pi}{2}}$$

$$+\ 2r^2\int_{\frac{\pi}{2}-\alpha}^{\frac{\pi}{2}} d\theta\ \sin^{-1}(\cot\alpha\cot\theta)\ \sin\theta\cos\theta\cos\alpha\ \Xi_\lambda(\theta)$$

$$+\ r^2\left[\overline{\Xi_\lambda(\theta)\left(\cos\theta\sqrt{\sin^{-2}\alpha-\cos^2\theta}\ +\ \sin^{-2}\alpha\sin^{-1}\frac{\cos\theta}{|\sin\alpha|}\right)}\right]_{\frac{\pi}{2}}^{\frac{\pi}{2}-\alpha}$$

(6-15)

where

$$\left[\overline{\Xi_\lambda(\theta)\ \frac{\sin^2\theta}{2}}\right]_{0}^{\frac{\pi}{2}-\alpha}$$

is the mean of ($\Xi_\lambda(\theta)\ \frac{\sin^2\theta}{2}$) in the interval of θ from 0 to $\frac{\pi}{2}-\alpha$. The same meaning applies to the third term of (6-15).

As a check of equation (6-15), if $\alpha=0$, that means when subsolar point and subearth point coinside, let $\Xi(\theta)$=constant evaluating (6-15) gives:

$$F\ =\ \pi r^2\Xi$$

If $\alpha=\frac{\pi}{2}$, that means the subsolar point and subearth point are 90° apart. With $\Xi(\theta)$ assumed to be constant, equation (6-15) gives

$$F\ =\ \frac{\pi r^2}{2}\ \Xi$$

which is as one expects since one is seeing half of Mercury.

Equation (6-15) can be readily integrated on a computer. It is applied to our case with the following physical parameters:

Date: August 3, 1976 .

Phase Angle: 53°

Radius vector: 0.414 A.U.

Orbital longitude: 198.09°

Mercury perihelion point: 0.3075 A.U.

Subsolar temperature at perihelion point: 700°K

Subsolar temperature at α=53°: 603°K

Equation (6-15) was computed on a LSI mini computer at each wavelength, from 10.6 to 13.2μm. The program and the result are shown in the Appendix D. The integral was divided into twenty steps. $\Xi(\theta)$ was evaluated from equation (6-8)

$$\Xi_\lambda(\theta) = \frac{C_1}{\lambda^5} \frac{1}{e^{C_2/kT(\theta)}-1}$$

where $T(\theta) = T_o \cos^{1/4}\theta$

The calculated spectrum is a measure of color temperature and is used to compare with the observed spectrum. Figure (6-16) shows the final Mercury spectrum conected for solar temperature, with a number of blackbody slopes shown to match. The calculated spectrum (cross) matches the blackbody temperature 525°K, which also matches the observed spectrum. We concluded that the best fit lies in the 500°K region. Murdock (1974) measured a effective brightness temperature at 10.8μm at the same phase angle to be around 650°K. Our results disagree with his results.

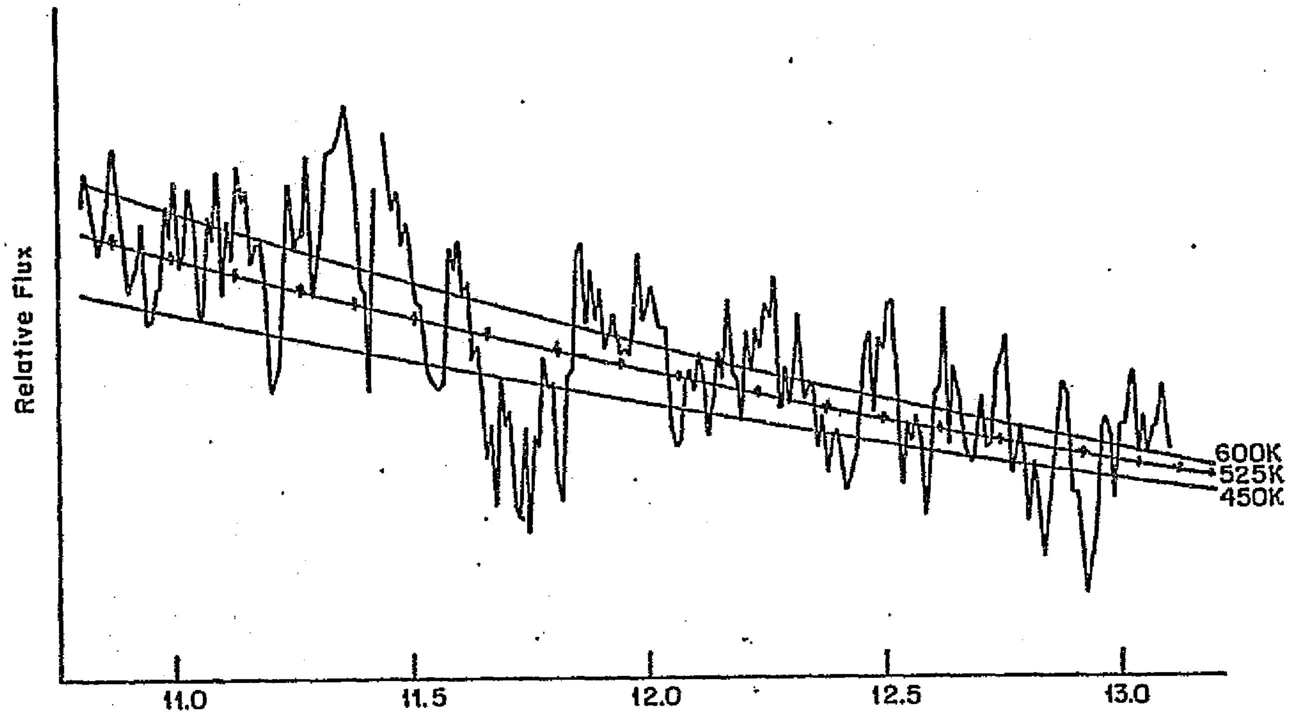

Figure 6-16. The final Mercury spectrum, corrected for solar temperature, with a number of blackbody slopes shown to match.

APPENDIX A

ESTIMATE OF CODING ERROR FOR FOURIER TRANSFORM SPECTROMETRY

Let ξ be the path difference in a two beam interferometer. $P(\nu)$ is the power at wavelength ν, (i.e. the spectral density function) ν here is taken to be $1/\lambda$. $S(\xi)$ is the power received for path difference ξ. Then (p.96 Stewart)

$$S(\xi) = \int_0^\infty P(\nu)\cos^2(2\pi\xi\nu)\,d\nu \qquad \text{A-1}$$

$$= 1/2P_o + 1/2\int_0^\infty P(\nu)\cos(4\pi\xi\nu)\,d\nu \qquad \text{A-2}$$

The reciprocal Fourier property is (Morse and Feshback P.454) that if

$$F(\xi) = \sqrt{\frac{2}{\pi}}\int_0^\infty \cos(\xi\nu) f(\nu)\,d\nu$$

Then $$f(\nu) = \sqrt{\frac{2}{\pi}}\int_0^\infty \cos(\xi\nu) F(\xi)\,d\xi$$

which implies, neglecting the constant term, that

$$P(\nu) = 16\int_0^\infty \cos(4\pi\xi\nu) s(\xi)\,d\xi \qquad \text{A-3}$$

Suppose we take measurement at (N+1) equally seperated steps in the variable ξ. Let the step length be τ, then

$$\xi = n\tau$$

In general τ is chosen such that

$$\tau = \frac{1}{4(\nu_{max} - \nu_{min})} \qquad \text{A-4}$$

which, if $\nu_{min} << \nu_{max}$, effectively implies sampling twice per cycle (Stewart, p.303).

One can now write the integral for $P(\nu)$ as

$$P(\nu) = 16\sum_{n=0}^{N} \tau S(n\tau) \cos(4\pi\nu n\tau) \qquad \text{A-5}$$

Now consider frequency $\nu = \nu_{min} + m\delta$

$$\text{where} \quad \delta = \frac{\nu_{max} - \nu_{min}}{N} \qquad \text{A-6}$$

and m is an integer. $m=0,1 \cdots N$

The $\delta P(\nu)$ is the power in the resolved spectral band width δ about frequency ν

$$\delta P(\nu) = 16\tau\delta \sum_{n=0}^{N} S(n\tau) \cos(4\pi\nu n\tau) \qquad \text{A-7}$$

but

$$\tau\delta = \frac{\delta}{4(\nu_{max} - \nu_{min})}$$

$$= \frac{\delta}{4N\delta}$$

$$= \frac{1}{4N} \qquad \text{A-8}$$

Therefore

$$\delta P(\nu) \quad = \quad \frac{4}{N} \sum_{n=0}^{N} S(n\tau) \cos(4\pi\nu n\tau) \qquad \text{A-9}$$

Writing this out in matrix form, with $\theta_1 = 4\pi\tau\nu_{min}$, $\theta_2 = 4\pi\tau(\nu_{min}+\delta)$ and with $\pi(\nu_{min}) \equiv \delta P(\nu_{min})$ we have

$$\begin{bmatrix} \pi(\nu_{min}) \\ \pi(\nu_{min}+\delta) \\ \vdots \\ \pi(\nu_{max}-\delta) \\ \pi(\nu_{max}) \end{bmatrix} \equiv \delta \begin{bmatrix} P(\nu_{min}) \\ P(\nu_{min}+\delta) \\ \vdots \\ P(\nu_{max}-\delta) \\ P(\nu_{max}) \end{bmatrix} - \frac{4}{N} \begin{bmatrix} 1 & \cos\theta_1 \cdots\cdots & \cos N\theta_1 \\ 1 & \cos\theta_2 \cdots\cdots & \cos N\theta_2 \\ \vdots & & \\ 1 & \cos\theta_{N-1} \cdots & \cos N\theta_{N-1} \\ 1 & \cos\theta_n \cdots\cdots & \cos N\theta_N \end{bmatrix} \begin{bmatrix} S(0) \\ S(1) \\ \vdots \\ S(N) \end{bmatrix}$$

$$\text{or} \qquad \pi \quad = \quad W^{-1}S \qquad \text{A-10}$$

From (2-8)

$$\Delta_j = (A_{j1} + \cdot \cdot \cdot + A_{jN})^{1/2}$$

$$= \sqrt{\frac{16}{N^2}} (1 + \cos^2\theta_j + \cdot \cdot \cdot + \cos^2 N\theta_j)^{1/2}$$

$$= \frac{4}{N} \left(\sum_{n=0}^{N} \cos^2 n\theta_j \right)^{1/2}$$

$$\sim \frac{4}{N} \sqrt{\frac{N+1}{2}}$$

$$\sim \sqrt{\frac{8}{N}} \qquad \text{for } N>>1 \qquad \text{A-11}$$

The SNR improvement is the reciprocal of this quantity.

APPENDIX B

```
0001                          NAM    CMND
0002                          EXTR   IER,ØTT,ØTL,CRLF
0003                          EXTR   ERR,XEQ,ØFPA
0004                          EXTR   XA,XB,FIX,FLT
0005  0100                    ABS    :100
0006                   *PRINT NAME
0007  0100  0110              ZAR
0008  0101  F900              JST    ØTL
            0000
0009  0102  017B              DATA   NAME
0010  0103  F201              JMP    S+2
0011                   *
0012                   *CØMMAND INTERPRETER
0013                   *
0014  0104  0800       CMND   ENT
0015  0105  0A00              EIN
0016  0106  4005              CIE                 ENABLE PANIC BUTTØN
0017  0107  F900              JST    CRLF         PRINT PRØMPT CHARACTER
            0000
0018  0108  C687              LAP    :87
0019  0109  F900              JST    ØTT
            0000
0020  010A  C6AA              LAP    '*'
0021  010B  F900              JST    ØTT
            0000
0022  010C  1200              RØV                 CLEAR MATH FLAG
0023  010D  0108              ZXR
0024  010E  F900              JST    IER          INPUT CØMMAND
            0000
0025  010F  C0D3              CAI    'S'
0026  0110  F25C              JMP    STATUS
0027  0111  C0D4              CAI    'T'
0028  0112  E24E              LDX    TRANS
0029  0113  C0D2              CAI    'R'
0030  0114  E24D              LDX    READ
0031  0115  C0C3              CAI    'C'
0032  0116  E24C              LDX    CLEAR
0033  0117  3809              JXN    ØKF
0034  0118  1400              SØV                 SET MATH FLAG
0035  0119  C0D0              CAI    'P'
0036  011A  E249              LDX    PUNCH
0037  011B  C0C7              CAI    'G'
0038  011C  E243              LDX    GRAPH
0039  011D  C0D6              CAI    'V'
0040  011E  E249              LDX    CRT
0041  011F  3801              JXN    ØKF
0042  0120  F900       BAD    JST    ERR
            0000
0043  0121  EA48       ØKF    STX    FUNC         SAVE CALL ADDRESS
0044  0122  0108              ZXR
0045  0123  F900              JST    IER          FETCH BEAM
            0000
0046  0124  C0AB              CAI    '+'
```

```
0125  E24C          LDX   NP
0126  C0AD          CAI   '-'
0127  E24F          LDX   NM
0128  3835          JXN   ØKB
0129  3249          JØR   BAD         IF MATH FLAG CLEAR
012A  0523          XRP               RESET INDICES
012B  E900          STX   XA
      0000
012C  E900          STX   XB
      0000
012D  EB1D          STX   *XC
012E  C5FF          LXM   255         RESET CØUNT
012F  EA3B          STX   CNT
0130  0108          ZXR
0131  C0C4          CAI   'D'
0132  E233          LDX   FSB
0133  C0D2          CAI   'R'
0134  E232          LDX   FDV
0135  2855          JXZ   BAD
0136  EA35          STX   MATH        SAVE MATH PØINTER
0137  F900          JST   XEQ         WAHT FØR GØ
      0000
              *MATH LØØP
0138  FB33    MLP   JST   *MATH
0139  9002          DATA  :9002,:9202,:9402
013A  9202
013B  9402
013C  D900          IMS   XA          BUMP CØUNTERS
      0000
013D  D900          IMS   XB
      0000
013E  211A          JAZ   ØKM         MATH ØK?
013F  1340          SAØ               NØ!
0140  C6D2          LAP   'R'         PRINT ERRØR MSG.
0141  3203          JØR   ØVFL
0142  F900          JST   ØTL
      0000
0143  0184          DATA  UNDER
0144  F202          JMP   FLØW
0145  F900    ØVFL  JST   ØTL
      0000
0146  0187          DATA  ØVER
0147  C600    FLØW  LAP   0
0148  F900          JST   ØTL
      0000
0149  018A          DATA  MSG
014A  F900          JST   FLT
      0000
014B          XC    REF
014C  0179          DATA  XCF
014D  F900          JST   ØFPA
      0000
014E  0179          DATA  XCF
```

```
014F  C63D          LAP    :8D
0150  F900          JST    ØTL
      0000
0151  0197          DATA   ZERØ
0152  B707          LDA    *XC        CLEAR BAD ELEMENT
0153  1050          ALA    1
0154  8A14          ADD    TP
0155  0043          TAX
0156  0110          ZAR
0157  9C00          STA    @0
0158  9C01          STA    @1
0159  DF0E   ØKM    IMS    *XC
015A  DA10          IMS    CNT
015B  F623          JMP    MLP
015C  E20C          LDX    TP
015D  F201          JMP    ØKB+1
015E  F900   ØKB    JST    XEQ        WAIT FØR GØ
      0000
015F  FB0A          JST    *FUNC      CALL FUNCTIØN
0160  F65B          JMP    CMND+1
0161         TRANS  REF
0162         READ   REF
0163         CLEAR  REF
0164         PUNCH  REF
0165         GRAPH  REF
0166         FSB    REF
0167         FDV    REF
0168         CRT    REF
0169  1400   TP     DATA   :1400
016A  0000   FUNC   DATA   0
016B  0000   CNT    DATA   0
016C  0000   MATH   DATA   0
016D  4006   STATUS CID               KILL PANIC SWITCH
016E  0110          ZAR
016F  F900          JST    ØTL
      0000
0170  01A1          DATA   TATUS
0171  F900          JST    ØFPA
      0000
0172  1000   NP     DATA   :1000
0173  0110          ZAR
0174  F900          JST    ØTL
      0000
0175  01A7          DATA   NMM
0176  F900          JST    ØFPA
      0000
0177  1200   NM     DATA   :1200
0178  F673          JMP    CMND+1
0179  0000   XCF    RES    2,0
017B  8D3A   NAME   DATA   :8D3A,:8AA0
017C  8AA0
017D  C8D4          TEXT   'HTS: 1X255'
017E  D3BA
```

```
           017F  A0B1
           0180  D3B2
           0181  B5B5
0133       0182  8D8A               DATA   :8D8A, 0
           0183  0000
0134       0184  8AD5   UNDER       DATA   :8AD5
0135       0185  CEC4               TEXT   'NDER'
           0186  C5D2
0136       0187  8ACF   ØVER        DATA   :8ACF
0137       0188  D6C5               TEXT   'VER'
           0189  D2A0
0138       018A  C6CC   MSG         TEXT   'FLØW ØCCURRED'
           018B  CFD7
           018C  A0CF
           018D  C3C3
           018E  D5D2
           018F  D2C5
           0190  C4A0
0139       0191  C1D4               TEXT   'AT ELEMENT'
           0192  A0C5
           0193  CCC5
           0194  CDC5
           0195  CED4
0140       0196  A000               DATA   :A000
0141       0197  ACA0   ZERØ        TEXT   ', REPLACED'
           0198  D2C5
           0199  D0CC
           019A  C1C3
           019B  C5C4
0142       019C  A0C2               TEXT   ' BY ZERØ'
           019D  D9A0
           019E  DAC5
           019F  D2CF
0143       01A0  AE8D               DATA   :AE8D
0144       01A1  D4C1   TATUS       TEXT   'TATUS: N+='
           01A2  D4D5
           01A3  D3BA
           01A4  A0CE
           01A5  ABBD
0145       01A6  A000               DATA   :A000
0146       01A7  ACA0   NMM         TEXT   ', N-= '
           01A8  CEAD
           01A9  BDA0
0147       01AA  0000               DATA   0
0148                                END
0000 ERRØRS
```

```
                      NAM   TRANS
                      NAM   RTTR,RTØP
                      EXTR  DISP
                      EXTR  IKB,ØTL,ØFPA,CRLF,ERR
                      EXTR  DPACC,DPFLT
                      EXTR  DPN:,DPSUB:,DPDIV:,DPSM:
                      EXTR  XB,XC,FAD
                      EXTR  DPFIX
0000                  REL   0
                *
                *IX255 HTS PRØCESSØR
                *
0000  0800      TRANS ENT
0001  E2BC            LDX   BPNT
0002  1328            LLX   1          INDIRECT BIT ØN
0003  1400            SØV
0004  11A8            RRX   1
0005  EA88            STX   BEAM
0006  EA88            STX   BEAM+1
0007  B2A0            LDA   ZCT        CLEAR BUFFERS
0008  9AA0            STA   CNT
0009  E2A1            LDX   NT
000A  0110            ZAR
000B  9C00      CLR   STA   @0
000C  0128            IXR
000D  DA9B            IMS   CNT
000E  F603            JMP   CLR
000F  C6BF            LAP   '?'
0010  F900            JST   ØTL
0011  0137            DATA  MØDE
0012  F900            JST   IKB
0013  C0CD            CAI   'M'
0014  F205            JMP   MØN
0015  C0D4            CAI   'T'
0016  F208            JMP   TAPE
0017  C0C9            CAI   'I'
0018  F209            JMP   INVS
0019  F900            JST   ERR
001A  0110      MØN   ZAR
001B  0210            CAR
001C  9AA0            STA   TETR
001D  0110            ZAR
001E  F20D            JMP   NEXT
001F  0110      TAPE  ZAR
0020  9A9C            STA   TETR
0021  F202            JMP   T4
0022  C601      INVS  LAP   1
0023  9A99            STA   TETR
0024  0108      T4    ZXR
0025  F900            JST   IKB
0026  C0AB            CAI   '+'
0027  0408            CXR
0028  C0AD            CAI   '-'
0029  0108            ZXR
```

```
002A  EA8E            STX   TREM
002B  0110            ZAR
002C  E292  NEXT      LDX   MASK
002D  0128            IXR
002E  0210            CAR                CHANGE DIRECTIØN
002F  9A7F            STA   DIR
0030  C0FF            CAI   :FF
0031  F203            JMP   FØWD
0032  0030            TXA
0033  8A7A            ADD   H255
0034  0048            TAX
0035  EA76  FØWD      STX   MSK1
0036  C7F5            LAM   245
0037  9A79            STA   DCT2
0038  C7FF            LAM   255          START DATA CØUNT
0039  9A76            STA   DCT
003A  FAB1            JST   TURNØN       WAIT FØR LIGHT
            *INPUT LØØP
003B  FABB  ILP       JST   MØNS         INPUT
003C  9A6C            STA   CNT          &SAVE
003D  EA6C            STX   CNT+1
003E  C7FF            LAM   255          SPECTRUM CØUNT
003F  9A72            STA   SCT
0040  B26B            LDA   MSK1         RESET MASK PØINTER
0041  9A6B            STA   MSK2
0042  B271            LDA   IB           GET BUFFER PØINTER
0043  9A0F            STA   IBP
            *TRANSFØRM CØLUMN TØ INPUT BUFFER
0044  E265  TLP       LDX   CNT+1
0045  0110            ZAR
0046  D366            CMS   *MSK2
0047  F208            JMP   T1A
0048  B274            LDA   TETR
0049  2163            JAL   $+4
004A  0110            ZAR
004B  0108            ZXR
004C  F204            JMP   T1
004D  B25B            LDA   CNT
004E  F900            JST   DPN:
004F  F201            JMP   T1
0050  B258  T1A       LDA   CNT
0051  DA5B  T1        IMS   MSK2
0052  F900            JST   DPACC        ADD
0053  0000  IBP       DATA  0
0054  C202            AXI   2            BUMP PØINTER
0055  EE02            STX   IBP
0056  DA5B            IMS   SCT          DØNE?
0057  F613            JMP   TLP          NØ
0058  E253            LDX   MSK1         YES, MØVE CØLUMN
0059  0128            IXR                +1IF FWD
005A  B254            LDA   DIR
005B  C000            CAI   0
005C  C302            SXI   2            -1IF REV.
005D  EA4E            STX   MSK1
```

```
005E  DA52         IMS   DCT2
005F  F201         JMP   S+2
0060  40C7         SEL   24,7
0061  DA4E         IMS   DCT        END ØF RØW?
0062  F627         JMP   ILP        NØ
            *END ØF RØW STØP TEST
0063  B259         LDA   TETR
0064  2081         JAM   S+2
0065  F2[illegible]         JMP   STØP
0066  3408         JSS   STØP       SS DØWN?
0067  48C7         SSN   :C7        NØ, STØP DØWN?
0068  F206         JMP   STØP       YES
0069  FA56         JST   ACC        NØ, SAVE DATA
006A  E24D         LDX   NØEM
006B  0110         ZAR
006C  F100         JMP   DISP
006D  B241  RTTR   LDA   DIR
006E  F642         JMP   NEXT
006F  E243  STØP   LDX   NI
0070  C601         LAP   I
0071  F100         JMP   DISP
0072  C6BF  RTØP   LAP   '?'
0073  F900         JST   ØTC
0074  011F         DATA  MSG
0075  F900         JST   IKB
0076  C0CE         CAI   'N'        ABØRT LAST PASS?
0077  F203         JMP   NØ         NØ
0078  C0D9         CAI   'Y'        YES
0079  F203         JMP   YES        YES
007A  F608         JMP   RTØP       WRØNG ENTRY
007B  FA44  NØ     JST   ACC        SAVE DATA
007C  F203         JMP   Y2
007D  C6AC  YES    LAP   ','        PRINT ABØRT
007E  F900         JST   ØTC
007F  0128         DATA  ABT
0080  B234  Y2     LDA   CT         SET CØUNTER
0081  9A30         STA   SCT
0082  0350         ARP              RESET SUBSCRIPTS
0083  9900         STA   XB
0084  9900         STA   XC
0085  E230         LDX   NPEM
            *ADD TØ BEAM ARRAY
0086  EE33  ALP    STX   IBP
0087  B400         LDA   @0         GET DATA
0088  E401         LDX   @1
0089  F900         JST   DPFLT      FLØAT IT
008A  9A21         STA   MSK1       SAVE IT
008B  EA21         STX   MSK2
008C  F900         JST   FAD        ADD TØ BEAM
008D  00AC         DATA  MSK1
008E  0000  BEAM   RES   2,0
0090  D900         IMS   XB         BUMP SUBSCRIPTS
0091  D900         IMS   XC
0092  E63F         LDX   IBP
```

```
0093  C202              AXI   2
0094  DA1D              IMS   SCT        DØNE?
0095  F60F              JMP   ALP        NØ
                  *PRINT PASS CØUNT
0096  F900              JST   CRLF
0097  C702              LAM   2
0098  9A23              STA   CØN1
0099  E21C              LDX   NPEM
009A  0110        MK    ZAR
009B  E401              LDX   @1
009C  F900              JST   DPFLT
009D  9A0E              STA   MSK1
009E  EA0E              STX   MSK2
009F  F900              JST   ØFPA
00A0  00AC              DATA  MSK1
00A1  0110              ZAR
00A2  F900              JST   ØTL
00A3  0130              DATA  RUNS
00A4  E212              LDX   NMEM
00A5  DA16              IMS   CØN1
00A6  F60C              JMP   MK
00A7  F7A7        T2    RTN   TRANS
                  *DATA STØRAGE
00A8  FA00        ZCT   DATA  -1536
00A9  0000        CNT   DATA  0,0
00AA  0000
00AB  1400        NT    DATA  :1400
00AC  0000        MSK1  DATA  0
00AD  0000        MSK2  DATA  0
00AE  00FF        H255  DATA  255
00AF  0000        DIR   DATA  0
00B0  0000        DCT   DATA  0
00B1  0000        DCT2  DATA  0
00B2  0000        SCT   DATA  0
00B3  1800        NI    DATA  :1800
00B4  1802        IB    DATA  :1802
00B5  FE00        CT    DATA  -512
00B6  1400        NPEM  DATA  :1400
00B7  1600        NMEM  DATA  :1600
00B8  0000        NØEM  DATA  0
00B9  0000        TREM  DATA  0
00BA  9002        PLS   DATA  :9002
00BB  9202        MINS  DATA  :9202
00BC  0000        CØN1  DATA  0
00BD  0000        TETR  DATA  0
00BE  1000        BPNT  DATA  :1000
00BF              MASK  REF
                  *
                  *ADD INPUT ARRAY TØ TEMP ARRAY
                  *
00C0  0800        ACC   ENT
00C1  B604              LDA   TETR
00C2  2083              JAM   $+4
00C3  B60A              LDA   TREM
```

```
00C4  0210           CAR
00C5  F201           JMP   S+2
00C6  B617           LDA   DIR
00C7  C000           CAI   0
00C8  F202           JMP   S+3
00C9  E613           LDX   NPEM
00CA  F201           JMP   S+2
00CB  E614           LDX   NMEM
00CC  EE14           STX   NØEM
00CD  DC01           IMS   @1       BUMP CØUNTER
00CE  C202           AXI   2
00CF  EA12           STX   TBP      SAVE TEMP PØINTER
00D0  C7FF           LAM   255      DATA CØUNT
00D1  9E28           STA   CNT
00D2  E61F           LDX   NI       INPUT PØINTER
00D3  C202   A1      AXI   2        BUMP CØUNTER
00D4  EE81           STX   IBP      +SAVE
00D5  B618           LDA   TETR
00D6  2188           JAL   T5
00D7  B400           LDA   @0
00D8  E401           LDX   @1
00D9  1328           LLX   1
00DA  1B86           LLR   7
00DB  13A8           LRX   1
00DC  1356           LLA   7
00DD  10D6           ARA   7
00DE  F202           JMP   T6
00DF  B400   T5      LDA   @0
00E0  E401           LDX   @1
00E1  F900   T6      JST   DPACC
00E2  0000   TBP     DATA  0
00E3  C202           AXI   2        BUMP TEMP
00E4  EE02           STX   TBP
00E5  E692           LDX   IBP
00E6  0110           ZAR
00E7  9C00           STA   @0
00E8  9C01           STA   @1
00E9  DE40           IMS   CNT      DØNE?
00EA  F617           JMP   A1       NØ
00EB  F72B           RTN   ACC
             *
             *WAIT FØR ALIGNMENT PULSE
             *
00EC  0800   TURNØN  ENT
00ED  4006           CID            DISABLE AUTØ
00EE  48C1           SSN   :C1      LIGHT ØFF?
00EF  F601           JMP   S-1      NØ
00F0  0E00           SEM            YES BYTE ØN
00F1  49C1           SEN   :C1      LIGHT ØN?
00F2  F601           JMP   S-1      NØ
00F3  0F00           SWM            YES, BYTE ØFF
00F4  40C4           SEL   :C4      CLEAR FLAG
00F5  4005           CIE            ENABLE AUTØ
00F6  F70A           RTN   TURNØN
```

```
                    *
                    *INPUT FRØM MØNSANTØ
                    *  CØNVERT BCD TØ BINARY
                    *
00F7  0800   MØNS   ENT
00F8  B63B          LDA   TETR
00F9  208F          JAM   T3
00FA  C6FF          LAP   255
00FB  8E4B          ADD   DCT
00FC  1050          ALA   1
00FD  E644          LDX   TRBM
00FE  3802          JXN   S+3
00FF  8A08          ADD   DMTR
0100  F201          JMP   S+2
0101  8A05          ADD   DPTR
0102  0048          TAX
0103  B400          LDA   @0
0104  E401          LDX   @1
0105  F900          JST   DPFIX
0106  F70F          RTN   MØNS
0107  1002   DPTR   DATA  :1002
0108  1202   DMTR   DATA  :1202
0109  49C6   T3     SEN   :C6        FLAG
010A  F601          JMP   S-1        NØ
010B  5AC6          INX   :C6        YES, INPUT TØ X
010C  2843          JXZ   S-3        IGNØRE ZERØES
010D  C704          LAM   4          SET DIGIT CØUNT
010E  9E65          STA   CNT
010F  0110          ZAR              CLEAR TALLY
0110  9E63          STA   MSK2
0111  F206          JMP   M2
0112  1350   M1     LLA   1          X10
0113  9E66          STA   MSK2
0114  1351          LLA   2
0115  8E68          ADD   MSK2
0116  9E69          STA   MSK2
0117  0110          ZAR
0118  1B03   M2     LLL   4          GET NEXT DIGIT
0119  8E6C          ADD   MSK2       ADD TØ TALLY
011A  DE71          IMS   CNT        LAST DIGIT?
011B  F609          JMP   M1         NØ
011C  0048          TAX
011D  0110          ZAR
011E  F727          RTN   MØNS       YES
                    *TEXT STØRAGE
011F  8D8A   MSG    DATA  :8D8A
0120  C1C2          TEXT  'ABØRT LAST RUN?'
0121  CFD2
0122  D4A0
0123  CCC1
0124  D3D4
0125  A0D2
0126  D5CE
0127  BFA0
```

```
0317  0128  8D8A  ABT   DATA :8D8A
0318  0129  B1A0        TEXT '1 RUN ABØRTED,'
      012A  D2D5
      012B  CEA0
      012C  C1C2
      012D  CFD2
      012E  D4C5
      012F  C4AC
0319  0130  A0D2  RUNS  TEXT ' RUNS KEPT'
      0131  D5CE
      0132  D3A0
      0133  CBC5
      0134  D0D4
0320  0135  8D8A        DATA :8D8A,0
      0136  0000
0321  0137  8D8A  MØDE  DATA :8D8A
0322  0138  CDCF        TEXT 'MØNSANTØ,TAPE ØR INVERSE?'
      0139  CED3
      013A  C1CE
      013B  D4CF
      013C  ACD4
      013D  C1D0
      013E  C5A0
      013F  CFD2
      0140  A0C9
      0141  CED6
      0142  C5D2
      0143  D3C5
      0144  BFA0
0323                    END
0000  ERRØRS
```

```
                         NAM    IKB, IER, BIPT, XEQ
                         NAM    ØTT, ERR, CRLF
                         NAM    ØTL, ØFPA
0000                     REL    0
                  *
                  * PANIC SWITCH
                  *
0000  FB00               JST    *CMND
0001              CMND   REF
                  *
                  *KEYBØARD INPUT
                  *
0002  0800        IKB    ENT
0003  4038               SEL    7, 0       AUTØ-ECHØ
0004  4039               SEL    7, 1       KBD MØDE
0005  5939               RDA    7, 1       READ ØN FLAG
0006  403C               SEL    7, 4       RESET
0007  F705               RTN    IKB
0008  0800        IER    ENT
0009  FE07               JST    IKB
000A  C0DF               CAI    :DF        BACK ARRØW?
000B  FF0A               JST    *CMND      YES
000C  C08A               CAI    :8A        LINE FEED?
000D  FF0C               JST    *CMND      YES
000E  F706               RTN    IER        NEITHER, RETURN
                  *
                  *PAPER TAPE INPUT
                  *  DS0 = 0 FØR TTY
                  *        1 FØR HSR
                  *
000F  0800        BIPT   ENT
0010  5801        BIP2   ISA               READ SWITCHES
0011  13D0               LRA    1          DS0 UP FØR TTY
0012  220A               JØS    HSR        DØWN FØR HSR
0013  493B               SEN    7, 3       TTY BUSY?
0014  F604               JMP    BIP2       YES
0015  403A               SEL    7, 2       NØ, STEP READER
0016  4839        WT     SSN    7, 1       FLAG?
0017  F203               JMP    IT         YES
0018  0150               IAR               NØ, BUMP CØUNT
0019  2149               JAZ    BIP2       RESTART IF TIME UP
001A  F604               JMP    WT         ELSE CHECK FLAG AGAIN
001B  5838        IT     INA    7, 0       INPUT FRØM TTY
001C  F70D               RTN    BIPT       & RETURN
001D  4933        HSR    SEN    6, 3       HSR BUSY?
001E  F60E               JMP    BIP2       YES
001F  4032               SEL    6, 2       NØ, STEP READER
0020  4835        WH     SSN    6, 5       FLAG?
0021  F203               JMP    IH         YES
0022  0150               IAR               NØ, BUMP CØUNT
0023  2153               JAZ    BIP2       RESTART IF TIME UP
0024  F604               JMP    WH         ELSE CHECK FLAG AGAIN
0025  5835        IH     INA    6, 5       INPUT FRØM HSR
```

```
0026  F717           RTN    BIPT        & RETURN
                *
                *WAIT FØR EXECUTE SIGNAL
                *
0027  0800    XEQ    ENT
0028  FE20           JST    IER         INPUT
0029  C08D           CAI    :8D         CARRIAGE RETURN?
002A  F703           RTN    XEQ         YES, RETURN
002B  F603           JMP    XEQ+1       NØ, GET MØRE
                *
                *ØUTPUT TØ TTY
                *
002C  0800    ØTT    ENT
002D  403C           SEL    7,4         RESET INTERFACE
002E  6D3B           WRA    7,3         WRITE ØN NØT BUSY
002F  493B           SEN    7,3         DØNE?
0030  F601           JMP    $-1         NØ
0031  F705           RTN    ØTT         YES
                *
                *CØMMAND ERRØR EXIT
                *
0032  0800    ERR    ENT
0033  C6DF           LAP    :DF         PRINT ARRØW
0034  FE08           JST    ØTT
0035  FF34           JST    *CMND       RESTART CØMMAND
                *
                *CARRIAGE-RETURN,LINE FEED
                *
0036  0800    CRLF   ENT
0037  C68D           LAP    :8D         CR
0038  FE0C           JST    ØTT
0039  C68A           LAP    :8A         LF
003A  FE0E           JST    ØTT
003B  F705           RTN    CRLF
                *
                *ØUTPUT TEXT FRØM BUFFER
                *
003C  0800    ØTL    ENT
003D  8A0F           ADD    CAI         MAKE CØMPARE INSTRUCTIØN
003E  9A06           STA    ØT2         &SAVE IT
003F  9A09           STA    ØT3
0040  E704           LDX    *ØTL        GET TEXT PØINTER
0041  DE05           IMS    ØTL         SET RETURN ADDRESS
0042  B400    ØT1    LDA    @0          GET WØRD
0043  11D7           RRA    8           PRINT FIRST BYTE
0044  FE18           JST    ØTT
0045  C000    ØT2    CAI    0           LAST ØNE
0046  F70A           RTN    ØTL         YES, RETURN
0047  1157           RLA    8           PRINT SECØND BYTE
0048  FE1C           JST    ØTT
0049  C000    ØT3    CAI    0           LAST ØNE?
004A  F70E           RTN    ØTL         YES RETURN
004B  0128           IXR                BUMP PØINTER
```

```
004C  F60A         JMP    ØT1       LØØP
004D  C000  CAI    CAI    0
                   *
                   *ØUTPUT FLØATING PØINT NUMBER
                   *
004E  0800  ØFPA   ENT
004F  E701         LDX    *ØFPA     GET PØINTER
0050  DE02         IMS    ØFPA      SET RETURN ADDRESS
0051  EA01         STX    ØPT       SAVE PØINTER
0052  FB0E         JST    *FAS      CØNVERT TØ ASCII
0053  0000  ØPT    DATA   0
0054  0059         DATA   BUF
0055  0110         ZAR              SET END FLAG
0056  FE1A         JST    ØTL       PRINT NUMBER
0057  0059         DATA   BUF
0058  F70A         RTN    ØFPA
0059  0000  BUF    RES    8,0
0061        FAS    REF
                   END
0000 ERRØRS
```

```
                     NAM    READ, CLEAR
                     NAM    PUNCH, GRAPH
                     EXTR   IKB, ØTT, BIPT
                     EXTR   ØTL, CRLF, FPLØT, ØFPA
                     EXTR   XA, XB, XC, FAD
0000                 REL    0
               *
               * READ PAPER TAPE & ADD TØ BUFFER
               *
0000  0800     READ  ENT
               *INITIALIZE VARIABLES
0001  1128           RLX    1         SET INDEX BIT
0002  1400           SØV
0003  11A8           RRX    1
0004  EA33           STX    R5        & SAVE PØINTER
0005  EA34           STX    R5+2
0006  0528           XRP              RESET SUBSCRIPTS
0007  E900           STX    XA
      0000
0008  E900           STX    XB
      0000
0009  E900           STX    XC
      0000
000A  B236           LDA    TP        SET INPUT BUFFER PØINTER
000B  9A38           STA    MPT
000C  B235           LDA    CT        SET INPUT CØUNT
000D  9A37           STA    CNT
               *SKIP LEADER & LABEL
000E  C68A           LAP    :8A       LINE FEED
000F  F900           JST    ØTT
      0000
0010  F900           JST    BIPT
      0000
0011  2141           JAZ    $-1       SKIP LEADER
0012  F900     R1    JST    ØTT       ECHØ LABEL
      0000
0013  F900           JST    BIPT      READ TAPE
      0000
0014  C092           CAI    :92       END ØF LABEL?
0015  F201           JMP    R2        YES
0016  F604           JMP    R1        NØ
0017  F900     R2    JST    BIPT      READ TAPE
      0000
0018  C0FF           CAI    :FF       FILE MARK?
0019  F201           JMP    R3        YES
001A  F603           JMP    R2        NØ
               *READ LØØP
001B  F900     R3    JST    BIPT      LØWER BYTE
      0000
001C  1B87           LLR    8         SAVE
001D  F900           JST    BIPT      UPPER BYTE
      0000
001E  1B07           LLL    8         RESTØRE
```

```
001F  E224           LDX   MPT       SAVE LØW BITS
0020  9C01           STA   @1
0021  F900           JST   BIPT      LØWER BYTE
      0000
0022  1B87           LLR   8
0023  F900           JST   BIPT      UPPER BYTE
      0000
0024  1B07           LLL   8
                *CØNVERT BASIC-F.P. TØ CAI-F.P.
0025  2109           JAZ   Z1        0=0=0
0026  0048           TAX             SAVE SIGN
0027  3081           JAP   $+2       ABS. VAL.
0028  0310           NAR
0029  1B87           LLR   8         REMØVE MSB
002A  1328           LLX   1
002B  8A17           ADD   D64       FIX CHARACTERISTIC
002C  1B07           LLL   8
002D  13C0           LAØ             RECØVER SIGN
002E  11D0           RRA   1
002F  9B14      Z1   STA   *MPT      SAVE HI BITS
0030  DA13           IMS   MPT       BUMP PØINTER
0031  DA12           IMS   MPT       TWICE!
0032  DA12           IMS   CNT       MØRE?
0033  F618           JMP   R3        YES
                *ADD INPUT BUFFER TØ BEAM ARRAY
                *PANIC SWITCH DISABLED FØR DURATIØN
0034  4006           CID             DISABLE AUTØ
0035  B20C           LDA   CT        RESET CØUNTER
0036  9A0E           STA   CNT
0037  F900      R4   JST   FAD       F.P. ADD
      0000
0038  0000      R5   DATA  0,:9400,0
0039  9400
003A  0000
003B  D900           IMS   XA        BUMP SUBSCRIPTS
      0000
003C  D900           IMS   XB
      0000
003D  D900           IMS   XC
      0000
003E  DA06           IMS   CNT       MØRE?
003F  F608           JMP   R4        YES
0040  F740           RTN   READ
                *STØRAGE
0041  1400      TP   DATA  :1400
0042  FF00      CT   DATA  -256
0043  0040      D64  DATA  64
0044  0000      MPT  DATA  0
0045  0000      CNT  DATA  0
                *
                *CLEAR BEAM ARRAY
                *
0046  0800      CLEAR ENT
```

```
0047  B605           LDA   CT        SET CØUNT
0048  9E03           STA   CNT
0049  0110           ZAR             CLEAR
004A  9C00   C1      STA   @0        HI BITS
004B  9C01           STA   @1        LØ BITS
004C  C202           AXI   2         BUMP PØINTER
004D  DE08           IMS   CNT       DØNE?
004E  F604           JMP   C1        NØ
004F  F709           RTN   CLEAR
                     *
                     *PUNCH BEAM ARRAY - BASIC FØRMAT
                     *
0050  0800   PUNCH   ENT
0051  FA22           JST   LEAD      LEADER
0052  B610           LDA   CT        START CØUNTER
0053  9E0E           STA   CNT
0054  F900   P1      JST   IKB       ECHØ LABEL
      0000
0055  C092           CAI   :92       CTRL/TAPE?
0056  F201           JMP   P2        YES
0057  F603           JMP   P1        NØ
0058  C6FF   P2      LAP   :FF       PUNCH FILE MARK
0059  F900           JST   ØTT
      0000
005A  B401   P3      LDA   @1        PUNCH LØ BITS
005B  F900           JST   ØTT
      0000
005C  13D7           LRA   8
005D  F900           JST   ØTT
      0000
005E  B400           LDA   @0        GET HI BITS
005F  C202           AXI   2         BUMP PØINTER
0060  EE1C           STX   MPT       AND SAVE
                     *CØNVERT CAI-F.P. TØ BASIC-F.P.
0061  210A           JAZ   Z2        0=0=0
0062  0048           TAX             SAVE SIGN
0063  1350           LLA   1         CLEAR A15
0064  1B87           LLR   8         SPLIT
0065  9622           SUB   D64       FIX CHARACTERISTIC
0066  1400           SØV             INSERT MSB
0067  1150           RLA   1
0068  1B06           LLL   7         RE-FØRMAT
0069  1329           LLX   2         RECØVER SIGN
006A  3201           JØR   $+2       CØRRECT FØR IT
006B  0310           NAR
006C  F900   Z2      JST   ØTT       PUNCH HI BITS
      0000
006D  1B87           LLR   8
006E  F900           JST   ØTT
      0000
006F  E62B           LDX   MPT       RECØVER PØINTER
0070  DE2B           IMS   CNT       DØNE?
0071  F617           JMP   P3        NØ
```

```
0072  FA01            JST    LEAD      YES, PUNCH LEADER
0073  F723            RTN    PUNCH
                *PUNCH 5" ØF LEADER
0074  0800  LEAD      ENT
0075  C732            LAM    50
0076  9E31            STA    CNT
0077  0110            ZAR
0078  F900  L2        JST    ØTT
      0000
0079  DE34            IMS    CNT
007A  F602            JMP    L2
007B  F707            RTN    LEAD
            *
            *PLØT DATA ARRAY
            *
007C  0800  GRAPH     ENT
007D  EA06            STX    T         SAVE CØUNT PØINTER
007E  C202            AXI    2
007F  EA08            STX    PT        SAVE DATA PØINTER
0080  0110            ZAR              PRINT CØUNT
0081  F900            JST    ØTL
      0000
0082  008A            DATA   CTX
0083  F900            JST    ØFPA
      0000
0084  0000  T         DATA   0
0085  F900            JST    CRLF
      0000
0086  C7FF            LAM    255       PLØT DATA
0087  F900            JST    FPLØT
      0000
0088  0000  PT        DATA   0
0089  F70D            RTN    GRAPH
008A  8A3A  CTX       DATA   :8A3A
008B  C3CF            TEXT   'CØUNT = '
008C  D5CE
008D  D4A0
008E  BDA0
008F  0000            DATA   0
                      END
0000 ERRØRS
```

```
                *
                *   FPLØT - FLØATING PØINT PLØTTER
                *
                *        CALLING SEQUENCE:
                *                                LDA MDIM
                *                                JST *FPLØT
                *                                DATA ARRAY
                *                               (RETURN)
                *
                        NAM     FPLØT
0000                    REL     0
0000    0800    FPLØT   ENT
0001    9A4C            STA     NRØW
0002    9A4C            STA     CNT
0003    B703            LDA     *FPLØT
0004    9A1F            STA     RP3
0005    9A24            STA     RP4
0006    A249            IØR     B15
0007    9A05            STA     RP1
0008    9A03            STA     RP2
0009    0350            ARP
000A    9B4F            STA     *XA
000B    F204            JMP     MØVE
000C    FB4E    LP1     JST     *FCP
000D    0000    RP1     DATA    0,MAX
000E    0051
000F    2183            JAL     INC
0010    FB4B    MØVE    JST     *FMV
0011    0000    RP2     DATA    0,MAX
0012    0051
0013    DB46    INC     IMS     *XA
0014    DA3A            IMS     CNT
0015    F609            JMP     LP1
0016    FB41            JST     *CRLF
0017    FB40            JST     *CRLF
0018    C6BD            LAP     '='
0019    FB3F            JST     *ØTL
001A    0061            DATA    SF
001B    FB43            JST     *FDV
001C    0055            DATA    F50,MAX,SCALE
001D    0051
001E    0053
001F    FB40            JST     *ØFPA
0020    0053            DATA    SCALE
0021    FB36            JST     *CRLF
0022    FB35            JST     *CRLF
0023    FB3C    LP2     JST     *ØFPA
0024    0000    RP3     DATA    0
0025    DE01            IMS     RP3
0026    DE02            IMS     RP3
0027    C6A0            LAP     ' '
0028    FB2E            JST     *ØTT
0029    FB34            JST     *FMP
```

```
002A  0000  RP4    DATA  0,SCALE,MAX
002B  0053
002C  0051
002D  DE03         IMS   RP4
002E  DE04         IMS   RP4
002F  FB2D         JST   *FIX
0030  0051         DATA  MAX,CNT
0031  004F
0032  B21C         LDA   CNT
0033  0048         TAX
0034  3085         JAP   PØS
0035  C6AD         LAP   '-'
0036  FB20         JST   *ØTT
0037  C6B0         LAP   '0'
0038  FB1E         JST   *ØTT
0039  F20E         JMP   ØUT
003A  C6A0  PØS    LAP   ' '
003B  FB1B         JST   *ØTT
003C  2809         JXZ   MARK
003D  C6B0         LAP   '0'
003E  FB18         JST   *ØTT
003F  0508         NXR
0040  EA0E         STX   CNT
0041  C6AA         LAP   '*'
0042  F201         JMP   $+2
0043  FB13         JST   *ØTT
0044  DA0A         IMS   CNT
0045  F602         JMP   $-2
0046  C6AA  MARK   LAP   '*'
0047  FB0F         JST   *ØTT
0048  FB0F  ØUT    JST   *CRLF
0049  DA04         IMS   NRØW
004A  F627         JMP   LP2
004B  FB0C         JST   *CRLF
004C  DE4C         IMS   FPLØT
004D  F74D         RTN   FPLØT
004E  0800  NRØW   HLT
004F  0800  CNT    HLT
0050  8000  B15    DATA  :8000
0051  0000  MAX    RES   2,0
0053  0000  SCALE  RES   2,0
0055  4348  F50    DATA  :4348,0
0056  0000
0057        ØTT    REF
0058        CRLF   REF
0059        ØTL    REF
005A        XA     REF
005B        FCP    REF
005C        FMV    REF
005D        FIX    REF
005E        FMP    REF
005F        FDV    REF
0060        ØFPA   REF
```

```
0099   0061   D3C3   SF     TEXT   'SCALFACTØR ='
       0062   C1CC
       0063   85C6
       0064   C1C3
       0065   D4CF
       0066   D2A0
       0067   BDA0
0100                        END
```

```
                    *
                    *CRT - FLØATING PØINT PLØTTER
                    *
                    *      CALLING SEQUENCE:
                    *                           JST *CRT
                    *                           (RETURN)
                    *
                           NAM    CRT
0000                       REL    0
0000  0800   CRT           ENT
0001  C7FF                 LAM    255
0002  9A5F                 STA    NRØW
0003  9A5F                 STA    CNT
0004  49C4                 SEN    24,4
0005  F601                 JMP    $-1
0006  40C7                 SEL    24,7
0007  C202                 AXI    2
0008  0030                 TXA
0009  A261                 IØR    B15
000A  9A0B                 STA    RP1
000B  9A0E                 STA    RP2
000C  9A10                 STA    RP3
000D  9A13                 STA    RP4
000E  9A36                 STA    RP5
000F  0110                 ZAR
0010  9A54                 STA    MIN
0011  9A54                 STA    MIN+1
0012  0350                 ARP
0013  9B5B                 STA    *XA
0014  F204                 JMP    MØVE
0015  FB5A   LP1           JST    *FCP
0016  0000   RP1           DATA   0,MAX
0017  0067
0018  2183                 JAL    INC1
0019  FB57   MØVE          JST    *FMV
001A  0000   RP2           DATA   0,MAX
001B  0067
001C  FB53   INC1          JST    *FCP
001D  0000   RP3           DATA   0,MIN
001E  0065
001F  3083                 JAP    INC2
0020  FB50                 JST    *FMV
0021  0000   RP4           DATA   0,MIN
0022  0065
0023  DB4B   INC2          IMS    *XA
0024  DA3E                 IMS    CNT
0025  F610                 JMP    LP1
                    *
0026  FB4F                 JST    *CRLF
0027  FB4E                 JST    *CRLF
0028  C6BD                 LAP    '='
0029  FB4D                 JST    *ØTL
002A  0079                 DATA   SF
```

```
                   *
002B  FB46                 JST    *FSB
002C  0067                 DATA   MAX,MIN,MAX
002D  0065
002E  0067
002F  FB43                 JST    *FDV
0030  006C                 DATA   F250,MAX,SCALE
0031  0067
0032  0069
0033  FB44                 JST    *ØFPA
0034  0069                 DATA   SCALE
0035  FB40                 JST    *CRLF
                   *
0036  FB3D                 JST    *FMP
0037  0069                 DATA   SCALE,MIN,MAX
0038  0065
0039  0067
003A  FB3A                 JST    *FIX
003B  0067                 DATA   MAX,MIN
003C  0065
003D  B227                 LDA    MIN
003E  0310                 NAR
003F  3081                 JAP    $+2
0040  0110                 ZAR
0041  9A22                 STA    X
0042  0350                 ARP
0043  9B2B                 STA    *XA
                   *
0044  FB2F         LP2     JST    *FMP
0045  0000         RP5     DATA   0,SCALE,MAX
0046  0069
0047  0067
0048  DB26                 IMS    *XA
0049  FB2B                 JST    *FIX
004A  0067                 DATA   MAX,CNT
004B  0063
004C  E217                 LDX    X
004D  B215                 LDA    CNT
004E  49C4         DØT     SEN    24,4
004F  F601                 JMP    $-1
0050  49C2                 SEN    24,2
0051  F601                 JMP    $-1
0052  6EC2                 ØTX    24,2
0053  2107                 JAZ    DØNE
0054  3183                 JAG    PØS
0055  00A8                 DXR
0056  0150                 IAR
0057  F609                 JMP    DØT
0058  0128         PØS     IXR
0059  00D0                 DAR
005A  F60C                 JMP    DØT
005B  B208         DØNE    LDA    X
005C  8A11                 ADD    H256
```

```
005D  9A06          STA    X
005E  DA03          IMS    NRØW
005F  F61B          JMP    LP2
0060  FB15          JST    *CRLF
0061  F761          RTN    CRT
                *
0062  0000  NRØW    DATA   0
0063  0000  CNT     DATA   0
0064  0000  X       DATA   0
0065  0000  MIN     RES    2,0
0067  0000  MAX     RES    2,0
0069  0000  SCALE   RES    2,0
006B  8000  B15     DATA   :8000
006C  447A  F250    DATA   :447A,0
006D  0000
006E  0100  H256    DATA   256
                *
006F            XA      REF
0070            FCP     REF
0071            FMV     REF
0072            FSB     REF
0073            FDV     REF
0074            FMP     REF
0075            FIX     REF
0076            CRLF    REF
0077            ØTL     REF
0078            ØFPA    REF
                *
0079  D3C3  SF      TEXT   'SCALE FACTØR ='
007A  C1CC
007B  C5A0
007C  C6C1
007D  C3D4
007E  CFD2
007F  A0BD
                *
                        END
0000 ERRØRS
```

```
                          NAM   VIEW
                          EXTR  DPN:, DPSUB:, DPDIV:, DPSM:
                          NAM   DISP
                          EXTR  RTTR, RTØP
0000  0800  VIEW          ENT
0001  9A71  DISP          STA   VEVR
0002  C202                AXI   2
0003  EA66                STX   RP1D        PØINTER
0004  EA66                STX   RP2D
0005  C7FF                LAM   255
0006  9A6A                STA   CNT
0007  9A64                STA   NRØW
0008  0110                ZAR               INITIALIZE MAX AMD MIN
0009  9A63                STA   MIN
000A  9A63                STA   MIN+1
000B  9A63                STA   MAX
000C  9A63                STA   MAX+1
000D  B400  STCM          LDA   @0
000E  D260                CMS   MAX
000F  F20A                JMP   MIN1        A1<MAX
0010  F205                JMP   MAX1        A1>MAX
0011  B401                LDA   @1          A1=MAX
0012  D25D                CMS   MAX+1
0013  F206                JMP   MIN1        A1=MAX  A2<MAX+1
0014  9A5B                STA   MAX+1       A1=MAX  A2>MAX+1
0015  F211                JMP   FICM
0016  9A58  MAX1          STA   MAX
0017  B401                LDA   @1
0018  9A57                STA   MAX+1
0019  F20D                JMP   FICM
001A  B400  MIN1          LDA   @0
001B  D251                CMS   MIN
001C  F206                JMP   MIN2        A1<MIN
001D  F209                JMP   FICM        A1>MIN
001E  B401                LDA   @1          A1=MIN
001F  D24E                CMS   MIN+1
0020  F202                JMP   MIN2        A1=MIN  A2<MIN+1
0021  F205                JMP   FICM        A1=MIN  A2>MIN+1
0022  F204                JMP   FICM        A1=MIN  A2=MIN+1
0023  B400  MIN2          LDA   @0
0024  9A48                STA   MIN
0025  B401                LDA   @1
0026  9A47                STA   MIN+1
0027  E242  FICM          LDX   RP1D
0028  C202                AXI   2
0029  EA40                STX   RP1D
002A  DA46                IMS   CNT
002B  F61E                JMP   STCM
            *
002C  B242                LDA   MAX
002D  E242                LDX   MAX+1
002E  F900                JST   DPSUB:
      0000
```

```
002F   006D          DATA   MIN
0030   1050          ALA    1
0031   1329          LLX    2
0032   3201          JØR    $+2
0033   0150          IAR
0034   13A3          LRX    1
0035   9A39          STA    MAX
0036   EA39          STX    MAX+1
              *
0037   B235          LDA    MIN
0038   E235          LDX    MIN+1
0039   F900          JST    DPDIV:
       0000
003A   006F          DATA   MAX
003B   9A2D          STA    TEM
003C   10D1          ARA    2
003D   0310          NAR
003E   8A2A          ADD    TEM
003F   10D5          ARA    6
              *
0040   0310          NAR
0041   3081          JAP    $+2
0042   0110          ZAR
0043   9A2E          STA    X
              *
0044   E226          LDX    RP2D
0045   B400   LPD    LDA    @0
0046   E401          LDX    @1
0047   F900          JST    DPDIV:
       0000
0048   006F          DATA   MAX
0049   9A1F          STA    TEM
004A   10D1          ARA    2
004B   0310          NAR
004C   8A1C          ADD    TEM
004D   10D5          ARA    6
              *
004E   E223          LDX    X
004F   49C4   DØT    SEN    24,4
0050   F601          JMP    $-1
0051   49C2          SEN    24,2
0052   F601          JMP    $-1
0053   6EC2          ØTX    24,2
0054   2107          JAZ    DØNE
0055   3183          JAG    PØS
0056   00A8          DXR
0057   0150          IAR
0058   F609          JMP    DØT
0059   0128   PØS    IXR
005A   00D0          DAR
005B   F60C          JMP    DØT
              *
005C   B215   DØNE   LDA    )
```

```
0104  005D  8A16         ADD    H256
0105  005E  9A13         STA    X
0106  005F  E20B         LDX    RP2D
0107  0060  C202         AXI    2
0108  0061  EA09         STX    RP2D
0109  0062  DA09         IMS    NRØW
0110  0063  F61E         JMP    LPD
0111  0064  B20E         LDA    VEVR
0112  0065  2101         JAZ    $+2
0113  0066  F100         JMP    RTØP
            0000
0114  0067  F100         JMP    RTTR
            0000
0115  0068  F768         RTN    VIEW
0116  0069  0000  TEM    DATA   0
0117  006A  0000  RP1D   DATA   0
0118  006B  0000  RP2D   DATA   0
0119  006C  0000  NRØW   DATA   0
0120  006D  0000  MIN    RES    2,0
0121  006F  0000  MAX    RES    2,0
0122  0071  0000  CNT    DATA   0
0123  0072  0000  X      DATA   0
0124  0073  0000  VEVR   DATA   0
0125  0074  0100  H256   DATA   256
0126                     END
0000 ERRØRS
```

```
                        NAM    DPACC
                        NAM    DPFLT
                        NAM    DPFIX
                        EXTR   DPN:
                        EXTR   DPN
0000                    REL    0
                 *
                 *DØUBLE PRECISIØN ACCUMULATE
                 *
0000  0800       DPACC  ENT
0001  9A10              STA    TEMP
0002  0030              TXA
0003  E703              LDX    *DPACC
0004  1200              RØV
0005  8C01              ADD    @1
0006  820C              AND    MASK
0007  9C01              STA    @1
0008  B209.             LDA    TEMP
0009  3204              JØR    DC1
000A  1200              RØV
000B  0150              IAR
000C  3201              JØR    DC1
000D  0110              ZAR
000E  8C00       DC1    ADD    @0
000F  9C00              STA    @0
0010  DE10              IMS    DPACC
0011  F711              RTN    DPACC
0012  0000       TEMP   DATA   0
0013  7FFF       MASK   DATA   :7FFF
                 *
                 *DØUBLE PRECISIØN TØ CAI-F. P.
                 *
0014  0800       DPFLT  ENT
0015  3801              JXN    DPF1
0016  2113              JAZ    DPF4
0017  BA13       DPF1   EMA    BITS
0018  0110              ZAR
0019  BA11              EMA    BITS
001A  9A11              STA    SIGN
001B  3081              JAP    DPF2
001C  F900              JST    DPN:
      0000
001D  1328       DPF2   LLX    1
001E  1B00       DPF3   LLL    1
001F  DA0B              IMS    BITS
0020  3242              JØR    DPF3
0021  1B88              LLR    9
0022  BA08              EMA    BITS
0023  0310              NAR
0024  8A08              ADD    D160
0025  1356              LLA    7
0026  A204              IØR    BITS
0027  BA04              EMA    SIGN
```

```
0028   8205          AND    DPM
0029   A202          IØR    SIGN
002A   F716   DPF4   RTN    DPFLT
002B   0000   BITS   DATA   0
002C   0000   SIGN   DATA   0
002D   00A0   D160   DATA   160
002E   8000   DPM    DATA   :8000
002F   0800   DPFIX  ENT
0030   9E04          STA    SIGN
0031   821C          AND    DPP
0032   13D6          LRA    7
0033   9606          SUB    D160
0034   9E09          STA    BITS
0035   B609          LDA    SIGN
0036   8218          AND    MANT
0037   A218          IØR    SBIT
0038   BE0D          EMA    BITS
0039   2109          JAZ    DPFX2
003A   3190          JAG    DPFX4
003B   BE10          EMA    BITS
003C   1B07          LLL    8
003D   1B30   DPFX1  LLR    1
003E   DE13          IMS    BITS
003F   F602          JMP    DPFX1
0040   1B00          LLL    1
0041   13A8          LRX    1
0042   F201          JMP    $+2
0043   BE18   DPFX2  EMA    BITS
0044   BE18          EMA    SIGN
0045   3083          JAP    DPFX3
0046   BE1A          EMA    SIGN
0047   F900          JST    DPN:
       0000
0048   F201          JMP    $+2
0049   BE1D   DPFX3  EMA    SIGN
004A   F71B          RTN    DPFIX
004B   0118   DPFX4  ZAX
004C   1400          SØV
004D   F71E          RTN    DPFIX
004E   7FFF   DPP    DATA   :7FFF
004F   007F   MANT   DATA   :7F
0050   0080   SBIT   DATA   :80
                     END
0000 ERRØRS
```

APPENDIX C

```
                    NAM   CMND
                    EXTR  IER,ØTT,ØTL,CRLF
                    EXTR  ERR,XEQ
0100                ABS   :100
               *PRINT NAME
0100  0110          ZAR
0101  F900          JST   ØTL
      0000
0102  012B          DATA  NAME
0103  F201          JMP   $+2
               *
               *CØMMAND INTERPRETER
               *
0104  0800     CMND ENT
0105  0A00          EIN
0106  4005          CIE               ENABLE PANIC BUTTØN
0107  F900          JST   CRLF        PRINT PRØMPT CHARACTER
      0000
0108  C687          LAP   :87
0109  F900          JST   ØTT
      0000
010A  C6AA          LAP   '*'
010B  F900          JST   ØTT
      0000
010C  0108          ZXR
010D  F900          JST   IER         INPUT CØMMAND
      0000
010E  C0D4          CAI   'T'
010F  E213          LDX   TRANS
0110  C0D2          CAI   'R'
0111  E212          LDX   READ
0112  C0C3          CAI   'C'
0113  E211          LDX   CLEAR
0114  380A          JXN   ØKF
0115  C0D0          CAI   'P'
0116  E20F          LDX   PUNCH
0117  C0C7          CAI   'G'
0118  E20F          LDX   FPLØT
0119  C0D6          CAI   'V'
011A  E20E          LDX   CRT
011B  C0C4          CAI   'D'
011C  E20A          LDX   DATUM
011D  3801          JXN   ØKF
011E  F900     BAD  JST   ERR
      0000
011F  EA0A     ØKF  STX   FUNC        SAVE CALL ADDRESS
0120  F900          JST   XEQ         WAIT FØR GØ
      0000
0121  FB08          JST   *FUNC       CALL FUNCTIØN
0122  F61D          JMP   CMND+1
0123           TRANS REF
0124           READ  REF
0125           CLEAR REF
```

```
0047  0126        PUNCH  REF
0048  0127        DATUM  REF
0049  0128        FPLØT  REF
0050  0129        CRT    REF
0051  012A  0000  FUNC   DATA   0
0052  012B  B1B5  NAME   TEXT   '15*255 FULL HTS'
      012C  AAB2
      012D  B5B5
      012E  A0C6
      012F  D5CC
      0130  CCA0
      0131  C8D4
      0132  D3A0
0053  0133  8D3A         DATA   :8D3A,0
      0134  0000
0054                     END
0000 ERRØRS
```

```
                           NAM    TRANS
                           NAM    RTTR
                           EXTR   DISP
0000                       REL    0
0000   0800   TRANS        ENT
0001   C6BF                LAP    '?'
0002   F900                JST    *ØTL
       8127
0003   013E                DATA   MØTA
0004   F900                JST    *IKB
       8128
0005   1200                RØV
0006   C0CD                CAI    'M'
0007   F203                JMP    MØN
0008   C0D4                CAI    'T'
0009   F204                JMP    TAP
000A   F900                JST    *ERR
       812A
000B   F900   MØN          JST    *CRLF
       8129
000C   0108                ZXR
000D   F20F                JMP    BEG
000E   F900   TAP          JST    *CRLF
       8129
000F   C68A                LAP    :8A
0010   F900                JST    *ØTT
       8126
0011   F900                JST    *BIPT
       8125
0012   2141                JAZ    $-1
0013   F900   T1           JST    *ØTT
       8126
0014   F900                JST    *BIPT
       8125
0015   C092                CAI    :92
0016   F201                JMP    T2
0017   F604                JMP    T1
0018   F900   T2           JST    *BIPT
       8125
0019   C0FF                CAI    :FF
001A   F201                JMP    T4
001B   F603                JMP    T2
001C   C401   T4           LXP    1
001D   E900   BEG          STX    TETR
       012B
001E   B100                LDA    MASK0
       0122
001F   9AF3                STA    MASK1
0020   F900                JST    *CRLF
       8129
0021   C6BF                LAP    '?'
0022   F900                JST    *ØTL
       8127
```

```
0023  0130          DATA   DIRE
0024  F900          JST    *IKB
      8123
0025  C0C6          CAI    'F'
0026  F205          JMP    FØRD
0027  C0C2          CAI    'B'
0028  F208          JMP    BACK
0029  C0CF          CAI    'Ø'
002A  F20A          JMP    BØTH
002B  FBFE          JST    *ERR
002C  C71E   FØRD   LAM    30
002D  9AE2          STA    CNT2
002E  0108          ZXR
002F  0403          CXR
0030  F207          JMP    TKF
0031  C71E   BACK   LAM    30
0032  9ADD          STA    CNT2
0033  0108          ZXR
0034  F203          JMP    TKF
0035  C70F   BØTH   LAM    15
0036  9AD9          STA    CNT2
0037  0358          AXP
0038  EAF5   TKF    STX    DIR1
0039  E2F1          LDX    TETR
003A  2802          JXZ    $+3
003B  C70F          LAM    15
003C  9AD3          STA    CNT2
003D  B2D4          LDA    ZCT
003E  9AD2          STA    CNT3
003F  E2E3          LDX    IBC
0040  0110          ZAR
0041  9C00   CLR    STA    @0
0042  0128          IXR
0043  DACD          IMS    CNT3
0044  F603          JMP    CLR
0045  EAD1          STX    IBP
0046  E2E4          LDX    TETR
0047  2803          JXZ    NEXT
0048  E2E5          LDX    DIR1
0049  3801          JXN    NEXT
004A  0210          CAR
004B  E2D8   NEXT   LDX    MASK
004C  0128          IXR
004D  0210          CAR
004E  C000          CAI    0
004F  C2FF          AXI    255
0050  EAB8          STX    MSK1
0051  9ABA          STA    DIR
0052  C7F5          LAM    245
0053  9ACC          STA    DCT2
0054  C7FF          LAM    255
0055  9AB7          STA    DCT
0056  B2D4          LDA    TETR
```

```
0057  2107          JAZ   TUR1
0058  FBCC  T3      JST   *BIPT
0059  1357          LLA   8
005A  9AD4          STA   TEMT
005B  FBC9          JST   *BIPT
005C  A2D2          IØR   TEMT
005D  9AB0          STA   VAL
005E  F209          JMP   PRØC
005F  FA89  TUR1    JST   TURNØN
0060  FA93  ILP     JST   MØNS
0061  9AAC          STA   VAL
0062  B2CB          LDA   DIR1
0063  C001          CAI   1
0064  F203          JMP   PRØC
0065  D2A6          CMS   DIR
0066  F235          JMP   FINØNE
0067  F234          JMP   FINØNE
0068  C70F  PRØC    LAM   15
0069  9AA5          STA   CNT1
006A  B2A8          LDA   MASK1
006B  9AA8          STA   MASK2
006C  B2B6          LDA   IBC
006D  9AA8          STA   IB
006E  C7FF  SPA     LAM   255
006F  9AA5          STA   SCT
0070  B298          LDA   MSK1
0071  9A98          STA   MSK2
0072  B2A3          LDA   IB
0073  9AA3          STA   IBP
0074  0110          ZAR
0075  D39E          CMS   *MASK2
0076  F201          JMP   $+2
0077  F213          JMP   TLP2
0078  E295  TLP1    LDX   VAL
0079  0110          ZAR
007A  D38F          CMS   *MSK2
007B  F201          JMP   $+2
007C  0508          NXR
007D  0030          TXA
007E  8B98          ADD   *IBP
007F  9B97          STA   *IBP
0080  DA89          IMS   MSK2
0081  DA95          IMS   IBP
0082  DA92          IMS   SCT
0083  F60B          JMP   TLP1
0084  DA8F          IMS   MASK2
0085  C6FF          LAP   255
0086  8A8F          ADD   IB
0087  9A8E          STA   IB
0088  DA86          IMS   CNT1
0089  F61B          JMP   SPA
008A  F211          JMP   FINØNE
008B  E282  TLP2    LDX   VAL
```

```
008C   0110            ZAR
008D   D37C            CMS    *MSK2
008E   0508            NXR
008F   0030            TXA
0090   8B86            ADD    *IBP
0091   9B35            STA    *IBP
0092   DA77            IMS    MSK2
0093   DA33            IMS    IBP
0094   DA80            IMS    SCT
0095   F60A            JMP    TLP2
0096   DA7D            IMS    MASK2
0097   C6FF            LAP    255
0098   8A7D            ADD    IB
0099   9A7C            STA    IB
009A   DA74            IMS    CNT1
009B   F62D            JMP    SPA
009C   E26C   FINØNE   LDX    MSK1
009D   0128            IXR
009E   B26D            LDA    DIR
009F   C000            CAI    0
00A0   C302            SXI    2
00A1   EA67            STX    MSK1
00A2   DA7D            IMS    DCT2
00A3   F201            JMP    $+2
00A4   40C7            SEL    24,7
00A5   DA67            IMS    DCT
00A6   F201            JMP    TUR2
00A7   F204            JMP    TUR3
00A8   B232   TUR2     LDA    TETR
00A9   2101            JAZ    $+2
00AA   F652            JMP    T3
00AB   F64B            JMP    ILP
00AC   C7FF   TUR3     LAM    255
00AD   9A6E            STA    CNT7
00AE   E263            LDX    IBP
00AF   0110            ZAR
00B0   9C00   CLR1     STA    @0
00B1   0128            IXR
00B2   DA69            IMS    CNT7
00B3   F603            JMP    CLR1
00B4   C7F1            LAM    241
00B5   9A63            STA    CNT4
00B6   C70F            LAM    15
00B7   9A62            STA    CNT5
00B8   9A62            STA    CNT6
00B9   B269            LDA    IBC
00BA   9A63            STA    IBD
00BB   C70E            LAM    14
00BC   9A60            STA    HM14
00BD   B260   NXBIN    LDA    IBD
00BE   9A60            STA    IBE
00BF   B35F   NXRØW    LDA    *IBE
00C0   10D3            ARA    4
```

```
00C1  8B55           ADD    *IBP
00C2  9B54           STA    *IBP
00C3  B254           LDA    H256
00C4  8A5A           ADD    IBE
00C5  9A59           STA    IBE
00C6  DA53           IMS    CNT5
00C7  F603           JMP    NXRØW
00C8  B252           LDA    CNT6
00C9  9A50           STA    CNT5
00CA  DA53           IMS    IBD
00CB  DA4B           IMS    IBP
00CC  DA4C           IMS    CNT4
00CD  F610           JMP    NXBIN
00CE  B24B           LDA    CNT5
00CF  0150           IAR
00D0  9A4A           STA    CNT6
00D1  9A48           STA    CNT5
00D2  C701           LAM    1
00D3  9A45           STA    CNT4
00D4  DA48           IMS    HM14
00D5  F618           JMP    NXBIN
00D6  0110           ZAR
00D7  9A49           STA    ØFFSET
00D8  F100           JMP    DISP
      0000
00D9  B251  RTTR     LDA    TETR
CODA  2104           JAZ    T5
00DB  B252           LDA    DIR1
00DC  3184           JAG    T6
00DD  0210           CAR
00DE  F206           JMP    T7
00DF  B24E  T5       LDA    DIR1
00E0  2182           JAL    $+3
00E1  B22A  T6       LDA    DIR
00E2  F202           JMP    T7
00E3  B223           LDA    DIR
00E4  3101           JAN    $+2
00E5  DA2D  T7       IMS    MASK1
00E6  DA29           IMS    CNT2
00E7  F69C           JMP    NEXT
00E8  F7E8           RTN    TRANS
00E9  0300  TURNØN   ENT
00EA  4006           CID
00EB  48C1           SSN    :C1
00EC  F601           JMP    $-1
00ED  0E00           SBM
00EE  49C1           SEN    :C1
00EF  F601           JMP    $-1
00F0  0F00           SWM
00F1  40C4           SEL    :C4
00F2  4005           CIE
00F3  F70A           RTN    TURNØN
00F4  0300  MØNS     ENT
```

```
00F5  49C6          SEN    :C6
00F6  F601          JMP    $-1
00F7  5AC6          INX    :C6
00F8  2843          JXZ    $-3
00F9  C704          LAM    4
00FA  9A10          STA    CNT
00FB  0110          ZAR
00FC  9A0D          STA    MSK2
00FD  F206          JMP    M2
00FE  1350  M1      LLA    1
00FF  9A0A          STA    MSK2
0100  1351          LLA    2
0101  8A08          ADD    MSK2
0102  9A07          STA    MSK2
0103  0110          ZAR
0104  1B03  M2      LLL    4
0105  8A04          ADD    MSK2
0106  DA04          IMS    CNT
0107  F609          JMP    M1
0108  F714          RTN    MØNS
0109  0000  MSK1    DATA   0
010A  0000  MSK2    DATA   0
010B  0000  CNT     DATA   0
010C  0000  DIR     DATA   0
010D  0000  DCT     DATA   0
010E  0000  VAL     DATA   0
010F  0000  CNT1    DATA   0
0110  0000  CNT2    DATA   0
0111  0000  CNT3    DATA   0
0112  F010  ZCT     DATA   -4080
0113  0000  MASK1   DATA   0
0114  0000  MASK2   DATA   0
0115  0000  SCT     DATA   0
0116  0000  IB      DATA   0
0117  0000  IBP     DATA   0
0118  0100  H256    DATA   256
0119  0000  CNT4    DATA   0
011A  0000  CNT5    DATA   0
011B  0000  CNT6    DATA   0
011C  0000  CNT7    DATA   0
011D  FFF2  HM14    DATA   -14
011E  0000  IBD     DATA   0
011F  0000  IBE     DATA   0
0120  0000  DCT2    DATA   0
0121  0000  ØFFSET  DATA   0
0122        MASK0   REF
0123        IBC     REF
0124        MASK    REF
0125        BIPT    REF
0126        ØTT     REF
0127        ØTL     REF
0128        IKB     REF
0129        CRLF    REF
```

```
0303  012A               ERR    REF
0304  012B   0000  TETR   DATA   0
0305  012C   0000  TEDA   DATA   0
0306  012D   0FF0  TCT1   DATA   4080
0307  012E   0000  DIR1   DATA   0
0308  012F   0000  TEMT   DATA   0
0309  0130   8D8A  DIRE   DATA   :8D8A
0310  0131   C6CF         TEXT   'FØRWARD, BACKWARD, ØR BØTH?'
      0132   D2D7
      0133   C1D2
      0134   C4AC
      0135   C2C1
      0136   C3CB
      0137   D7C1
      0138   D2C4
      0139   ACCF
      013A   D2A0
      013B   C2CF
      013C   D4C8
      013D   BFA0
0311  013E   8D8A  MØTA   DATA   :8D8A
0312  013F   C6D2         TEXT   'FRØM MØNSANTØ ØR FRØM TAPE?'
      0140   CFCD
      0141   A0CD
      0142   CFCE
      0143   D3C1
      0144   CED4
      0145   CFA0
      0146   CFD2
      0147   A0C6
      0148   D2CF
      0149   CDA0
      014A   D4C1
      014B   D0C5
      014C   BFA0
0313                      END
0000  ERRØRS
```

```
                        NAM    DATUM, RTDA
                        EXTR   DISD
0000   0800   DATUM     ENT
0001   C6BF             LAP    '?'
0002   FB63             JST    *ØTL
0003   0067             DATA   DIRE
0004   FB71             JST    *IKB
0005   C0C6             CAI    'F'
0006   F205             JMP    FØRD
0007   C0C2             CAI    'B'
0008   F208             JMP    BACK
0009   C0CF             CAI    'Ø'
000A   F20A             JMP    BØTH
000B   FB6C             JST    *ERR
000C   C71E   FØRD      LAM    30
000D   9A73             STA    DNT2
000E   0108             ZXR
000F   0408             CXR
0010   F207             JMP    PKF
0011   C71E   BACK      LAM    30
0012   9A6E             STA    DNT2
0013   0108             ZXR
0014   F203             JMP    PKF
0015   C70F   BØTH      LAM    15
0016   9A6A             STA    DNT2
0017   0358             AXP
0018   EA60   PKF       STX    DIR1
0019   B260             LDA    ZCT1
001A   9A60             STA    CT1
001B   E25B             LDX    IBC
001C   EA5F             STX    IB
001D   0110             ZAR
001E   9C00   CLR       STA    @0
001F   0128             IXR
0020   DA5A             IMS    CT1
0021   F603             JMP    CLR
0022   9A61             STA    RØN
0023   0210   NEXT      CAR
0024   9A58             STA    DIR0
0025   C7F5             LAM    245
0026   9A58             STA    DDT2
0027   C7FF             LAM    255
0028   9A55             STA    DDT
0029   FA19             JST    DURNØN
002A   FA23   DLP       JST    DØNS
002B   9A54             STA    DAT
002C   B24C             LDA    DIR1
002D   C001             CAI    1
002E   F203             JMP    STØ
002F   D24D             CMS    DIR0
0030   F232             JMP    DLP2
0031   F231             JMP    DLP2
0032   B24D   STØ       LDA    DAT
```

```
0033   E248          LDX   IB
0034   9C00          STA   @0
0035   DA46          IMS   IB
0036   DA48          IMS   DDT2
0037   F201          JMP   $+2
0038   40C7          SEL   24,7
0039   DA44          IMS   DDT
003A   F610          JMP   DLP
003B   DA48          IMS   RØN
003C   B247  DLP1    LDA   RØN
003D   2101          JAZ   $+2
003E   F100          JMP   DISD
       0000
003F   B23D  RTDA    LDA   DIRO
0040   DA40          IMS   DNT2
0041   F61E          JMP   NEXT
0042   F742          RTN   DATUM
0043   0800  DURNØN  ENT
0044   4006          CID
0045   48C1          SSN   :C1
0046   F601          JMP   $-1
0047   0E00          SBM
0048   49C1          SEN   :C1
0049   F601          JMP   $-1
004A   0F00          SWM
004B   40C4          SEL   :C4
004C   4005          CIE
004D   F70A          RTN   DURNØN
004E   0800  DØNS    ENT
004F   49C6          SEN   :C6
0050   F601          JMP   $-1
0051   5AC6          INX   :C6
0052   2843          JXZ   $-3
0053   C704          LAM   4
0054   9A2D          STA   CNT
0055   0110          ZAR
0056   9A2C          STA   MSK2
0057   F206          JMP   M2
0058   1350  M1      LLA   1
0059   9A29          STA   MSK2
005A   1351          LLA   2
005B   8A27          ADD   MSK2
005C   9A26          STA   MSK2
005D   0110          ZAR
005E   1B03  M2      LLL   4
005F   8A23          ADD   MSK2
0060   DA21          IMS   CNT
0061   F609          JMP   M1
0062   F714          RTN   DØNS
0063   DA1A  DLP2    IMS   DDT
0064   F63A          JMP   DLP
0065   F629          JMP   DLP1
0066         ØTL     REF
```

```
0106   0067   8D8A   DIRE    DATA   :8D8A
0107   0068   C6CF           TEXT   'FØRWARD, BACKWARD ØR BØTH?'
       0069   D2D7
       006A   C1D2
       006B   C4AC
       006C   C2C1
       006D   C3CB
       006E   D7C1
       006F   D2C4
       0070   A0CF
       0071   D2A0
       0072   C2CF
       0073   D4C8
       0074   BFA0
0108   0075          CRLF    REF
0109   0076          IKB     REF
0110   0077          IBC     REF
0111   0078          ERR     REF
0112   0079   0000   DIR1    DATA   0
0113   007A   F00B   ZCT1    DATA   -4085
0114   007B   0000   CT1     DATA   0
0115   007C   0000   IB      DATA   0
0116   007D   0000   DIRO    DATA   0
0117   007E   0000   DDT     DATA   0
0118   007F   0000   DDT2    DATA   0
0119   0080   0000   DAT     DATA   0
0120   0081   0000   DNT2    DATA   0
0121   0082   0000   CNT     DATA   0
0122   0083   0000   MSK2    DATA   0
0123   0084   0000   RØN     DATA   0
0124                         END
0000 ERRØRS
```

```
                              NAM    IKB,IER,BIPT,XEQ
                              NAM    ØTT,ERR,CRLF
                              NAM    ØTL,ØFPA,ØDEC
0000                          REL    0
                      *
                      * PANIC SWITCH
                      *
0000   FB00                   JST    *CMND
0001                  CMND    REF
                      *
                      *KEYBØARD INPUT
                      *
0002   0800           IKB     ENT
0003   4038                   SEL    7,0         AUTØ-ECHØ
0004   4039                   SEL    7,1         KBD MØDE
0005   5939                   RDA    7,1         READ ØN FLAG
0006   403C                   SEL    7,4         RESET
0007   F705                   RTN    IKB
0008   0800           IER     ENT
0009   FE07                   JST    IKB
000A   C0DF                   CAI    :DF         BACK ARRØW?
000B   FF0A                   JST    *CMND       YES
000C   C08A                   CAI    :8A         LINE FEED?
000D   FF0C                   JST    *CMND       YES
000E   F706                   RTN    IER         NEITHER,RETURN
                      *
                      *PAPER TAPE INPUT
                      * DS0 = 0 FØR TTY
                      * 1 FØR HSR
                      *
000F   0800           BIPT    ENT
0010   5801           BIP2    ISA                READ SWITCHES
0011   13D0                   LRA    1           DS0 UP FØR TTY
0012   220A                   JØS    HSR         DØWN FØR HSR
0013   493B                   SEN    7,3         TTY BUSY?
0014   F604                   JMP    BIP2        YES
0015   403A                   SEL    7,2         NØ,STEP READER
0016   4839           WT      SSN    7,1         FLAG?
0017   F203                   JMP    IT          YES
0018   0150                   IAR                NØ,BUMP CØUNT
0019   2149                   JAZ    BIP2        RESTART IF TIME UP
001A   F604                   JMP    WT          ELSE CHECK FLAG AGAIN
001B   5838           IT      INA    7,0         INPUT FRØM TTY
001C   F70D                   RTN    BIPT        & RETURN
001D   4933           HSR     SEN    6,3         HSR BUSY?
001E   F60E                   JMP    BIP2        YES
001F   4032                   SEL    6,2         NØ, STEP READER
0020   4835           WH      SSN    6,5         FLAG?
0021   F203                   JMP    IH          YES
0022   0150                   IAR                NØ, BUMP CØUNT
0023   2153                   JAZ    BIP2        RESTART IF TIME UP
0024   F604                   JMP    WH          ELSE CHECK FLAG AGAIN
0025   5835           IH      INA    6,5         INPUT FRØM HSR
```

```
0026  F717          RTN   BIPT     & RETURN
                *
                *WAIT FØR EXECUTE SIGNAL
                *
0027  0800  XEQ     ENT
0028  FE20          JST   IER      INPUT
0029  C03D          CAI   :8D      CARRIAGE RETURN?
002A  F703          RTN   XEQ      YES, RETURN
002B  F603          JMP   XEQ+1    NØ, GET MØRE
                *
                *ØUTPUT TØ TTY
                *
002C  0800  ØTT     ENT
002D  403C          SEL   7,4      RESET INTERFACE
002E  6D3B          WRA   7,3      WRITE ØN NØT BUSY
002F  493B          SEN   7,3      DØNE?
0030  F601          JMP   $-1      NØ
0031  F705          RTN   ØTT      YES
                *
                *CØMMAND ERRØR EXIT
                *
0032  0800  ERR     ENT
0033  C6DF          LAP   :DF      PRINT ARRØW
0034  FE03          JST   ØTT
0035  FF34          JST   *CMND    RESTART CØMMAND
                *
                *CARRIAGE-RETURN,LINE FEED
                *
0036  0800  CRLF    ENT
0037  C68D          LAP   :8D      CR
0038  FE0C          JST   ØTT
0039  C68A          LAP   :8A      LF
003A  FE0E          JST   ØTT
003B  F705          RTN   CRLF
                *
                *ØUTPUT TEXT FRØM BUFFER
                *
003C  0800  ØTL     ENT
003D  8A0F          ADD   CAI      MAKE CØMPARE INSTRUCTIØN
003E  9A06          STA   ØT2      &SAVE IT
003F  9A09          STA   ØT3
0040  E704          LDX   *ØTL     GET TEXT PØINTER
0041  DE05          IMS   ØTL      SET RETURN ADDRESS
0042  B400  ØT1     LDA   @0       GET WØRD
0043  11D7          RRA   8        PRINT FIRST BYTE
0044  FE13          JST   ØTT
0045  C000  ØT2     CAI   0        LAST ØNE
0046  F70A          RTN   ØTL      YES, RETURN
0047  1157          RLA   8        PRINT SECØND BYTE
0048  FE1C          JST   ØTT
0049  C000  ØT3     CAI   0        LAST ØNE?
004A  F70E          RTN   ØTL      YES RETURN
004B  0128          IXR            BUMP PØINTER
```

```
004C  F60A         JMP   ØT1      LØØP
004D  C000  CAI    CAI   0
                   *
                   *ØUTPUT FLØATING PØINT NUMBER
                   *
004E  0800  ØFPA   ENT
004F  E701         LDX   *ØFPA    GET PØINTER
0050  DE02         IMS   ØFPA     SET RETURN ADDRESS
0051  EA01         STX   ØPT      SAVE PØINTER
0052  FB0E         JST   *FAS     CØNVERT TØ ASCII
0053  0000  ØPT    DATA  0
0054  0059         DATA  BUF
0055  0110         ZAR            SET END FLAG
0056  FE1A         JST   ØTL      PRINT NUMBER
0057  0059         DATA  BUF
0058  F70A         RTN   ØFPA
0059  0000  BUF    RES   8,0
0061        FAS    REF
                   *
                   * ØDEC ØUTPUT DECIMAL (+/-DDDDD)
                   ** ØDEC CØNVERTS THE BINARY VALUE IN THE
                   *A REG AND PRINTS IT AS A SIGNED 5
                   * DIGIT DECIMAL NUMBER ØN THE TELETYPE.
                   * AR AND OV ARE DESTRØYED.
                   *
                   * LDA VAL AR = VALUE
                   * SWM  MUST BE IN WØRD MØDE
                   * JST *ØDEC CALL RØUTINE
                   * *** RETURN XR UNCHANGED
0062  0800  ØDEC   ENT
0063  EA19         STX   S        SAVE XR
0064  C4AB         LXP   '+'
0065  3032         JAP   $+3
0066  0310         NAR            MAKE VALUE +
0067  C202         AXI   2        MAKE SIGN -
0068  9A15         STA   V        SAVE VALUE
0069  0030         TXA
006A  FE3E         JST   ØTT      PRINT SIGN
006B  B215         LDA   STRT
006C  9A13         STA   PTR      INITIALIZE TEL PTR
006D  C705         LAM   5
006E  9A10         STA   T        SET FØR 5 DIGITS
006F  B20E  Ø1     LDA   V
0070  C4AF         LXP   :AF      ZERØ TØ -1
0071  930E         SUB   *PTR
0072  0128         IXR
0073  30C2         JAP   $-2
0074  8B0B         ADD   *PTR
0075  9A08         STA   V
0076  0030         TXA
0077  FE4B         JST   ØTT      PRINT DIGIT
0078  DA07         IMS   PTR
0079  DA05         IMS   T
```

```
007A  F60B          JMP    Ø1
007B  E201          LDX    S             RESTØRE XR
007C  F71A          RTN    ØDEC          RETURN
007D  0800  S       HLT                  TEMP FØR XR
007E  0800  V       HLT                  VALUE
007F  0800  T       HLT                  CØUNT
0080  0800  PTR     HLT                  PØINTER
0081  0082  STRT    DATA   TBL           TABLE ADDR
0082  2710  TBL     DATA   10000,1000,100
0083  03E8
0084  0064
0085  000A          DATA   10,1
0086  0001
                    END
0000 ERRØRS
```

```
                         NAM   READ, PUNCH, CLEAR
                         EXTR  IKB, ØTT, BIPT, ØTL, CRLF, IER, ERR
0000                     REL   0
0000   0800    READ      ENT
0001   F900              JST   CRLF
       0000
0002   F900              JST   IER
       0000
0003   C0B0              CAI   '0'
0004   F203              JMP   REZE
0005   C0C7              CAI   'G'
0006   F204              JMP   RESN
0007   F900              JST   ERR
       0000
0008   E21F    REZE      LDX   IBC
0009   B21F              LDA   ZCT0
000A   F204              JMP   RDLP
000B   B21C    RESN      LDA   IBC
000C   8A1E              ADD   SN0
000D   0048              TAX
000E   B21B              LDA   ZCT1
000F   9A1C    RDLP      STA   CNT
0010   C68A              LAP   :8A
0011   F900              JST   ØTT
       0000
0012   F900              JST   BIPT
       0000
0013   2141              JAZ   $-1          SKIP LEADER
0014   F900    R1        JST   ØTT
       0000
0015   F900              JST   BIPT         READ TAPE
       0000
0016   C092              CAI   :92          END ØF LABEL
0017   F201              JMP   R2           YES
0018   F604              JMP   R1           NØ
0019   F900    R2        JST   BIPT         READ TAPE
       0000
001A   C0FF              CAI   :FF          FILE MARK
001B   F201              JMP   R3           YES
001C   F603              JMP   R2           NØ
001D   F900    R3        JST   BIPT
       0000
001E   1357              LLA   8
001F   9A0E              STA   TEMP
0020   F900              JST   BIPT
       0000
0021   A20C              IØR   TEMP
0022   8C00              ADD   @0
0023   9C00              STA   @0
0024   0128              IXR
0025   DA06              IMS   CNT
0026   F609              JMP   R3
0027   F727              RTN   READ
```

```
002B            IBC     REF
0029    F010    ZCT0    DATA    -4080
002A    FF01    ZCT1    DATA    -255
002B    0EF1    SN0     DATA    3825
002C    0000    CNT     DATA    0
002D    0000    PNT     DATA    0
002E    0000    TEMP    DATA    0
                *
                * PUNCH
002F    0800    PUNCH   ENT
0030    F900            JST     CRLF
        0000
0031    F900            JST     IER
        0000
0032    C0B0            CAI     '0'
0033    F203            JMP     PNZE
0034    C0C7            CAI     'G'
0035    F204            JMP     PNSN
0036    F900            JST     ERR
        0000
0037    E60F    PNZE    LDX     IBC
0038    B60F            LDA     ZCT0
0039    F204            JMP     PNLP
003A    B612    PNSN    LDA     IBC
003B    8E10            ADD     SN0
003C    0048            TAX
003D    B613            LDA     ZCT1
003E    9E12    PNLP    STA     CNT
003F    FA0D            JST     LEAD
0040    F900    P1      JST     IKB             ECHØ LABEL
        0000
0041    C092            CAI     :92             CTRL/TAPE
0042    F201            JMP     P2              YES
0043    F603            JMP     P1              NØ
0044    C6FF    P2      LAP     :FF             PUNCH FILE MARK
0045    F900            JST     ØTT
        0000
0046    B400    P3      LDA     @0              PUNCH BITS
0047    FA0D            JST     ØTW
0048    0128            IXR
0049    DE1D            IMS     CNT
004A    F604            JMP     P3
004B    FA01            JST     LEAD
004C    F71D            RTN     PUNCH
                *PUNCH 5" ØF LEADER
004D    0800    LEAD    ENT
004E    C732            LAM     50
004F    9E22            STA     PNT
0050    0110            ZAR
0051    F900    L2      JST     ØTT
        0000
0052    DE25            IMS     PNT
0053    F602            JMP     L2
```

```
0091  0054  F707         RTN    LEAD
0092               *
0093  0055  0800   ØTW   ENT
0094  0056  11D7         RRA    8
0095  0057  F900         JST    ØTT
            0000
0096  0058  1157         RLA    8
0097  0059  F900         JST    ØTT
            0000
0098  005A  F705         RTN    ØTW
0099               *CLEAR PRØGRAM
0100  005B  0800   CLEAR ENT
0101  005C  F900         JST    CRLF
            0000
0102  005D  F900         JST    IER
            0000
0103  005E  C0B0         CAI    'O'
0104  005F  F203         JMP    CLZE
0105  0060  C0C7         CAI    'G'
0106  0061  F204         JMP    CLSN
0107  0062  F900         JST    ERR
            0000
0108  0063  E63B   CLZE  LDX    IBC
0109  0064  B63B         LDA    ZCTO
0110  0065  F204         JMP    CLLP
0111  0066  B63E   CLSN  LDA    IBC
0112  0067  8E3C         ADD    SNO
0113  0068  0048         TAX
0114  0069  B63F         LDA    ZCT1
0115  006A  9E3E   CLLP  STA    CNT
0116  006B  0110         ZAR
0117  006C  9C00   CR    STA    @0
0118  006D  0128         IXR
0119  006E  DE42         IMS    CNT
0120  006F  F603         JMP    CR
0121  0070  F715         RTN    CLEAR
0122                     END
0000 ERRØRS
```

```
     0000                    NAM   FPLØT
0000                         REL   0
0000 0800  FPLØT             ENT
0001 C70F                    LAM   15
0002 9ABB                    STA   NRØW
0003 B2D0                    LDA   IBC
0004 9ABA                    STA   IB
0005 0108                    ZXR
0006 FBCF                    JST   *CRLF
0007 FBD1                    JST   *IER
0008 C0B0                    CAI   '0'
0009 F221                    JMP   FZRØ
000A C0B1                    CAI   '1'
000B F222                    JMP   FØNE
000C C0B2                    CAI   '2'
000D F222                    JMP   FTWØ
000E C0B3                    CAI   '3'
000F F222                    JMP   FTHRE
0010 C0B4                    CAI   '4'
0011 F222                    JMP   FFØUR
0012 C0B5                    CAI   '5'
0013 F222                    JMP   FFIVE
0014 C0B6                    CAI   '6'
0015 F222                    JMP   FSIX
0016 C0B7                    CAI   '7'
0017 F222                    JMP   FSEVE
0018 C0B8                    CAI   '8'
0019 F222                    JMP   FEIGH
001A C0B9                    CAI   '9'
001B F222                    JMP   FNINE
001C C0C1                    CAI   'A'
001D F222                    JMP   FTEN
001E C0C2                    CAI   'B'
001F F222                    JMP   FELE
0020 C0C3                    CAI   'C'
0021 F222                    JMP   FTWVE
0022 C0C4                    CAI   'D'
0023 F222                    JMP   FTHD
0024 C0C5                    CAI   'E'
0025 F222                    JMP   FFRTN
0026 C0C6                    CAI   'F'
0027 F222                    JMP   FFVTN
0028 C0C7                    CAI   'G'
0029 F222                    JMP   FSXTN
002A FBAF                    JST   *ERR
002B 0110  FZRØ              ZAR
002C 9A9C                    STA   CALL
002D F22A                    JMP   FØØP1
002E C601  FØNE              LAP   1
002F F21E                    JMP   FSTØ
0030 C602  FTWØ              LAP   2
0031 F21C                    JMP   FSTØ
0032 C603  FTHRE             LAP   3
```

```
0033  F21A          JMP   FSTØ
0034  C604  FFØUR   LAP   4
0035  F218          JMP   FSTØ
0036  C605  FFIVE   LAP   5
0037  F216          JMP   FSTØ
0038  C606  FSIX    LAP   6
0039  F214          JMP   FSTØ
003A  C607  FSEVE   LAP   7
003B  F212          JMP   FSTØ
003C  C608  FEIGH   LAP   8
003D  F210          JMP   FSTØ
003E  C609  FNINE   LAP   9
003F  F20E          JMP   FSTØ
0040  C60A  FTEN    LAP   10
0041  F20C          JMP   FSTØ
0042  C60B  FELE    LAP   11
0043  F20A          JMP   FSTØ
0044  C60C  FTWVE   LAP   12
0045  F208          JMP   FSTØ
0046  C60D  FTHD    LAP   13
0047  F206          JMP   FSTØ
0048  C60E  FFRTN   LAP   14
0049  F204          JMP   FSTØ
004A  C60F  FFVTN   LAP   15
004B  F202          JMP   FSTØ
004C  C610  FSXTN   LAP   16
004D  F200          JMP   FSTØ
004E  9A7A  FSTØ    STA   CALL
004F  0310          NAR
0050  9A79          STA   FRØW
0051  B26D          LDA   IB
0052  DA77  FRØNØ   IMS   FRØW
0053  F201          JMP   $+2
0054  F202          JMP   $+3
0055  8A75          ADD   H255
0056  F604          JMP   FRØNØ
0057  9A67          STA   IB
0058  B270  FØØP1   LDA   CALL
0059  2101          JAZ   $+2
005A  F204          JMP   $+5
005B  B26C          LDA   ZCT
005C  0150          IAR
005D  9A63          STA   CNT
005E  F203          JMP   $+4
005F  C7FF          LAM   255
0060  0150          IAR
0061  9A5F          STA   CNT
0062  B25C          LDA   IB
0063  9A5E          STA   IPB1
0064  B35D          LDA   *IPB1
0065  9A5E          STA   MAX
0066  DA5B  LØØP2   IMS   IPB1
0067  B35A          LDA   *IPB1
```

```
0068  D25B          CMS   MAX
0069  F201          JMP   $+2
006A  9A59          STA   MAX
006B  DA55          IMS   CNT
006C  F606          JMP   LØØP2
006D  0350          ARP
006E  9A56          STA   SCALE
006F  9A56          STA   RØUND
0070  B256          LDA   H50
0071  D252          CMS   MAX
0072  F202          JMP   $+3
0073  F20C          JMP   LØØP
0074  F20B          JMP   LØØP
0075  B24E          LDA   MAX
0076  0108          ZXR
0077  924F          SUB   H50
0078  0128          IXR
0079  31C2          JAG   $-2
007A  EA4A          STX   SCALE
007B  1200          RØV
007C  11A8          RRX   1
007D  3201          JØR   $+2
007E  0128          IXR
007F  EA46          STX   RØUND
0080  FB55  LØØP    JST   *CRLF
0081  FB54          JST   *CRLF
0082  C6BD          LAP   '='
0083  FB54          JST   *ØTL
0084  00CD          DATA  SF
0085  C6A0          LAP   ' '
0086  FB50          JST   *ØTT
0087  B23D          LDA   SCALE
0088  FB4C          JST   *ØDEC
0089  C601          LAP   1
008A  9A41          STA   RØNØ
008B  FB4A          JST   *CRLF
008C  FB49          JST   *CRLF
008D  B23E          LDA   RØNØ
008E  FB48          JST   *ØTT
008F  C7FF          LAM   255
0090  9A2F          STA   NCØL
0091  B22D          LDA   IB
0092  9A30          STA   IPB2
0093  FB42  LØØP1   JST   *CRLF
0094  B32E          LDA   *IPB2
0095  FB3F          JST   *ØDEC
0096  C6A0          LAP   ' '
0097  FB3F          JST   *ØTT
0098  C6B0          LAP   '0'
0099  FB3D          JST   *ØTT
009A  B328          LDA   *IPB2
009B  2192          JAL   CLØSE
009C  0108          ZXR
```

```
009D  9227          SUB   SCALE
009E  0128          IXR
009F  31C2          JAG   $-2
00A0  8A24          ADD   SCALE
00A1  00A8          DXR
00A2  D223          CMS   RØUND
00A3  F202          JMP   $+3
00A4  0000          NØP
00A5  0128          IXR
00A6  0030          TXA
00A7  2166          JAL   CLØSE
00A8  C6AA          LAP   '*'
00A9  0503          NXR
00AA  EA16          STX   CNT
00AB  FB2B          JST   *ØTT
00AC  DA14          IMS   CNT
00AD  F602          JMP   $-2
00AE  DA14   CLØSE  IMS   IPB2
00AF  0000          NØP
00B0  DA0F          IMS   NCØL
00B1  F61E          JMP   LØØP1
00B2  FB23          JST   *CRLF
00B3  B215          LDA   CALL
00B4  2101          JAZ   $+2
00B5  F206          JMP   FSH
00B6  C6FF          LAP   255
00B7  8A07          ADD   IB
00B8  9A06          STA   IB
00B9  DA12          IMS   RØNØ
00BA  DA03          IMS   NRØW
00BB  F628          JMP   LØØP1
00BC  FB19   FSH    JST   *CRLF
00BD  F7BD          RTN   FFLØT
00BE  0000   NRØW   DATA  0
00BF  0000   IB     DATA  0
00C0  0000   NCØL   DATA  0
00C1  0000   CNT    DATA  0
00C2  0000   IPB1   DATA  0
00C3  0000   IPB2   DATA  0
00C4  0000   MAX    DATA  0
00C5  0000   SCALE  DATA  0
00C6  0000   RØUND  DATA  0
00C7  0032   H50    DATA  50
00C8  F10F   ZCT    DATA  -3825
00C9  0000   CALL   DATA  0
00CA  0000   FRØW   DATA  0
00CB  00FF   H255   DATA  255
00CC  0000   RØNØ   DATA  0
00CD  D3C3   SF     TEXT  'SCALE FACTØR='
00CE  C1CC
00CF  C5A0
00D0  C6C1
00D1  C3D4
```

```
      00D2   CFL2
      00D3   BDA0
0209  00D4          IBC     REF
0210  00D5          ØDEC    REF
0211  00D6          CRLF    REF
0212  00D7          ØTT     REF
0213  00D8          ØTL     REF
0214  00D9          IER     REF
0215  00DA          ERR     REF
0216                        END
0000 ERRØRS
```

```
                        NAM   CRT
                        NAM   DISP
                        NAM   DISD
                        EXTR  RTDA
                        EXTR  RTTR
0000                    REL   0
0000  0800  CRT         ENT
0001  C70F              LAM   15
0002  9900              STA   NRØW
      0112
0003  49C4              SEN   24,4
0004  F601              JMP   $-1
0005  40C7              SEL   24,7
0006  0110              ZAR
0007  9900              STA   ØFFSET
      0113
0008  C601              LAP   1
0009  9900  DISP        STA   TR1
      0116
000A  3106              JAN   $+7
000B  B100              LDA   AD16
      0126
000C  8900              ADD   IBC
      0133
000D  9900              STA   IB
      0114
000E  0110              ZAR
000F  9900              STA   CALL
      0117
0010  F25F              JMP   MXMI
0011  B100              LDA   IBC
      0133
0012  9900              STA   IB
      0114
0013  0108              ZXR
0014  F900              JST   *CRLF
      8133
0015  F900              JST   *IER
      8134
0016  C0B0              CAI   '0'
0017  F221              JMP   ZERØ
0018  C0B1              CAI   '1'
0019  F222              JMP   ØNE
001A  C0B2              CAI   '2'
001B  F222              JMP   TWØ
001C  C0B3              CAI   '3'
001D  F222              JMP   THREE
001E  C0B4              CAI   '4'
001F  F222              JMP   FØUR
0020  C0B5              CAI   '5'
0021  F222              JMP   FIVE
0022  C0B6              CAI   '6'
0023  F222              JMP   SIX
```

```
0024  C0B7          CAI   '7'
0025  F222          JMP   SEVEN
0026  C0B8          CAI   '8'
0027  F222          JMP   EIGHT
0028  C0B9          CAI   '9'
0029  F222          JMP   NINE
002A  C0C1          CAI   'A'
002B  F222          JMP   TEN
002C  C0C2          CAI   'B'
002D  F222          JMP   ELE
002E  C0C3          CAI   'C'
002F  F222          JMP   TWVE
0030  C0C4          CAI   'D'
0031  F222          JMP   THD
0032  C0C5          CAI   'E'
0033  F222          JMP   FRTN
0034  C0C6          CAI   'F'
0035  F222          JMP   FVTN
0036  C0C7          CAI   'G'
0037  F222          JMP   SXTN
0038  FBFC          JST   *ERR
0039  0110  ZERØ    ZAR
003A  9ADC          STA   CALL
003B  F22E          JMP   LØØP1
003C  C601  ØNE     LAP   1
003D  F222          JMP   STØRE
003E  C602  TWØ     LAP   2
003F  F220          JMP   STØRE
0040  C603  THREE   LAP   3
0041  F21E          JMP   STØRE
0042  C604  FØUR    LAP   4
0043  F21C          JMP   STØRE
0044  C605  FIVE    LAP   5
0045  F21A          JMP   STØRE
0046  C606  SIX     LAP   6
0047  F218          JMP   STØRE
0048  C607  SEVEN   LAP   7
0049  F216          JMP   STØRE
004A  C608  EIGHT   LAP   8
004B  F214          JMP   STØRE
004C  C609  NINE    LAP   9
004D  F212          JMP   STØRE
004E  C60A  TEN     LAP   10
004F  F210          JMP   STØRE
0050  C60B  ELE     LAP   11
0051  F20E          JMP   STØRE
0052  C60C  TWVE    LAP   12
0053  F20C          JMP   STØRE
0054  C60D  THD     LAP   13
0055  F20A          JMP   STØRE
0056  C60E  FRTN    LAP   14
0057  F208          JMP   STØRE
0058  C60F  FVTN    LAP   15
```

```
0059  F206         JMP  STØRE
005A  C610  SXTN   LAP  16
005B  F204         JMP  STØRE
005C  0108  DISD   ZXR
005D  EAB8         STX  TR1
005E  E2D4         LDX  IBC
005F  EAB4         STX  IB
0060  9AB6  STØRE  STA  CALL
0061  0310         NAR
0062  9AB5         STA  RØWVA
0063  B2B0         LDA  IB
0064  DAB3  RØWNØ  IMS  RØWVA
0065  F201         JMP  $+2
0066  F202         JMP  $+3
0067  8ABB         ADD  H255
0068  F604         JMP  RØWNØ
0069  9AAA         STA  IB
006A  B2AC  LØØP1  LDA  CALL
006B  2101         JAZ  $+2
006C  F203         JMP  $+4
006D  B2AC         LDA  ZCT
006E  9AAC         STA  CNT
006F  F202         JMP  $+3
0070  C7FF  MXMI   LAM  255
0071  9AA9         STA  CNT
0072  B2A1         LDA  IB
0073  9AA8         STA  IBP1
0074  0110         ZAR
0075  9AA8         STA  MIN
0076  9AA8         STA  MAX
0077  B3A4  LØØP2  LDA  *IBP1
0078  D2A6         CMS  MAX
0079  F202         JMP  $+3
007A  9AA4         STA  MAX
007B  F203         JMP  $+4
007C  D2A1         CMS  MIN
007D  9AA0         STA  MIN
007E  0000         NØP
007F  DA9C         IMS  IBP1
0080  DA9A         IMS  CNT
0081  F60A         JMP  LØØP2
0082  0350         ARP
0083  9A9C         STA  SCALE
0084  9A9C         STA  RØUND
0085  B299         LDA  MAX
0086  9297         SUB  MIN
0087  9A97         STA  MAX
0088  B28D         LDA  TR1
0089  2106         JAZ  SCA
008A  B28C         LDA  CALL
008B  2101         JAZ  $+2
008C  F203         JMP  $+4
008D  B294         LDA  H100
```

```
008E   9A98          STA    TØTDØT
008F   F202          JMP    $+3
0090   B293   SCA    LDA    H200
0091   9A95          STA    TØTDØT
0092   B294          LDA    TØTDØT
0093   D28B          CMS    MAX
0094   F202          JMP    $+3
0095   F20C          JMP    LØØP
0096   F20B          JMP    LØØP
0097   B287          LDA    MAX
0098   0108          ZXR
0099   928D          SUB    TØTDØT
009A   0128          IXR
009B   31C2          JAG    $-2
009C   EA83          STX    SCALE
009D   1200          RØV
009E   11A3          RRX    1
009F   3201          JØR    $+2
00A0   0128          IXR
00A1   EA7F          STX    RØUND
00A2   B273   LØØP   LDA    TR1
00A3   210B          JAZ    MI
00A4   FB93          JST    *CRLF
00A5   FB92          JST    *CRLF
00A6   C6BD          LAP    '='
00A7   FB8F          JST    *ØTL
00A8   012C          DATA   SF
00A9   C6A0          LAP    ' '
00AA   FB8B          JST    *ØTT
00AB   B274          LDA    SCALE
00AC   FB8C          JST    *ØDEC
00AD   FB8A          JST    *CRLF
00AE   FB89          JST    *CRLF
00AF   B26E   MI     LDA    MIN
00B0   0310          NAR
00B1   0108          ZXR
00B2   926D          SUB    SCALE
00B3   0128          IXR
00B4   31C2          JAG    $-2
00B5   8A6A          ADD    SCALE
00B6   00A8          DXR
00B7   D269          CMS    RØUND
00B8   F202          JMP    $+3
00B9   0000          NØP
00BA   0128          IXR
00BB   EA6C          STX    X1
00BC   B26B   LØØP4  LDA    X1
00BD   9A6B          STA    X
00BE   C7FF          LAM    255
00BF   9A59          STA    NCØL
00C0   B253          LDA    IB
00C1   9A5B          STA    IBP2
00C2   B250   LØØP3  LDA    ØFFSET
```

```
00C3  8A65          ADD   X
00C4  9A66          STA   TØTØFF
00C5  B357          LDA   *IBP2
00C6  1200          RØV
00C7  1150          RLA   1
00C8  2207          JØS   NEG
00C9  11D0          RRA   1
00CA  0108          ZXR
00CB  9254          SUB   SCALE
00CC  0128          IXR
00CD  31C2          JAG   $-2
00CE  8A51          ADD   SCALE
00CF  F206          JMP   $+7
00D0  1400   NEG    SØV
00D1  11D0          RRA   1
00D2  0108          ZXR
00D3  8A4C          ADD   SCALE
00D4  00A8          DXR
00D5  20C2          JAM   $-2
00D6  9249          SUB   SCALE
00D7  00A8          DXR
00D8  D248          CMS   RØUND
00D9  F202          JMP   $+3
00DA  0000          NØP
00DB  0128          IXR
00DC  0030          TXA
00DD  9A4C          STA   DØTNØ
00DE  E24C          LDX   TØTØFF
00DF  49C4   DØT    SEN   24,4
00E0  F601          JMP   $-1
00E1  49C2          SEN   24,2
00E2  F601          JMP   $-1
00E3  6EC2          ØTX   24,2
00E4  B231          LDA   TR1
00E5  2108          JAZ   $+9
00E6  B230          LDA   CALL
00E7  2101          JAZ   $+2
00E8  F205          JMP   $+6
00E9  B240          LDA   DØTNØ
00EA  8A40          ADD   TØTØFF
00EB  0048          TAX
00EC  6EC2          ØTX   24,2
00ED  F20B          JMP   DØNE
00EE  B23B          LDA   DØTNØ
00EF  2109          JAZ   DØNE
00F0  3184          JAG   PØS
00F1  00A8          DXR
00F2  0150          IAR
00F3  9A36          STA   DØTNØ
00F4  F615          JMP   DØT
00F5  0128   PØS    IXR
00F6  00D0          DAR
00F7  9A32          STA   DØTNØ
```

```
0255  00F8  F619          JMP   DØT
0256  00F9  B22F  DØNE    LDA   X
0257  00FA  8A2A          ADD   H256
0258  00FB  9A2D          STA   X
0259  00FC  DA20          IMS   IBP2
0260  00FD  DA1B          IMS   NCØL
0261  00FE  F63C          JMP   LØØP3
0262  00FF  B216          LDA   TR1
0263  0100  3104          JAN   $+5
0264  0101  B215          LDA   CALL
0265  0102  2101          JAZ   $+2
0266  0103  F100          JMP   RTDA
            0000
0267  0104  F100          JMP   RTTR
            0000
0268  0105  B211          LDA   CALL
0269  0106  2101          JAZ   $+2
0270  0107  F208          JMP   FIN
0271  0108  C60A          LAP   10
0272  0109  8A09          ADD   ØFFSET
0273  010A  9A08          STA   ØFFSET
0274  010B  B217          LDA   H255
0275  010C  8A07          ADD   IB
0276  010D  9A06          STA   IB
0277  010E  DA03          IMS   NRØW
0278  010F  F653          JMP   LØØP4
0279  0110  FB27  FIN     JST   *CRLF
0280  0111  F100          RTN   CRT
            8000
0281  0112  0000  NRØW    DATA  0
0282  0113  0000  ØFFSET  DATA  0
0283  0114  0000  IB      DATA  0
0284  0115  0000  IBQ     DATA  0
0285  0116  0000  TR1     DATA  0
0286  0117  0000  CALL    DATA  0
0287  0118  0000  RØWVA   DATA  0
0288  0119  0000  NCØL    DATA  0
0289  011A  F10E  ZCT     DATA  -3826
0290  011B  0000  CNT     DATA  0
0291  011C  0000  IBP1    DATA  0
0292  011D  0000  IBP2    DATA  0
0293  011E  0000  MIN     DATA  0
0294  011F  0000  MAX     DATA  0
0295  0120  0000  SCALE   DATA  0
0296  0121  0000  RØUND   DATA  0
0297  0122  0064  H100    DATA  100
0298  0123  00FF  H255    DATA  255
0299  0124  00C8  H200    DATA  200
0300  0125  0100  H256    DATA  256
0301  0126  0EF1  AD16    DATA  3825
0302  0127  0000  TØTDØT  DATA  0
0303  0128  0000  X1      DATA  0
0304  0129  0000  X       DATA  0
```

```
0305   012A   0000   DØTNØ   DATA    0
0306   012B   0000   TØTØFF  DATA    0
0307   012C   D3C3   SF      TEXT    'SCALE FACTØR='
       012D   C1CC
       012E   C5A0
       012F   C6C1
       0130   C3D4
       0131   CFD2
       0132   BDA0
0308   0133          IBC     REF
0309   0134          IER     REF
0310   0135          ERR     REF
0311   0136          ØTT     REF
0312   0137          ØTL     REF
0313   0138          CRLF    REF
0314   0139          ØDEC    REF
0315                         END
0000 ERRØRS
```

```
PAGE  0001

                         NAM   MASKO
0000                     REL   0
0000  0001  MASKO        DATA  1
0001  0001               DATA  1
0002  0001               DATA  1
0003  0001               DATA  1
0004  FFFF               DATA  -1
0005  0001               DATA  1
0006  FFFF               DATA  -1
0007  0001               DATA  1
0008  0001               DATA  1
0009  FFFF               DATA  -1
000A  FFFF               DATA  -1
000B  0001               DATA  1
000C  FFFF               DATA  -1
000D  FFFF               DATA  -1
000E  FFFF               DATA  -1
000F  0001               DATA  1
0010  0001               DATA  1
0011  0001               DATA  1
0012  0001               DATA  1
0013  FFFF               DATA  -1
0014  0001               DATA  1
0015  FFFF               DATA  -1
0016  0001               DATA  1
0017  0001               DATA  1
0018  FFFF               DATA  -1
0019  FFFF               DATA  -1
001A  0001               DATA  1
001B  FFFF               DATA  -1
001C  FFFF               DATA  -1
                         END
0000 ERRØRS
```

```
0001                              NAM    IBC
0002  0000                        REL    0
0003  0000  0000  IBC             DATA   0000
0004                              END
0000 ERRORS
```

APPENDIX D

```
1    DEF FNR(X)=INT(100*X+0.5)/100
10   DIM Ø(255),F(255),X(255)
20   PRINT "SPECTRUM CØRRECTED FØR NEGETIVE DIP"
25   PRINT
26   PRINT
30   CALL (20)
40   CALL (5,Ø(0),256,2)
50   LET F(0)=Ø(0)
60   FØR N=1 TØ 255
70   LET I1=N-1
75   IF I1>0 THEN 85
80   LET I1=255
85   LET I2=N+1
90   IF I2<256 THEN 100
95   LET I2=I2-255
100  LET I3=N+24
105  IF I3<256 THEN 115
110  LET I3=I3-255
115  LET I4=N+25
120  IF I4<256 THEN 130
125  LET I4=I4-255
130  LET C=(Ø(I3)+Ø(I4)-Ø(I1)-Ø(I2))/20
140  LET F(N)=Ø(N)+C
150  NEXT N
160  PRINT "A: 1 FØR DISPLAY, 2 FØR GRAPH, 3 FØR TAPE"
170  PRINT "B: 0 FØR ØRIGINAL, 1 FØR FINAL"
180  PRINT
200  PRINT "A=";
210  INPUT A
220  PRINT "B=";
230  INPUT B
240  PRINT "RESØLUTIØN D=";
250  INPUT D
260  PRINT "INITIAL WAVE LENGTH L0=";
270  INPUT L0
280  PRINT
290  PRINT
300  IF A=3 THEN 730
310  LET Z=0
320  LET M=1E10
330  FØR N=1 TØ 255
```

```
350   IF B=1 THEN 400
360   LET X(N)=Ø(N)
370   GØTØ 410
400   LET X(N)=F(N)
410   IF X(N)>=M THEN 430
420   LET M=X(N)
430   IF X(N)<=Z THEN 450
440   LET Z=X(N)
450   NEXT N
460   IF M>=0 THEN 510
470   LET S0=255/(Z-M)
480   LET S1=48/(Z-M)
490   LET Y0=-M*S
500   GØTØ 540
510   LET S0=255/Z
520   LET S1=48/Z
530   LET Y0=0
540   PRINT "MAX=";Z;"MIN=";M
550   IF A=2 THEN 630
560   PRINT "SCALE FACTØR=";S0
570   FØR N=1 TØ 255
580   LET E=INT(S0*X(N)+0.5)
590   CALL (3,N,Y0,2,E)
600   NEXT N
620   GØTØ 160
630   PRINT "SCALE FACTØR="; S1
635   PRINT
636   PRINT
640   FØR N=1 TØ 255
650   LET E=INT(S1*X(N)+0.5)
660   LET L=L0+(N-1)*D
670   PRINT FNR(L);TAB(8);X(N)
715   NEXT N
730   IF B=0 THEN 760
740   IF B=1 THEN 780
750   GØTØ 200
760   CALL(6,Ø(0),256,2)
770   GØTØ 790
780   CALL(6,F(0),256,2)
790   CALL(6,0,0,3)
800   STØP
```

BIBLIOGRAPHY

1. Aitken, D.K., and Jones, B., (1972), Nature, 240, 230.
2. Allen, J.D., Jr., and Schweitzer, G.K., (1972, 1973), J. Electron Spectroscopy 1, 509.
3. Baumert, L.D., (1964), Digital Communication with Space Application, Prentice-Hall Inc., Canada, S.W. Golomb, Ed. pp.17-32.
4. Combes, M., Encrenaz, TH., Vapillon, L., and Ze'au, Y., (1974), Astron & Astrophys, 34, 33.
5. Colpa, J.P., and Keltelaar, J.A.A.,(1958), Mol. Phys., 1,14.
6. Cudaback, D.D., and Gaustad, J.E., (1971), 166, L49.
7. Day, K.L., (1974), Ap.J., 192, L15.
8. Decker, J.A., Jr., and Harwit, M., (1968), Appl. Opt., 7, 2205.
9. Decker, J.A., Jr., (1969), Appl. Opt., 8, 2552.
10. Decker, J.A., Jr., (1971), Appl. Opt., 10, 510.
11. Decker, J.A., Jr., (1974), Appl. Opt., 13, 1296.
12. Encrenaz, Th., (1972), Astron and Astrophys, 16, 237.
13. Fellgett, P., (1951), Cambridge Univ., PH.D. thesis.
14. Fellgett, P., (1958), J. Phys., 19, 187.
15. Fink, U., Larson, H.P., and Poppen, R.F., (1974), Ap.J., 187, 407.
16. Finkbeiner, D.T., II(1960), Introduction to Matrices and Linear Transformations, W.H. Freeman and Co., San Francisco.

17. Gamown, R.H., Gaustad, J.E., and Treffers, R.R., (1973), Ap.J., 175, 687.

18. Gillett, F.C., Low, F.J., and Stein, W.A., (1968), Ap.J., 154,677.

19. Gillett, F.C., Low, F.J., and Stein, W.A., (1969), Ap.J., 157, 925.

20. Gilman, R.C., (1969), Ap.J., 155, L185.

21. Golay M.J.E., (1949), J. Opt. Soc. Amer. 39, 437.

22. de Graauw, Th., Veltman, B.P. Th., (1970), Appl. Opt., 9, 2658.

23. Hall, M., Jr., (1967), Combinational Theory, Blaisdell Publ. Co., Waltham, Mass., 204.

24. Harwit, M., Phillips, P.G., Fine, T., and Sloane, N.J.A., (1970), Appl. Opt., 9, 1149.

25. Harwit, M., (1971), Appl. Opt., 10, 1415.

26. Harwit, M., (1973), Appl. Opt., 12, 285.

27. Harwit, M., Phillips, P.G., King, L.W., and Briotta, D.H., (1974a), Appl. Opt., 13, 2669.

28. Harwit, M., and Decker, J.A., Jr., (1974b), Progress in Optics XII, North-Holland.

29. Hirschfeld, T., and Wijntjes, G., (1973), Appl. Opt., 12, 2876.

30. Hirschfeld, T., and Wijntjes, G., (1974), Appl. Opt., 13, 1740.

31. Hirschy, V.L., and Aldridge, J.P., (1971), Rev. Sci. Inotrum. 42, 381.

32. Hotelling, H., (1944), Ann. Math. Stat. 15, 297.

33. Houck, J., Pollack, J.B., Schaack, D., Sagan, C., and Decker, J.A., (1973), Icarus, 18, 470.

34. Ibbett, R.N., Aspinall, D., Grainger, J.F., (1968), Appl. Opt., 7, 1089.

35. Ingersoll, A.P., submitted to space Sci. Rev. July, 1975.

36. Jacquinot, P., (1954), J.O.S.A., 44, 761.

37. Jacquinot, P., (1960), Rep. Prog. Phys., 23, 267.

38. Kittel, C., (1966), Introduction to Solid State Physics, John Wiley and Sons, N.Y., 548.

39. Kowalski, B.R., and Bender, C.F., (1973), Anal. Chem. 45, 2234.

40. Kranendonk, J.Van. and Kiss, Z.J., (1959), Can. J. Phys., 37, 1187.

41. Lacy, J.H., Larrabee, A.I., Wollman, E.R., Geballe, T.R., Townes, L.H., Bregman, J.D., and Rank, D.M., (1975), Ap. J., 198, L145.

42. Larson, N., Crosmun, R., and Taimi, Y., (1974), Appl. Opt., 13, 2662.

43. Lewis, J.S., and Prinn, R.G., (1970), Science, 169, 472.

44. Linsky, J.L., (1973), Ap.J., Supp., 216, 25, 163.

45. Low, F.J., and Swamy, K.S.K., (1970), Nature, 227, 1333.

46. Maas, R.W., Ney, E.F., and Woolf, N.J., (1970), Ap.J., letters, 160, L101.

47. McCord, T.B., and Adams, J.B., (1972), Icarus, 17, 585.

48. McElroy, M.B., (1973), Space Sci. Rev., 14, 460.

49. Mertz, L., (1965), Transformation in Optics, John Wiley and Sons, Inc., N.Y.

50. Mertz, L., (1976) Private communication.

51. Mertz, L., and Flamand, J., (1976), Private communication.

52. Morrison, D., and Sagan, C., (1967), Ap.J., 150, 1105.

53. Morrison, D., (1970), Spa. Sci. Rev., 11, 271.

54. Murcray, F.H., Murcray, D.G., and Williams, W.J., (1970), J. Geo. Res. 75, 14, 2662.

55. Murdock, T.L., (1974), Ap.J., 79, 1457.

56. Nelson, E.D., and Fredman, M.L., (1970), J.O.S.A., 60, 1664.

57. Oliver, C., and Pike, E., (1974), Appl. Opt., 13, 158.

58. Penman, (1976), Mon. Not. R. Astr.Soc., 175, 149.

59. Pettingill, G.H., and Dyce, R.B., (1965), Nature, 206, 1240.

60. Phillips, P.G., and Harwit, M., (1971), Appl. Opt., 10, 1415.

61. Planky, F.W., Winefordner, J.D., (1974), paper No.200, Pittsburgh Conference on Analytical Chemistry and Applied Spectroscopy.

62. Podolak, M., and Cameron, A.F.W., (1974), Icarus, 22, 123.

63. Pratt, W.K., Kane, J., and Andrew, H.C., (1969), Proc IEEE, 57, 58.

64. Putley, E.H., (1964), Phys, Stat. Solidi, 6, 571.

65. Rage and Sagan, C., (1977), in preparation.

66. Ridgway, S.T., (1974), Ap.J., 187, L41.

67. Sagan, C., and Salpeter, E.E., (1976), Ap.J., Suppl 76.

68. Saiedy, F., and Goody, R.M., (1959) R.A.S.M.N. 119, 213.

69. Salpeter, E.E., (1974a), Ap.J., 193, 579.

70. Salpeter, E.E., (1974b), Ap.J., 193, 585.

71. Sloane, N.J.A., Fine, T., Phillips, P.G., and Harwit M., (1969), Appl. Opt., 8, 2103.

72. Sloane, N.J.A., and Harwit, M., (1976), Appl. Opt., 15, 107.

73. Smith, L.G., (1949), J. Chem. Phys., 17, 139.

74. Soter, S.L., and Ulrichs, J., (1967), Nature, 214, 1315.

75. Stewart, J.E., (1970), Infrared Spectroscopy: Experimental Methods and Techniques, Marcel Dekper, Inc., N.Y.

76. Strobel, D.F., (1973), J. Atmos, Sci., 30, 489.

77. Swift, R.D., Wattson, R.B., Decker, J.A., Paganetti, R., and Harwit, M., (1976), Appl. Opt., 15, 1595.

78. Tai, M.H., Briotta, D.A., Kamath, N.S., and Harwit, M., (1975a), Appl. Opt., 14, 2533.

79. Tai, M.H., Harwit, M., and Sloane, N.J.A., (1975b), Appl. Opt., 14, 2678.

80. Terrile, R.J., and Westphal J.A., (1976), preprint.

81. Trafton, L.M., and Münch, G., (1969), J. Atm. Sci., 26, 813.

82. Treffers, R., and Cohen, M., (1974), Ap.J., 188, 545.

83. Vanasse, G.A., Sakai, H., (1967), Progress in Optics, 7, 298, E. Wolf, Ed., Wiley-Interscience, N.Y.

84. Vanasse, G.A., (1974), Application of Walsh Functions and Sequency Theory. The Institute of Electronic Engineering, Inc., New York, N.Y. 10017.

85. de Vancouleurs, G., (1964), Icarus, 3, 187.

86. Wallace, L., Caldwell, J.J., and Savage, B.D., (1972), Ap. J., 172, 755.

87. Wallace, L. Prather, M., and Belton, M.J.S., (1974), Ap.J., 193, 481.

88. Weidenschilling, S.J., and Lewis, J.S., (1973), Icarus, 20, 465.

89. Woolf, N.J., and Ney, E.P., (1969), Ap.J., 155, L181.

90. Wyatt, C., and Esplin, R., (1974), Appl. Opt., 13, 2651.